Western Michigan University
ScholarWorks at WMU

Masters Theses

Graduate College

12-2012

The Implementation of a Versatile Pseudodynamic Hybrid Simulation for Seismic Evaluation of Structural Systems

Chelsea Griffith
Western Michigan University

Follow this and additional works at: https://scholarworks.wmich.edu/masters_theses

 Part of the Construction Engineering and Management Commons

Recommended Citation

Griffith, Chelsea, "The Implementation of a Versatile Pseudodynamic Hybrid Simulation for Seismic Evaluation of Structural Systems" (2012). *Masters Theses*. 88.
https://scholarworks.wmich.edu/masters_theses/88

This Masters Thesis-Open Access is brought to you for free and open access by the Graduate College at ScholarWorks at WMU. It has been accepted for inclusion in Masters Theses by an authorized administrator of ScholarWorks at WMU. For more information, please contact wmu-scholarworks@wmich.edu.

THE IMPLEMENTATION OF A VERSATILE PSEUDODYNAMIC HYBRID SIMULATION FOR SEISMIC EVALUATION OF STRUCTURAL SYSTEMS

by

Chelsea Griffith

A Thesis
Submitted to the
Faculty of The Graduate College
in partial fulfillment of the
requirements for the
Degree of Master of Science in Engineering (Civil)
Department of Civil and Construction Engineering
Advisor: Xiaoyun Shao, Ph.D.

Western Michigan University
Kalamazoo, Michigan
December 2012

THE IMPLEMENTATION OF A VERSATILE PSEUDODYNAMIC HYBRID SIMULATION FOR SEISMIC EVALUATION OF STRUCTURAL SYSTEMS

Chelsea Griffith, M.S.E.

Western Michigan University, 2012

Pseudodynamic hybrid simulation technique was developed to evaluate structural seismic performance by physically testing the critical portion with the remaining structure simulated using a numerical model in the computer. An incremental approach was adopted in developing the control scheme to suit multiple testing facilities and test specimens. First the small scale, predictable specimen was utilized to investigate techniques of improving stability, slowing down the loading rate and triggering the accurate force measurement in a series of at benchmark scale experiments in the Laboratory of Earthquake and Structural Simulation at Western Michigan University (WMU). A step/hold command scheme was developed and results matched well to those obtained from the purely numerical simulations of the analytical model setup based on the cyclic tests. Then a series of open and closed loop PSD hybrid simulations of increasing amplitude were conducted at large scale in the Structural Engineering Laboratory at University of Alabama. A ramp/hold displacement command scheme with flexible definition on the ramp phase were developed to the address the excessive vibrations due to the very high speed actuator. The final control scheme was applied the large scale PSD hybrid simulation of a two story woodframe building with a physical first story wood shear wall and numerical second story and reasonable seismic response were achieved. The results of this study serve as a basis for developing the simulation technique for the large scale hybrid simulation that that will be conducted at the NEES equipment site at the University of Buffalo.

ACKNOWLEDGMENTS

This thesis and the material presented herein would not have been possible without the assistance and encouragement of several professors, colleagues, and devoted friends and family. First and foremost, I would like to thank my advisor, Dr. Xiaoyun Shao for all her insights and diligence during my research. She has truly taught me to strive for excellence. I would also like to thank the rest of my committee, Dr. Upul Attanayake and Dr. Haluk Aktan.

In addition, I would like to thank the National Science Foundation for funding the NEES-Soft project, on which much of my thesis is based. The principal investigator John van de Lindt and the staff at the Large Scale Structural Engineering Laboratory at the University of Alabama deserve special recognition.

Last but not least, the immense support I have received from friends and family has helped motivate me to complete this thesis, especially that of and my colleagues Adam Mueller and Christopher Sawyer.

Chelsea Griffith

TABLE OF CONTENTS

Table of Contents - Continued

CHAPTER

Table of Contents - Continued

CHAPTER

Table of Contents - Continued

CHAPTER

LIST OF TABLES

LIST OF FIGURES

List of Figures - Continued

List of Figures - Continued

CHAPTER 1

INTRODUCTION

One of the main objectives of earthquake engineering is to design, construct and maintain structures to perform up to the expectations when subjected to an earthquake. A grand challenge associated with this objective is predicting the seismic response of generally large scale civil structural systems. Though numerical simulation have advanced greatly during the past two decades, experimental investigation remains indispensable as it provides critical insight into structural seismic response. Additionally, experimental investigation is used to calibrate/establish necessary numerical models for computational analysis. Several experimental methods are currently in place to study dynamic response of structures subject to seismic excitations, including quasi-static testing (QST), shake table testing (STT), and relatively newly developed various hybrid simulation methods.

1.1 Earthquake Experimentation Methods

1.1.1 Conventional Seismic Testing

Conventional seismic testing methods include STT and QST. These conventional methods are generally open loop (see Figure 1.1) during which the loadings applied to the test specimen are predetermined (i.e. predefined cyclic displacement/force histories in QST or earthquake acceleration histories in STT). No feedback from the testing specimen is needed for the control of experimental execution. During STT, servo-hydraulic actuators apply simulated earthquake ground motion to a large scale specimen. While this is the most direct approach to earthquake simulation, it is limited in the size and weight of the specimen; the cost of

the table increases rapidly with capacity. QST tests involve the application of slow, cyclic loading pattern to evaluate the hysteretic behavior of structural elements. Generally, this method is used for individual structural elements and/or simple structural assemblies (i.e beam-column connections).

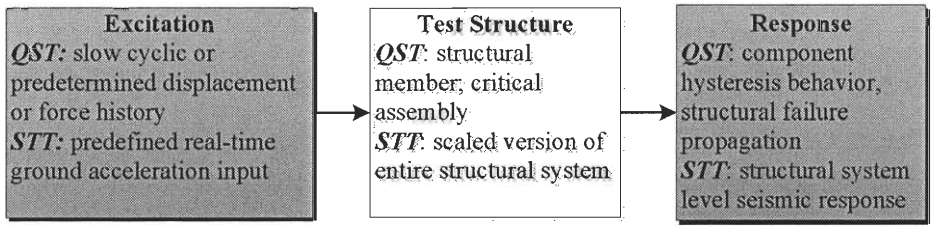

Figure 1.1. Conventional Open Loop Simulation

1.1.2 Hybrid Simulation

Hybrid simulation, on the other hand, is closed-loop (see Figure 1.2) testing that requires the testing specimen's response feedback such as the restoring force and/or displacement response to determine the loading command for the next time step. In this context, hybrid simulation is defined as a structural seismic response simulation involving both computational simulation of a *numerical substructure* and physical testing of an *experimental substructure.* A physical substructure, loaded using hydraulic loading devices, usually represents a critical portion of the structural system for which the response is difficult to predict analytically. The *numerical substructure* is the remainder of the structural system for which the response is relatively simple to be modeled and analyzed. The combination of analytical and experimental simulation is then carried out in a step-by-step format to determine the overall structural response to earthquake excitation. The two major classes of hybrid simulation are pseudodynamic and dynamic hybrid simulation.

1.1.2.1 Pseudodynamic Hybrid Simulation

Pseudodynamic (PSD) hybrid simulation is a displacement-based hybrid simulation method during which the inertia and viscous damping effects are simulated computationally, employing a numerical model of the prototype structure. This method is essentially identical to the traditional time history analysis but rather than idealizing the non-linear stiffness characteristics of the structure, the static restoring forces are directly measured from the specimen as the experiment proceeds. The numerical model and physical restoring force feedback are integrated to calculate simulated displacements, applied to the experimental substructure statically or at a real-time rate. Both the dynamic effects and progressive damage of the specimen are included in the imposed displacements, and the procedure allows for an in-depth monitoring of the performance of the structure for the entire duration of realistic earthquake excitation.

1.1.2.2 Dynamic Hybrid Simulation

Dynamic hybrid simulation is a force-based hybrid simulation method where inertial effects associated with the mass forces are physically developed within the physical substructure specimen. The test specimen, as a physical model (at small or full scale) representing the prototype structure under investigation, contains all the structural dynamic properties such as mass, damping and stiffness. Shake table with substructure testing (Igarashi et al. 2000), effective force substructure testing (EFT) (Dimig et al. 1999; Chen 2007) and real time dynamic hybrid simulation (Reinhorn et al. 2004) belong to the dynamic hybrid simulation category. They utilize shake tables, dynamic rated actuators and a combination of the two, respectively. The load applied to the physical substructure consists of the ground acceleration input and the dynamic

effects due to interaction with the numerical substructure; the dynamic responses of the physical substructure are fed back to the numerical substructure to determine the interface loading applied to each other for the next step.

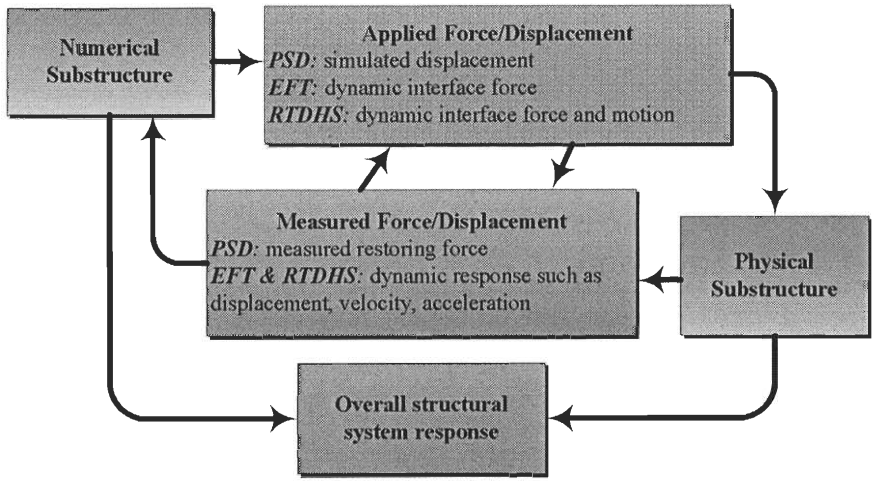

Figure 1.2. Hybrid Simulation

1.2 NEES-Soft Project

1.3 Project Description

In 1977, the United States Congress established The National Earthquake Hazards Reduction Program (NEHRP) to reduce the risks of life and property from future earthquakes in the United States through the establishment and maintenance of an effective earthquake hazards reduction program. Among the measures developed to reduce seismic risk, the NEHRP coordinated The George E. Brown, Jr. Network for Earthquake Engineering Simulation (NEES). NEES is a National Science Foundation funded organization of interdisciplinary research organizations collectively committed to the mitigation of seismic risk. The collaborative efforts of participants in the United States, as well as cross-continental partnerships consistently lead in advances in earthquake engineering simulation practices.

The Seismic Risk Reduction for Soft Story Woodframe Buildings (NEES-Soft) project is a NEES research project. A soft story is characterized as a story with large openings, such as those required for garage doors and commercial windows in a first-story used for parking or commercial spaces; and/or an open floor plan lacking partition walls. The lateral stiffness in a soft story is greatly reduced relative to upper stories and the building is prone to large lateral movements and even collapse during an earthquake. The objectives of NEES-Soft project are twofold; first, to design and experimentally validate performance based seismic retrofit options for soft story woodframe buildings, focusing on upper story effects. Second, the NEES-Soft project aims to provide fundamental understanding of collapse mechanisms in woodframe buildings through multiple seismic testing methods.

NEES-Soft is a collaborative project among five universities: Colorado State University (CSU), Clemson University (CU), Rensselaer Polytechnic Institute (RPI), Western Michigan University (WMU) and California Polytechnic State University. Retrofits have been designed and numerically modeled using a performance based seismic design method developed by Bahmani and van de Lindt at CSU (Bahmani and van de Lindt 2012) and utilizing energy dissipation devices proposed by Tian and Symans at RPI (2012). Numerical models of 3-D collapse mechanisms are being developed at CU (Pang and Shirazi 2012; Pang and Ziaei 2012). Hybrid simulation is proposed for testing the retrofit options as the relatively low cost of hybrid simulation allows testing multiple configurations without change the physical testing setup. Experimental protocol for hybrid simulation, such as control scheme and error compensations, is being developed in the Laboratory of Earthquake and Structural Simulation (LESS) at WMU (Shao 2012). The small and large scale hybrid simulations described in Chapters 4 and 5, respectively, will provide a basis for

developing the hybrid simulation control technique for the proposed experiments; they will be carried out at the large scale NEES structural testing laboratory at the State University of New York at Buffalo (UB-NEES).

1.4 NEES-Soft Hybrid Simulation

To develop a better understanding of the effects of soft story retrofits on upper stories, a PSD hybrid simulation of a full-scale, three-story wood-framed building at UB-NEES is proposed. The prototype building is representative of typical woodframe buildings in San Francisco constructed mid-20th century deemed structurally deficient due to a weak or soft story. A total of eight retrofits will be analytically modeled as numerical substructures. One physical substructure representing the remaining upper two stories will be constructed at full scale. Six servo-hydraulic actuators, two at each floor level, will slowly apply the translational and rotational simulated seismic responses to the physical substructure. The restoring force will be recorded and fed back to the numerical model, which calculates the displacement commands for the next step. PSD hybrid simulation controller with necessary compensations developed in this study will be implemented to ensure seamless integration with the real-time hybrid simulation controller at UB-NEES (Shao et al. 2011). Figure 1.3 illustrates the concept of the proposed PSD hybrid simulation.

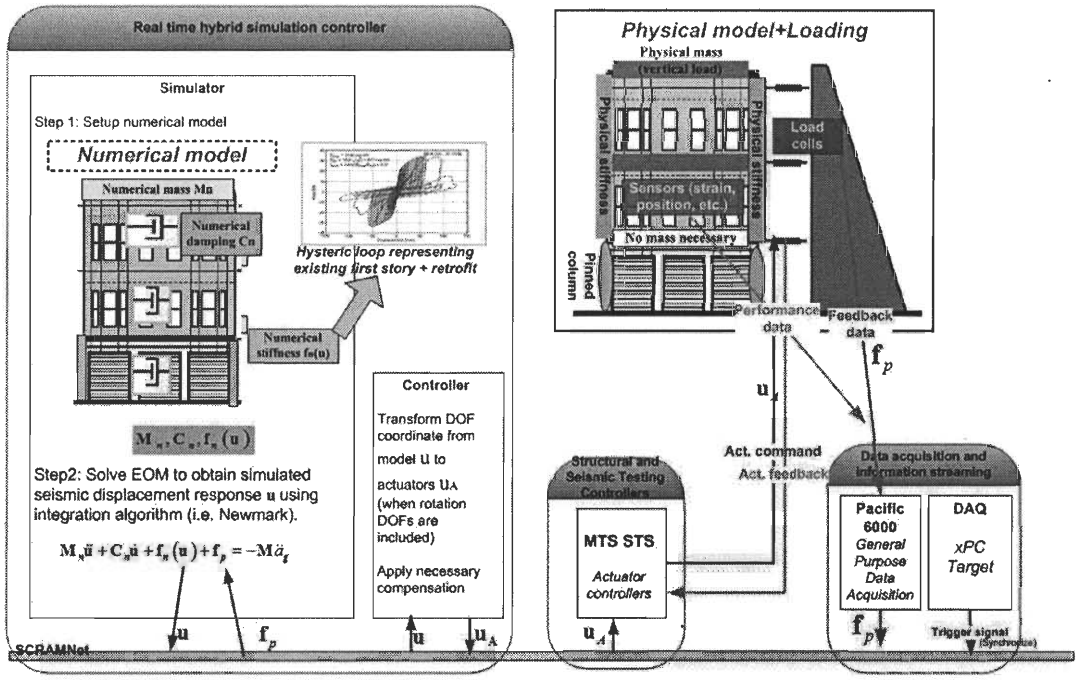

Figure 1.3. Conceptual Diagram of NEES-Soft PSD Hybrid Simulation

NEES-Soft is the first project conducting PSD hybrid simulation experiment utilizing a full scale woodframe building; knowledge gained in the experiment will be used as a basis for hybrid simulation in future wood specimen projects. The simulated dynamic response will be validated by direct comparison to the dynamic response obtained in a STT of a full-scale, four-story wood-framed building with selected retrofit(s) on the outdoor shake table at the NEES equipment site at University of California at San Diego.

1.5 Research Objectives and Scope

The main objective of this study is to develop the PSD hybrid simulation technique for benchmark and large scale experiments. Knowledge gained during this study will serve as a basis for developing the simulation technique for the NEES-Soft

project. Since, the NEES-Soft project is the first to adopt hybrid simulation for a wood specimen, the feasibility is verified herein. Developing the NEES-Soft control technique will be based on the series of PSD hybrid simulations conducted in this study. The secondary objective was to establish the state-of-the-practice of PSD hybrid simulation as it pertains to the NEESR sponsored projects.

As a relatively new practice, the experimental protocol of PSD hybrid simulation varies by laboratory and testing objectives. A detailed review of PSD hybrid simulation fundamentals provides a comprehensive understanding of the background theory including the formulation of dynamic analysis (equation of motion), substructure partitioning and numerical integration algorithms. Knowledge of various PSD hybrid simulation projects is essential when developing the simulation control scheme for an experiment. In this study, a review of literature available in the NEESR Project Warehouse establishes the state-of-the-practice in NEESR projects. A total of 22 projects adopting hybrid simulation are reviewed. Conclusions on the effect of the experimental specimen, numerical integration algorithm, compensation technique, and validation procedures are directly applied to the experiments conducted in this study.

To develop the initial PSD hybrid simulation control technique, a series of benchmark scale PSD hybrid simulations are conducted in the LESS facility at WMU. This part of the study explores methods of achieving a stable control scheme with accurate force feedback and compensation for error in the actuator command tracking. The dynamic response of a predictable specimen is simulated to empirically characterize the effect of control system performance on the accuracy and stability of the simulation. The control scheme is then adopted in a large scale PSD hybrid simulation of a wood shear wall specimen in a series of experiments conducted at the

University of Alabama (UA). This portion of the study investigates methods of addressing excessive vibration of the testing specimen and force measurement due to a higher performing control system and faster actuator.

1.6 Outline of Thesis

Chapter 2 provides an overview of the fundamentals of PSD hybrid simulation, followed by the establishment of the state-of-the-practice of its application in the NEESR projects in Chapter 3. The major components of the PSD hybrid simulation are introduced, including experimental equipment, physical and numerical substructuring and integration algorithms. Additionally real-time and geographically distributed applications are introduced as well as methods of validating experimental procedures and hybrid simulation results.

Chapters 4 and 5 are dedicated to the development of accurate, reliable and scalable PSD hybrid simulation techniques in two sets of experiments. First in Chapter 4, a series of benchmark scale PSD hybrid simulations are presented at LESS at WMU. Methods of slowing the loading rate, achieving accurate force measurement and compensating for actuator tracking error are discussed. Then in Chapter 5, a series of large scale PSD hybrid simulations are conducted at the newly constructed Structural Engineering Laboratory at UA. A method of ramping the loading commands, achieving accurate force measurement is discussed. This thesis is concluded in Chapter 6, with a summary of achievements and a brief discussion of future research needs for PSD hybrid simulation.

CHAPTER 2

PSEUDODYNAMIC HYBRID SIMULATION FUNDAMENTALS

2.1 Introduction

Earthquake experimentation is necessary for the safe design and evaluation of new and existing structures. Ideally an entire full scale prototype structure would be constructed in a laboratory to evaluate its dynamic response, a practice that is extremely expensive and infeasible. An increased demand for the realistic evaluation and performance based design of complex structures led to the development of pseudodynamic (PSD) hybrid simulation (Takanashi 1987, Nakashima et al. 1988, Nakashima 1990, Shing 1996). As discussed in Chapter 1, PSD simulation is a displacement-based hybrid simulation method during which inertia and viscous damping effects are simulated computationally employing a numerical model of the prototype structure. In this context, PSD hybrid simulation employs substructuring to addresses large scale testing requirements in civil engineering by dividing the structure under investigation into physical and numerical components. The physical substructure is an experimental model of the region of a structure critical to its restoring force and the numerical substructure is a computational model of the structure's mass, damping and the remainder of its stiffness properties. The numerical model and physical restoring force feedback are integrated to determine simulated displacement responses by solving the idealized structure's equation of motion (EOM) over small time increments time through a time-step integration procedure. Chapter 2 provides an overview of the fundamentals of PSD hybrid simulation.

2.2 Equation of Motion

When subjected to earthquake excitation, the effective external force acting on the structure is equal to mass times ground acceleration. This force is counteracted by the structure's inertial, elastic and energy dissipation properties. To characterize dynamic behavior, a structure is idealized into a three part system with mass (inertial) component, stiffness (elastic) component and damping (energy dissipation) components. Elastic and energy dissipation properties are related to the displacement and velocity of the system, respectively. According to Newton's second law of motion, at any instant of time the deformation of the idealized MDOF structure is governed by the following second order differential equation known as the EOM:

$$[m]\{\ddot{u}\}+[c]\{\dot{u}\}+[k]\{u\}=[p] \qquad 2.1$$

Where $[m]$, $[c]$, $[k]$ and $[p]$ are the mass, damping , stiffness and external excitation matrices, respectively. The acceleration, velocity and displacement vectors of the structure relative to the ground are represented as $\{\ddot{u}\}$, $\{\dot{u}\}$ and $\{u\}$, respectively. External excitation is equal to the mass times the earthquake ground acceleration, vector $\{\ddot{u}_g\}$. For a nonlinear structure, the stiffness component $[k]\{u\}$ is replaced with the restoring force, $[f_s]$ and the EOM becomes:

$$[m]\{\ddot{u}\}+[c]\{\dot{u}\}+[f_s]=[p] \qquad 2.2$$

2.3 Substructuring

Structural dynamic response to severe earthquake excitation often exhibits nonlinear behavior. Due to the resulting uncertainties in structural displacement-response force relationship, analytically modeling its dynamic behavior is not reliable. Unpredictable nonlinear dynamic response can often be attributed to the displacement-force relation of a localized critical subassembly within the whole structure. The implementation of PSD hybrid simulation is based on the practice that is widely used in finite element analysis: a complex structure can be divided into several components, known as substructures. Individual substructures can be analyzed separately and combined through predefined laws to obtain the results of the whole structural system. When this practice is introduced into PSD simulation, the structure under investigation is partitioned into one or more numerical and physical substructures (Takanashi and Nakashima 1987). Substructuring in PSD hybrid simulation addresses capacity limitations of large scale experimentation without degrading the accuracy of the results, as is usually seen in scaled experiments (Dermitzakis 1986). Introducing a numerical component greatly increases the versatility and decreases the cost of implementing PSD hybrid simulation when compared to traditional seismic testing methods involving the whole structure models such as those used in shake table test (STT). Additionally, stability concerns that arise in PSD simulation with multiple physical DOFs, discussed in the following section, are addressed by substructuring.

The physical substructure is an experimental model of the isolated critical subassembly from which the restoring force of at least one DOF is measured. A physical specimen as close to prototype size as possible is ideal as structural behavior

does not scale accurately (Nakashima 2001; Kumar et al. 1997). The inertial and energy dissipation forces of the entire prototype structure are computationally modeled in a numerical substructure. Additionally, the restoring force of the remaining DOFs is modeled in the numerical substructure.

The numerical substructure is formed by idealizing the prototype structure as a subassemblage of elements, forming a series of interconnected nodes. The displacements at each node are a DOF and are generally considered to be in a planar two dimensional frame. The tributary mass of the prototype structure is idealized as a lumped mass distributed at each node. For a nonlinear structure, a hysteretic model determines the restoring force of the numerical specimen with respect to its displacement even after yield displacement has been reached. In the case that the numerical substructure's hysteretic characteristics have not been adequately studied, the analytical model is generally calibrated experimentally by a cyclic test. Equation 2.3 is the EOM to be solved during a PSD hybrid simulation of a structure with $\boldsymbol{n}$ numerical and $\boldsymbol{p}$ physical DOFs, denoted by the subscripts n and p. The physical and numerical restoring forces are denoted $f_{s,p}$ and $f_{s,n}$, respectively. Note that the mass and damping coefficient matrices and external excitation vector are completely numerical for all DOFs.

$$\begin{bmatrix} m_n & 0 \\ 0 & m_p \end{bmatrix} \begin{Bmatrix} \ddot{u}_n \\ \ddot{u}_p \end{Bmatrix} + \begin{bmatrix} c_{nn} & c_{np} \\ c_{pn} & c_{pp} \end{bmatrix} \begin{Bmatrix} \dot{u}_n \\ \dot{u}_p \end{Bmatrix} + \begin{bmatrix} f_{s,n} \\ f_{s,p} \end{bmatrix} = \begin{bmatrix} p_n \\ p_p \end{bmatrix} \qquad 2.3$$

The modal mass(es) and damping influence coefficients of the physical DOFs $\left[\boldsymbol{m}_p\right]$ and $\left[\boldsymbol{c}_p\right]$ the numerical DOFs $\left[\boldsymbol{m}_n\right]$ and $\left[\boldsymbol{c}_n\right]$, respectively, and diagonal damping influence coefficients $\left[c_{np}\right]$ and $\left[c_{pn}\right]$ are numerical for all DOFs. In a substructured PSD hybrid simulation, the physical restoring forces $\left\{f_{s,p}\right\}$ are

measured from the physical substructure and combined with the numerical restoring force $\{f_{s,n}\}$ to form the overall restoring force vector. The restoring force vector is then used in the calculation of the displacement response of the next step. Unlike linear system described in Equations 2.1, 2.2 and 2.3 describe the dynamic equilibrium of nonlinear system and does not contain a displacement component. A time stepping numerical integration is adopted during which the restoring force vector is replaced with the product of secant stiffness and the displacement vector of the current step to solve the displacement, this procedure is described in details in Section 2.4.2. Once the displacement responses are solved, the ones related to the DOFs of the physical substructure are applied to the specimen and the restoring forces are again measured.

In this study, a two story shear frame building is idealized as a two DOF system, one physical and one numerical. The overall dynamic response is obtained through PSD hybrid simulation. The physical substructure is the second story in the experiment described Chapter 4, and the first story in Chapter 5. The prototype mass, viscous damping and the displacement-force response from a predefined hysteresis of the numerical DOF are the numerical substructure. The formulation of the numerical substructure for each model is presented in each chapter, respectively.

2.4 Numerical Integration Algorithms

When using an integration step method to solve the EOM of the nonlinear structure, the incremental forms of Equations 2.2 is adopted as shown below:

$$[m]\{\Delta\ddot{u}\}_i + [c]\{\Delta\dot{u}\}_i + [\Delta f_s]_i = [\Delta p]_i \qquad 2.4$$

Where $\{\Delta\ddot{u}\}_i$, $\{\Delta\dot{u}\}_i$, $[\Delta f_s]_i$ and $[\Delta p]_i$ are the incremental acceleration, velocity, restoring force and external excitation vectors, respectively. Several numerical integration algorithms are available, both explicit and implicit, with two main challenges: stability and accuracy. Explicit algorithms calculate structural response for the next time step based on response of the current step. Implicit algorithms' calculation of the structural response of the next time step requires information from both the current and the next time steps. A family of integration algorithms, known collectively as the Newmark method (1959) is an example of such integration algorithm. Newmark method is commonly adopted in PSD hybrid simulation and was also adopted in this study. Therefore a detailed discussion of this method is described below. Equations 2.5 and 2.6 shows the incremental velocity and displacement vectors approximated in the Newmark method.

$$\{\Delta\dot{u}\}_i = \Delta t\left[(1-\gamma)\{\ddot{u}\}_i + \gamma\{\ddot{u}\}_{i+1}\right] \qquad 2.5$$

$$\{\Delta u\}_i = \Delta t\{\dot{u}\}_i + \Delta t^2\left[\left(\frac{1}{2}-\beta\right)\{\ddot{u}\}_i + \beta\{\ddot{u}\}_{i+1}\right] \qquad 2.6$$

Where $\{\ddot{u}\}_{i+1}$ the acceleration vector from the next time is step and Δt is the time step in seconds. The parameter β is defined based on the assumed variation of acceleration over each time step. For average acceleration approximation, $\beta = \frac{1}{4}$ and for linear acceleration approximation, $\beta = \frac{1}{6}$. Typically $\gamma = \frac{1}{2}$. When $\gamma > \frac{1}{2}$ positive numerical damping is added, when $\gamma < \frac{1}{2}$ negative numerical damping is added to the numerical substructure (Carrion and Spencer 2007). Equation 2.6 can be rewritten for incremental acceleration vector $\{\Delta\ddot{u}\}_i$ as:

$$\{\Delta\ddot{u}\}_i = \frac{1}{\beta\Delta t^2}\{\Delta u\}_i - \frac{1}{\beta\Delta t}\{\dot{u}\}_i - \frac{1}{2\beta}\{\ddot{u}\}_i \qquad 2.7$$

Equations 2.5 and 2.6 are combined with Equation 2.4 to calculate the displacement, velocity and acceleration of the next time step. Newmark methods with average and linear acceleration approximations are more accurate than the explicit version; however, since $\beta \neq 0$, calculating displacement of the next step is implicit as it depends on the acceleration of the next step, which is unknown at current step. In purely numerical simulation, iterations within each step can be implemented to obtain updating secant stiffness and displacement increment that will satisfy the equilibrium condition of both the current step and the next step as discussed in the next section. However, iterations are not applicable in PSD hybrid simulation involving physical simulation as they can lead to spurious loading cycles on the physical specimen. In this case, either an explicit format or a modified implicit format is used that are discussed in sections 2.4.3 and 2.4.4 respectively.

2.5 Integration Algorithm for Numerical Simulation

To solve Equation 2.4 implicitly using the Newmark method, the restoring force vector is replaced with a secant stiffness vector that is being updated at each time step and solved using an iterative procedure. The following steps are used a purely numerical simulation as an illustration.

Substitute Equation 2.7 into 2.5 for the incremental velocity:

$$\{\Delta\dot{u}\}_i = \frac{\gamma}{\beta\Delta t}\{\Delta u\}_i - \frac{\gamma}{\beta}\{\dot{u}\}_i + \Delta t\left(1 - \frac{\gamma}{2\beta}\right)\{\ddot{u}\}_i \qquad 2.8$$

The incremental restoring force vector in Equation 2.4 is reasonably approximated to the product of secant stiffness (k_{sec}) matrix and incremental displacement of that time step due to small time step:

$$\left[\Delta f_s\right]_i = \left[k_{\text{sec}}\right]_i \left\{\Delta u\right\}_i \qquad 2.9$$

Equation 2.9 is still implicit; the secant stiffness matrix at each time step is formulated from the displacement and restoring force of both the current and next time step. The displacement of the next step and the secant stiffness needs to be determined simultaneously as illustrated in Figure 2.1.

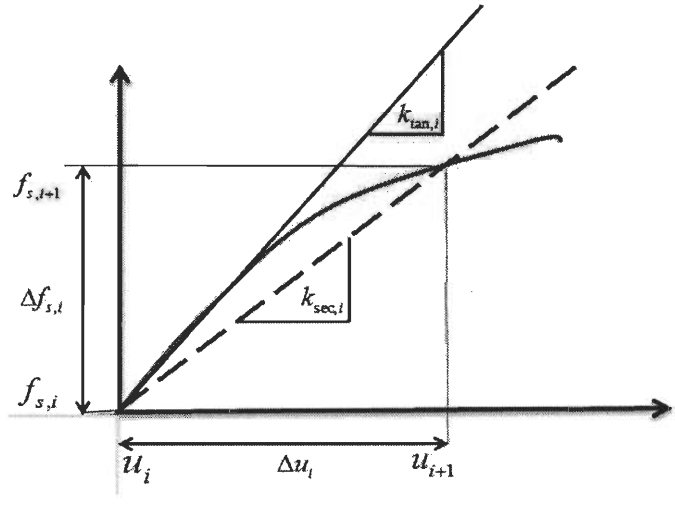

Figure 2.1. Secant and Tangent Stiffness Determination

Therefore a further approximation of the secant stiffness is adopted in numerical simulation. Assuming that over a small time interval, the secant stiffness (k_{sec}) is equal to the tangent stiffness (k_T).

$$\left[\Delta f_s\right]_i \cong \left[k_T\right]_i \left\{\Delta u\right\}_i \qquad 2.10$$

An iterative-corrective procedure, such as the Newton-Raphson procedure (Lindstrom 1988), can be employed within each time step to determine the tangent

stiffness component(s), k_T at each time step. Figure 2.2 shows three Newton Raphson iterations, noted in the superscript, within a single time step as described by Chopra (2007).

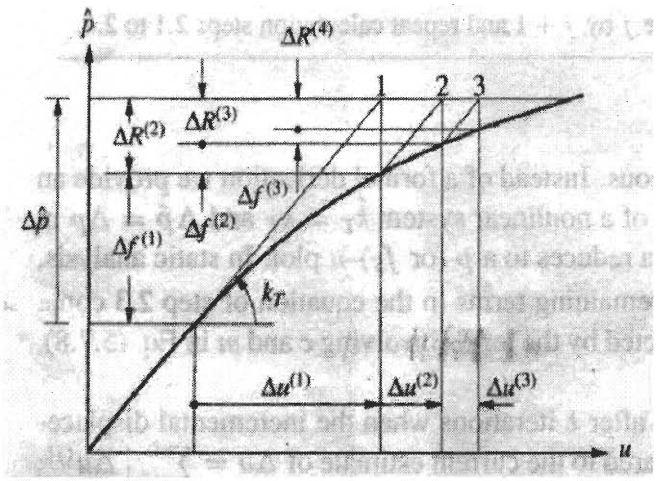

Figure 2.2. Newton Raphson Iteration within Time Step for Nonlinear System

For each Newton-Raphson iteration, j, $\Delta u^{(j)}$ is the incremental displacement associated with the true incremental force, $\Delta f^{(j)}$, which is less than $\Delta \hat{p}$, calculated in Equation 2.11 from the inertial, damping and external forces. The residual force, $\Delta R^{(j)}$ is defined as the difference between $\Delta f^{(j)}$ and $\Delta \hat{p}$. The additional displacement, $\Delta u^{(j+1)}$ due to the residual force is calculated:

$$k_T \Delta u^{(j+1)} = \Delta R^{j+1} = \Delta \hat{p} - \Delta f^{j} \qquad 2.11$$

This process is continued until convergence is achieved and the final tangent stiffness value(s) are used to formulate the stiffness matrix in Equation 2.10. Substitute Equation 2.10 into Equation 2.4 and eliminate the 'T' subscript for simple presentation:

$$[m]\{\Delta \ddot{u}\}_i + [c]\{\Delta \dot{u}\}_i + [k]_i \{\Delta u\}_i = [\Delta p]_i \qquad 2.12$$

Substitute Equations 2.7 and 2.8 into 2.1 and $\{\Delta u\}_i$ can be determined from:

$$\left[\frac{1}{\beta\Delta t^2}[m]+\frac{\lambda}{\beta\Delta t^2}[c]+[k]_i\right]\{\Delta u\}_i = [p]+\left[\frac{1}{\beta\Delta t^2}[m]+\frac{\lambda}{\beta\Delta t^2}[c]\right]\{\Delta\dot{u}\}_i+\left(\frac{1}{2\beta}[m]-[c]\Delta t\left(1-\frac{\gamma}{2\beta}\right)\right)\{\ddot{u}\}_i \quad 2.13$$

To minimize step calculations, constants are calculated in advance. The following equations show the initial calculations and the step-by-step procedure to determine structural response using the implicit Newmark integration algorithm as follows.

Table 2.1. Procedure for Newmark Integration for Numerical Simulation

2.1.0 Initial calculations

2.1.1 $$k_{C1}=\frac{1}{\beta\Delta t^2}[m],\ k_{C2}=\frac{\gamma}{\beta\Delta t}$$

2.1.2 $$dp_{C1}=\frac{1}{\beta\Delta t}[m],\ dp_{C2}=\frac{\gamma}{\beta}[c],\ dp_{C3}=\frac{1}{2\beta}[m],$$

2.1.3 $$dp_{C4}=\Delta t\left[\frac{\gamma}{2\beta}-1\right][c]$$

2.1.4 $$v_{C1}=\frac{\gamma}{\beta\Delta t},\ v_{C2}=\frac{\gamma}{\beta},\ v_{C3}=\Delta t\left[1-\frac{\gamma}{2\beta}\right]$$

2.1.5 $$a_{C1}=\frac{1}{\beta\Delta t^2},\ a_{C2}=\frac{1}{\beta\Delta t},\ a_{C3}=\frac{1}{2\beta}$$

Calculations for each step (*i=1:n*):

2.1.6 $$[\Delta\hat{p}]_i=[\Delta p]_i+[dp_{C1}+dp_{C2}]\{\ddot{u}\}_i+[dp_{C3}+dp_{C4}]\{\ddot{u}\}_i$$

Solve for the tangent stiffness $[k]_i$ using iteration

2.1.7 $$\left[\hat{k}\right]_i = [k]_i + [k_{C1}] + k_{C2}[c]$$

2.1.8 $$\{\Delta u\}_i = \left[\hat{k}\right]_i^{-1} [\Delta \hat{p}]_i$$

2.1.9 $$\{\Delta \dot{u}\}_i = v_{C1}\{\Delta u\}_i - v_{C2}\{\dot{u}\}_i + v_{C3}\{\ddot{u}\}_i$$

2.1.10 $$\{\Delta \ddot{u}\}_i = a_{C1}\{\Delta u\}_i - a_{C2}\{\dot{u}\}_i - a_{C3}\{\ddot{u}\}_i$$

2.1.11 $$\{u\}_{i+1} = \{\Delta u\}_i + \{u\}_i ; \{\dot{u}\}_{i+1} = \{\Delta \dot{u}\}_i + \{\dot{u}\}_i ; \{\ddot{u}\}_{i+1} = \{\Delta \ddot{u}\}_i + \{\ddot{u}\}_i$$

2.6 Integration for PSD Hybrid Simulation

2.6.1 Explicit Algorithm

As previously stated, the iterative versions of implicit algorithms are not suitable for experiments with a physical specimen, as is the case with PSD hybrid simulation. Early PSD hybrid simulation adopted explicit forms of the Newmark and the explicit central difference methods. In the explicit Newmark integration algorithm, no knowledge of the updated stiffness matrix is required. Except for the initial stiffness of the physical substructure that is usually estimated from the cyclic test and used to obtain the displacement response of the first step. When applying this first step displacement through actuator, the restoring force measurement of the first is yielded and the integration stepping continues without stiffness calculation (Shing 2006). Setting $\gamma = \frac{1}{2}$ and $\beta = 0$ eliminates the $\{\ddot{u}\}_{i+1}$ from Equation 2.5, the incremental displacement becomes:

$$\{\Delta u\}_i = \Delta t\{\dot{u}\}_i + \frac{\Delta t^2}{2}\{\ddot{u}\}_i \qquad 2.14$$

After the displacement has been applied to the specimen, the restoring force is measured and the acceleration for the next time step is calculated at the end of the current time step to satisfy dynamic equilibrium. Substitute 2.14 into 2.4 for acceleration of the next time step:

$$\{\ddot{u}\}_{i+1} = \left[\frac{\Delta t}{2}[c]+[m]\right]^{-1}\left[[p]_{i+1}-[f_s]_{i+1}-[c]\left[\{\dot{u}\}_i+\frac{\Delta t}{2}\{\ddot{u}\}_i\right]\right] \qquad 2.15$$

Velocity of the next time step is then solved from the non-incremental form of Equation 2.8:

$$\{\dot{u}\}_{i+1} = \{\dot{u}\}_i + \frac{\Delta t}{2}\left[\{\ddot{u}\}_i + \{\ddot{u}\}_{i+1}\right] \qquad 2.16$$

Most explicit algorithms are conditionally stable; the size of the time step must be smaller than a critical value, known as the stability limit, for the test to remain stable. The stability limit is governed by the structure's highest natural frequency. Stability of the explicit Newmark method is governed by Equation 2.17.

$$\Delta t \ll \frac{2}{\omega_{\max}} \qquad 2.17$$

Due to conditional stability, explicit algorithms cannot be used with infinitely stiff structures and are impractical for simulations with many physical DOFs, as they often exhibit high natural frequencies.

2.6.2 Implicit Algorithm

Alternative to explicit algorithms, implicit algorithms are ideal for structures having high stiffness or several physical degrees of freedom. To overcome the aforementioned difficulties when implementing implicit algorithm in PSD hybrid simulation, implicit methods are modified to limit or eliminate iterations. Four implicit algorithms modified to be suitable for PSD hybrid simulation are discussed in

the following section; implicit Newmark integration algorithm modified for this study is presented below.

Implicit schemes with iteration using sub-step feedback limit the number of iterations for each time step. The implicit Hilber-Hughes-Taylor alpha method (HHT α-method) accounts for nonlinear behavior in a structure by an iterative solution procedure; it is unconditionally stable for linearly elastic structures and introduces controllable numerical damping at higher frequencies. Numerical damping suppresses the excitation of higher modes due to experimental errors propagating within the numerical solutions, as they are more pronounced at higher modes (Shing and Mahin 1983). Shing (2004) modified the HHT α-method with a set number of iterations for RT-PSD simulations, reducing the computational delay introduced by iterations. Chen and Ricles (2012) proposed another modified version of the HHT α-method for improved stability for nonlinear specimens and real time testing. The proposed method incorporates a technique that bases the predicted restoring force on the end of the time-step instead of the prior sub step.

Another way to implement implicit algorithm in PSD hybrid simulation is to introduce predictor-corrector schemes to eliminate iterations all together. Predictor-corrector methods are implicit schemes modified to not require iteration within each time. The operator-splitting (OS) method, combining linearly implicit and non-linearly explicit schemes, provides explicit target displacement and unconditional stability in slow PSD hybrid simulation (Nakashima 1990). It assumes that the difference between the elastic and nonlinear restoring forces at the predicted displacement and target displacement are approximately equal. The target velocity calculated in the OS method is implicit, therefore it still presents stability concerns for RT-PSD hybrid simulations. To provide unconditional stability for RT-PSD hybrid

simulation, the OS method was modified, named OS-RST, by formulating an explicit target velocity based on the difference of predicted displacements. This method was proven unconditionally stable for specimens with softening behavior (Wu et al. 2006). Alternatively Combescure and Pegon (1997) proposed the α-operator splitting (α-OS) for specimens displaying stiffening behavior. The α-OS method combines the Newmark α-method with the OS method and is ideal for specimens not experiencing high stiffness degradation and its accuracy is dependent on predicted stiffness.

In this study, an implicit Newmark integration algorithm was adopted, modified with stiffness components, to replace iterations required in purely numerical simulation. This method greatly improves the overall accuracy of the hybrid simulation, especially with a highly nonlinear specimen (Mehdi 2007). Recalling Equation 2.3, the following equations show the step-by-step procedure for the general PSD hybrid simulation of a structural system with ***n*** numerical and ***p*** physical DOFs. In a PSD hybrid simulation with a numerical and physical substructure, the restoring force is split into a physical, $\left[f_{s,p}\right]_i$ and numerical component, $\left[f_{s,n}\right]_i$ for the physical DOF, p and numerical DOF, n. Similar to Equation 2.4, an incremental form of Equation 2.3 with the substructural partition is shown:

$$\begin{bmatrix} m_n & 0 \\ 0 & m_p \end{bmatrix} \begin{Bmatrix} \Delta\ddot{u}_n \\ \Delta\ddot{u}_p \end{Bmatrix}_i + \begin{bmatrix} c_{nn} & c_{np} \\ c_{pn} & c_{pp} \end{bmatrix} \begin{Bmatrix} \Delta\dot{u}_n \\ \Delta\dot{u}_p \end{Bmatrix}_i + \begin{bmatrix} \Delta f_{s,n} \\ \Delta f_{s,p} \end{bmatrix}_i = \begin{bmatrix} \Delta p_n \\ \Delta p_p \end{bmatrix}_i \qquad 2.18$$

As noted in Section 2.3, Equation 2.18 must be modified to obtain an incremental displacement vector, comprised of the numerical and physical displacements, $\{\Delta u_n\}_i$ and $\{\Delta u_p\}_i$, respectively. In this study, the updating tangent stiffness is adopted to provide reasonable approximation of the displacement

increment corresponding to the restoring force term that is necessary for the PSD hybrid simulation

The tangent stiffness of each DOF is determined at the end of each time step during the hybrid simulation from the incremental restoring force and the incremental displacement vectors. As discussed in Section 2.5, this is based on the assumption that the secant stiffness is approximately equal to the tangent stiffness of the previous step over a short increment of time (Equation 2.10). The estimated tangent stiffness component ('tan' subscript is eliminated for simple presentation) :

$$k_{nn,i+1} = \frac{\Delta f_{s,n_i}}{\Delta u_{n,i}}, k_{pp,i+1} = \frac{\Delta f_{s,p,i}}{\Delta u_{p,i}} \qquad 2.19$$

Where $k_{nn,i+1}$ and $k_{pp,i+1}$ are the stiffness component(s), of the next time step *i+1,* relating to the numerical restoring force and the numerical displacements and the physical restoring force and physical displacements, respectively; these components comprise the diagonal terms of the stiffness matrix. Note that the incremental displacement of each DOF is relative to the other DOFs based on the geometry of the specimen and the actuator coordinate system. The stiffness matrix is formulated for the prototype structure with respect the geometry and configuration of structural elements such as the beams, columns and floor diaphragms and the structural material. The off diagonal terms of the stiffness matrix, relating the physical restoring force and numerical displacements and vice versa, $k_{np,i+1}$ and $k_{pn,i+1}$, respectively, are calculated based on the diagonal terms. To correct for error associated with inaccurate stiffness approximation, acceleration is calculated for the next time step after the target displacement has been applied to the specimen (Equation 2.2.4) using the EOM

consisting of the velocity, displacement of the current step and the measured restoring force to ensure dynamic equilibrium.

To minimize step calculations constants are calculated before the hybrid simulation. The following shows the initial calculations and the step-by-step procedure of the implicit Newmark integration algorithm used in this study:

Table 2.2. Procedure for Newmark Integration for Hybrid Simulation

2.2.0 Initial calculations:

2.2.1 $$\begin{bmatrix} k_{C1,n} & 0 \\ 0 & k_{C1,p} \end{bmatrix} = \frac{1}{\beta \Delta t^2}\begin{bmatrix} m_n & 0 \\ 0 & m_p \end{bmatrix}; \begin{bmatrix} k_{C2,nn} & k_{C2,np} \\ k_{C2,pn} & k_{C2,pp} \end{bmatrix} = \frac{\gamma}{\beta \Delta t}\begin{bmatrix} c_{nn} & c_{np} \\ c_{pn} & c_{pp} \end{bmatrix}$$

2.2.2 $$\begin{bmatrix} dp_{C1,n} & 0 \\ 0 & dp_{C1,p} \end{bmatrix} = \frac{1}{\beta \Delta t}\begin{bmatrix} m_n & 0 \\ 0 & m_p \end{bmatrix}; \begin{bmatrix} dp_{C2,nn} & dp_{C2,np} \\ dp_{C2,pn} & dp_{C2,pp} \end{bmatrix} = \frac{\gamma}{\beta}\begin{bmatrix} c_{nn} & c_{np} \\ c_{pn} & c_{pp} \end{bmatrix}$$

$$\begin{bmatrix} dp_{C3,n} & 0 \\ 0 & dp_{C3,p} \end{bmatrix} = \frac{1}{2\beta}\begin{bmatrix} m_n & 0 \\ 0 & m_p \end{bmatrix}; \begin{bmatrix} dp_{C4,nn} & dp_{C4,np} \\ dp_{C4,pn} & dp_{C4,pp} \end{bmatrix} = \Delta t\left[\frac{\gamma}{2\beta} - 1\right]\begin{bmatrix} c_{nn} & c_{np} \\ c_{pn} & c_{pp} \end{bmatrix}$$

2.2.3 $$v_{C1} = \frac{\gamma}{\beta \Delta t},\ v_{C2} = \frac{\gamma}{\beta},\ v_{C3} = \Delta t\left[1 - \frac{\gamma}{2\beta}\right]$$

Calculations for each step ($i=1:n$):

2.2.4 $$\begin{bmatrix} \Delta \hat{p}_n \\ \Delta \hat{p}_p \end{bmatrix}_i = \begin{bmatrix} \Delta p_n \\ \Delta p_p \end{bmatrix}_i + \left[\begin{bmatrix} dp_{C1,n} & 0 \\ 0 & dp_{C1,p} \end{bmatrix} + \begin{bmatrix} dp_{C2,nn} & dp_{C2,np} \\ dp_{C2,pn} & dp_{C2,pp} \end{bmatrix}\right]\begin{Bmatrix} \dot{u}_n \\ \dot{u}_p \end{Bmatrix}_i + \cdots$$
$$\left[\begin{bmatrix} dp_{C3,n} & 0 \\ 0 & dp_{C3,p} \end{bmatrix} + \begin{bmatrix} dp_{C4,nn} & dp_{C4,np} \\ dp_{C4,pn} & dp_{C4,pp} \end{bmatrix}\right]\begin{Bmatrix} \ddot{u}_n \\ \ddot{u}_p \end{Bmatrix}_i$$

2.2.5 $$\begin{bmatrix} \hat{k}_{nn} & \hat{k}_{np} \\ \hat{k}_{pn} & \hat{k}_{pp} \end{bmatrix}_i = \begin{bmatrix} k_{nn} & k_{np} \\ k_{pn} & k_{pp} \end{bmatrix}_i + \begin{bmatrix} k_{C1,n} & 0 \\ 0 & k_{C1,p} \end{bmatrix} + \begin{bmatrix} k_{C2,nn} & k_{C2,np} \\ k_{C2,pn} & k_{C2,pp} \end{bmatrix}$$

2.2.6 $$\begin{Bmatrix} \Delta u_n \\ \Delta u_p \end{Bmatrix}_i = \begin{bmatrix} \hat{k}_{nn} & \hat{k}_{np} \\ \hat{k}_{pn} & \hat{k}_{pp} \end{bmatrix}_i^{-1}\begin{bmatrix} \Delta \hat{p}_n \\ \Delta \hat{p}_p \end{bmatrix}_i$$

Displacement of physical DOFs , $\{\Delta u_p\}_i$ is imposed on the physical

2.2.7 specimen: $\begin{Bmatrix} \ddot{u}_n \\ \ddot{u}_p \end{Bmatrix}_{i+1} = \begin{bmatrix} m_n & 0 \\ 0 & m_p \end{bmatrix}^{-1} \left[\begin{bmatrix} p_n \\ p_p \end{bmatrix}_{i+1} - \begin{bmatrix} f_{s,n} \\ f_{s,p} \end{bmatrix}_{i+1} - \begin{bmatrix} c_{nn} & c_{np} \\ c_{pn} & c_{pp} \end{bmatrix} \begin{Bmatrix} \dot{u}_n \\ \dot{u}_p \end{Bmatrix}_{i+1} \right]$

2.2.8 $k_{n,i+1} = \dfrac{\Delta f_{s,n_{i}}}{\Delta u_{n,i}}, k_{p,i+1} = \dfrac{\Delta f_{s,p,i}}{\Delta u_{p,i}}$

2.2.9 Formulate the modal stiffness matrix of the prototype specimen: $\begin{bmatrix} k_{nn} & k_{np} \\ k_{pn} & k_{pp} \end{bmatrix}_{i+1}$

2.2.10 $\{u\}_{i+1} = \{\Delta u\}_i + \{u\}_i ; \{\dot{u}\}_{i+1} = \{\Delta \dot{u}\}_i + \{\dot{u}\}_i$

2.7 Experimental Equipment

Specific experimental equipment is needed for conducting PSD hybrid simulation. Hydraulic actuators with the associated hydraulic controller are required to apply the step-by-step simulated displacement responses on the physical specimen during PSD hybrid simulation. For slow rate simulation, a static actuator is appropriate while a dynamic actuator is necessary for faster loading rates of real-time simulation. The actuator is mounted against a reaction wall / frame, which must be much stronger (i.e. stiffer) than the physical specimen so that it will not introduce undesired deformations to the test structure. The data acquisition (DAQ) hardware provides force and displacement feedback via load cells and linear variable displacement transducers (LVDTs), respectively. Displacement commands are generated in a hybrid testing controller which feeds the measured responses of the physical system from the DAQ hardware to the numerical models and runs the numerical simulation. Additionally, discrepancies between the command and the feedback displacements are monitored and compensated accordingly in the hybrid testing controller. As an example, the schematic of the LESS equipment that is

capable of conducting PSD hybrid simulation is illustrated in Figure 2.3 ; specific details of the equipment used in this study are discussed in Chapter 4.

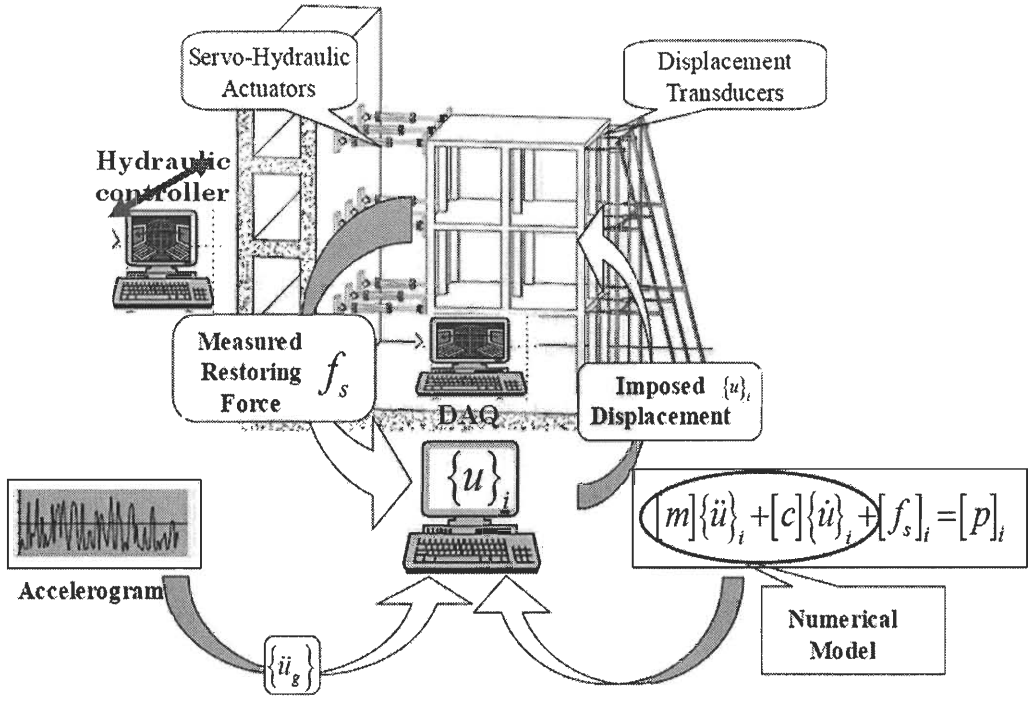

Figure 2.3. General Requirements for PSD Hybrid Simulation

2.8 Real-Time PSD Hybrid Simulation

When subject to earthquake excitation, structure's performance is greatly dependent on energy dissipation through its inherent damping and/or additional damping provided by specially designed and installed devices. Seismic response mitigation devices, such as magneto-rheological (MR) dampers and base isolations, show potential for reducing the threat to life and property posed by large earthquake excitations. Structural systems installed with such devices exhibit rate-dependent behavior that cannot be accurately evaluated using the conventional (slow) PSD testing. Therefore RT-PSD simulation becomes imperative for these structures. Early

RT-PSD hybrid simulation was attempted on a small scale specimen by Darby (1999) and Darby et al. (2001). Later on large scale specimen and testing equipment were used in the development of RT-PSD hybrid simulation (Chen et al. 2009). Stability and accuracy issues arise in RT-PSD hybrid simulation when delay is introduced into the hybrid control system. This delay is attributed to computational time of the numerical integration and communication time of the data acquisition system and most of all, inherent latency of the hydraulic actuator. Horiuchi et al. (1999,2001) noted that actuator delay increases total energy of system, resulting in negative damping. If negative damping is greater than inherent structural damping, the RT hybrid simulation system becomes unstable. Integration algorithms were modified for stability in real-time simulations and are discussed in Section 2.4. Additionally, methods of achieving more accurate actuator control, and control compensation based on adaptive and predictive control theory have been explored to address delay errors.

One way to compensate time delay is to predict the displacement of the actuator after the delay, equal to one time step by polynomial extrapolation (Horiuchi et al. 1999) and then a linear acceleration assumption (Horiuchi et al. 2001). Actuator delay compensations were also developed based on virtual coupling and the Smith predictor; both require an accurate estimation of delay value in the RT testing system. When highly nonlinear behavior and large dynamic responses are expected in the physical specimen, virtual coupling improves the real time system stability by connecting the numerical and physical models via a parallel virtual spring-damper model. The virtual spring set so that with the maximum physical force, the virtual spring displacement is less than the quantified displacement error present in the actuator (Lin 2010). The Smith predictor method (Smith 1959) employs an estimated model of the physical setup to predict its delayed behavior and compensates for such

in the controller. Smith's predictor method addressed communication delay in distributed RT-PSD (Christenson et al. 2008) and real time dynamic hybrid simulations to accommodate control delay in the structure actuator and shake table (Reinhorn et al. 2004; Shao et al. 2011).

Compensation based on adaptive control theory minimizes the effect of variable control delay. Darby (1999) developed a procedure which estimated actuator delay based on polynomial extraction, assuming delay is constant equal to or greater than the integration time step, Δt (Darby 1999). Ahmadizadeh (2008) incorporated this method into a linear acceleration extrapolation, addressing variability in actuator delay (Ahmadizadeh et al. 2008). An inverse compensation method (Chen et al. 2008) assumes that the actuator reaches a command displacement at $\alpha\delta t$ where α is greater than 1.0 when actuator delay is present and δt is a substep, j , of the integration step, i . The actuator is assumed to reach the measured displacement of the next time step, $(i+1)$ at the end of the $(j-1)$ substep:

$$d_{i+1}^{m(j)} = d_{i+1}^{m(j-1)} + \frac{1}{\alpha}\cdot\left(d_{i+1}^{c(j)} - d_{i+1}^{m(j-1)}\right) \qquad 2.20$$

The inverse of the discrete z- transform of Equation 2.20 sends the predicted displacement associated with the actuator delay to the controller to compensate for delay. To accommodate for errors due to inaccurately estimated time delay, Chen and Ricles (2009) introduced an estimated actuator delay, α and an evolutionary variable, $\Delta\alpha$ as an error tracking indicator to the inverse compensation method, in an adaptive inverse compensation method.

2.9 Geographical Distributed Simulation

PSD hybrid simulation of complex structures such as multi-span bridges has several components that are unique in their dynamic behavior. The large scale physical substructures cannot feasibly be loaded in a single laboratory as simulating such a structure requires different experimental equipment, and simultaneous loading of each substructure. In geographically distributed hybrid simulation, numerical and physical substructures located in multiple laboratories are integrated and simulated in a single experimental procedure. Robust internet communication and flexible software are fundamental to distributed simulation to quickly communicate essential information for a seamless execution of PSD hybrid simulations. The information being transferred in between laboratories includes test initialization, stiffness estimation, integration parameters and loading commands. To load both numerical and physical substructures pseudo-dynamically at multiple sites, the University of Illinois Simulation Coordinator (UI-SimCor) was developed at University of Illinois, Urbana-Champagne (UIUC) (Kwon et al. 2005). Schellenberg et al. (2007) developed Open source framework for experimental setup and control (OpenFresco) at University of California, Berkeley as a middleware to standardize the deployment of PSD hybrid simulation. It is capable of linking many common simulations software such as Matlab /Simulink, Abacus and UI-Simcor with DAQ and control systems of the physical setup. Additionally, OpenFresco permits flexibility of Open System for Earthquake Engineering Simulation (OpenSees), finite element application software specifically for simulating structural response to earthquake excitation. With OpenFresco, OpenSees components are easily added and interchanged within the OpenSees framework and made available in the library without the need to change the

existing code, offering a wide variety of experimental elements and setups (Schellenberg and Mahin 2006). Support for real time distributed hybrid testing is not included in UI-SimCor nor OpenFresco, however a project to develop these capabilities is currently underway (Kim et al. 2012).

2.10 Validation of Hybrid Simulation Results

PSD hybrid simulation results are validated to serve as a basis in developing analytical models and future research projects. Validation of the PSD hybrid simulation results is generally conducted through direct comparison to results from other experimental simulation methods, such as STT or QST. Full dynamic simulation such as STT, will confirm that inertial forces are properly modeled in the numerical model. Component level experiments such as QST characterize hysteretic behavior of critical subassemblies and provide a basic numerical force-displacement model for preparation of PSD hybrid simulation.

As a relatively new topic, the hybrid simulation protocol itself often requires validation. Equipment setup, structural idealization, numerical algorithms and compensation techniques are all major sources for unexplained error within a hybrid simulation. Therefore a predictable specimen, small scale simulations, and an incremental approach are usually adopted to verify the overall hybrid simulation procedure. These methods are particularly necessary to advance simulation techniques such as RT-PSD hybrid simulation and geographically distributed hybrid simulations. As discussed in Chapter 3, a more stable integration algorithm (Chen and Ricles 2008) and an actuator delay compensation technique (Chen and Ricles 2009) for more accurate real-time PSD simulations were validated by a predictable specimen. The

communication framework and delay compensations for distributed slow and real time PSD hybrid simulations (Kwon 2005, Christenson 2008) were validated by an incremental approach. Also in this study, the development of a PSD hybrid simulation procedure is approached incrementally from benchmark scale development (Chapter 4) to large scale implementation (Chapter 5).

2.11 Conclusion

Chapter 2 provides a detailed overview of the fundamentals in PSD hybrid simulation. First, an explanation of the basics in PSD hybrid simulation was presented, including equation of motion, formulation of the numerical substructure and physical specimen, numerical integration procedures; explicit and implicit numerical integration algorithms and modified versions of each commonly adopted in slow and RT- PSD hybrid simulation were discussed. Next, experimental equipment, real-time applications and related time delay compensation techniques followed by geographically distributed applications are discussed. Finally, validation of the simulation development and experimental results are discussed. In summary, hybrid simulation, especially the PSD hybrid method, is a viable approach in earthquake engineering to generate reasonable structural seismic responses that is essential for seismic design of new structural systems and evaluation of existing structures. Chapter 3 establishes the state-of-the-practice of hybrid simulation in the NEESR projects. The knowledge established in this chapter serves as a basis for developing the PSD hybrid simulation control schemes described in Chapters 4 and 5.

CHAPTER 3

HYBRID SIMULATION IN NEESR PROJECTS

3.1 Introduction

The National Earthquake Hazards Reduction Program, established by the US Congress, initiated the George E. Brown, Jr. Network for Earthquake Engineering Simulation (NEES) program in 1999. The primary objective of NEES is providing the tools necessary for researchers and engineers to develop innovations that reduce the threat imposed by seismic disasters. The NEES research infrastructure features fourteen geographically-distributed, shared-use equipment sites and a cyber-infrastructure capable of large scale, complex experiments including all types of conventional and hybrid simulations. Since its establishment in 2004, the NEES Research program (NEESR) has sponsored 213 projects in seismic and tsunami simulation research. Hybrid simulation has been adopted in twenty-two NEESR projects, to date. Table 3.1 lists the project name, completion year, NEES equipment sites, experimental methods, prototype specimen and NEEShub project warehouse ID of 22 NEESR projects which adopted hybrid simulation. Among them, fourteen projects completed their experimental program including the hybrid simulation. All completed hybrid simulations were conventional displacement-based pseudodynamic (PSD) type, six were executed in real-time (RT-PSD) and three were carried out via geographic distribution. Five projects focused developing hybrid simulation techniques such as delay compensation in RT-PSD local and geographically distributed simulations. Half of the completed projects were accompanied by other experimental methods for structural response investigation and simulation

development; three projects used shake-table testing (STT) and six also conducted quasi-static (QST) tests.

Chapter 3 establishes the state-of-the - practice of PSD hybrid simulation in NEESR projects based on the information available at the project warehouse hosted at NEEShub (NEEShub 2009). Projects described herein are referred to by their ID number as assigned in the project warehouse (see also Table 3.1). The construction of NEES equipment sites that are capable of conducting hybrid simulation and their accompanying simulation development are discussed first. Next, details are provided on each hybrid simulation including the physical specimen material and scaling, substructuring method, and numerical integration algorithm. The stability and accuracy of numerical integration algorithms have been significantly improved by NEESR projects. Finally those projects including RT-PSD and geographically distributed PSD hybrid simulation are presented, highlighting the research contributions to both methods.

Table 3.1. Summary of NEESR Hybrid Simulation Projects in NEESHub Project Warehouse

ID	Completion Year	NEESR project title	NEES facility	Experiment methods	Prototype Structure(s)
A 21	2003	Semiactive Control of Nonlinear Structures	CUB FHT	RT-PSD	Magneto-Rheological (MR) fluid dampers as seismic protection in steel structures
B 135	2005	Hybrid Sim. and STT on RC Buildings With Masonry Infill Walls	UCB	STT; PSD	RC building with masonry infill walls
C 47	2005	Damage Tolerant Fiber-Reinforced Cementitious Materials for New EQ Resistant Structural Systems and Retrofit of Existing Structures	UCB; UMich*	PSD,QST	Steel building with easily installed/replaceable ductile cementitious materials in critical regions
D 570; 605	2006	International Hybrid Simulation of Tomorrow's Steel Braced Frames	UCB; NCREE; UM; UW*	PSD;QST	Concentric braced steel frames with various brace configurations
E 120	2006	Multi-Site Soil-Structure-Foundation Interaction Test	UIUC, Lehigh, RPI*	Distributed PSD	Simulation development: distributed testing and analytical simulation; Santa Monica Freeway 5-span off-ramp bridge damaged in Northridge EQ (1994)

Table 3.1. – Continued

ID	Completion Year	NEESR project title	NEES facility	Experiment methods	Prototype Structure(s)
F 72	2008	Development of a Real-Time Multi-Site Hybrid simulation Tool for NEES	UIUC, Lehigh; UCONN*	RT-PSD local and distributed	Simulation development : distributed RT-PSD testing
G 711	2008	Advanced Servo-Hydraulic Control and Real-Time Testing of Damped Structures	Lehigh	RT-PSD	Simulation development: actuator control and integration algorithm for RT-PSD
H 24	2009	Behavior of Braced Steel Frames with Innovative Bracing Schemes	UCB, UB, CUB, Georgia Tech*	QST; STT; PSD slow and distributed	Structural steel frames with various braces displaying complex behavior
I 77	2009	Self-Centering Damage-Free Seismic-Resistant Steel Frame Systems	Lehigh	PSD	Multi-story buildings with self-centering steel frames designed to mitigate seismic damage seen in conventional steel frames
J 75	2010	Controlled Rocking of Steel-Framed Buildings	UIUC;Stanford*; E-Defense, Japan*	QST; PSD; STT	Steel frame assemblies equipped with replaceable fuses for easier repair after damage
K 973	2012	Real-Time Hybrid Simulation Test-Bed for Structural Systems with Smart Dampers	Lehigh	RTPSD	Simulation development using various dampers and structural design cases

Table 3.1. – Continued

ID	Completion Year	NEESR project title	NEES facility	Experiment methods	Prototype Structure(s)
L 685	2011	Framework for Development of Hybrid Simulation in an Earthquake Impact Assessment Context	UIUC	QST; PSD	Simulation development using small scale bridge piers
M 648	2012	Performance-Based Design and Real-time Large-scale Testing to Enable Implementation of Advanced Damping	Lehigh, UIUC	RT-PSD	Simulation development for control strategies using simple damped frames
N 1018	In Progress	Performance-Based Design for Cost-Effective Seismic Hazard Mitigation in New Buildings Using Supplemental Passive Damper Systems	Lehigh	RT-PSD	MR dampers as passive damping in structural design
O 71	In Progress	Seismic Simulation and Design of Bridge Columns under Combined Actions, and Implications on System Response	UCLA, UIUC, UMR*, UNR*	QST; PSD; STT	Piers of 5-Span Continuous Bridge subjected to combined actions/deformations
P 676	In Progress	Performance-Based Design of Squat Reinforced Concrete Shear Walls	UB; UCB	Static; Cyclic; Hybrid (ST)	Structural walls typical for seismic lateral force resistance in buildings and nuclear facilities

Table 3.1. – Continued

	ID	Completion Year	NEESR project title	NEES facility	Experiment methods	Prototype Structure(s)
Q	912/974	In Progress	Collapse Simulation of Multi-Story Buildings Through Hybrid simulation	UB	ST; PSD local and distributed	Validation of collapse predictions using a 4 story frame
R	922	In Progress	CR: Post-Tensioned Coupled Shear Wall Systems	Lehigh; Notre Dame*	PSD	RC coupled building wall systems
S	921	In Progress	Enabling Performance-Based Seismic Design of Multi-Story Cold-Formed Steel (CFS) Structures	UB	STT (substructured)	Low and mid-rise buildings equipped with lightweight CFS for primary beams and columns
T	1084	In Progress	NEESR: Near Collapse Performance of Existing Reinforced Concrete Frame Buildings	UIUC	Distributed PSD	
U	934	In Progress	NEESsoft: Seismic Risk Reduction of Soft-story Wood-frame Buildings	UB; UCSD	PSD; STT	Older multi- story wood building with large openings and few partition walls at ground level

* Non-NEESR funded sites

3.2 Development of NEES Structural Testing Facilities

Construction of the NEES equipment sites took place between 2000 and 2004, among them, six sites are equipped with shake tables and large-scale structural testing facilities that are capable of conducting hybrid simulation (see Table 3.2). Testing facility constructions were accompanied by the development *local* and *geographically distributed* hybrid simulation techniques. The following paragraphs describe facilities developed during the initial construction period and the associated advancement in hybrid simulation method.

Equipped with real time hydraulic actuator control system and reaction walls, the University of Colorado-Boulder (CUB) and Lehigh University focused on developing stable and accurate large scale, *real time* PSD (RT-PSD) hybrid simulation methods. At CUB, Shing (2006) attempted to reduce time delay; the first simulations to approach a real-time rate were achieved by improving conventional time-step integrations to achieve continuous actuator movement. Real-time capabilities were added to OpenSees and numerical simulations were carried out at a much higher speed, reducing the delay imposed by processing actuator command displacements. Chen and Ricles (2008, 2009) developed an explicit integration algorithm and compensation schemes to achieve accurate actuator control based on adaptive control law at Lehigh University.

Strong walls and multi-axial control systems at the University of Illinois, Urbana-Champagne (UIUC) and the University of Minnesota (UM) were built for *multi-directional* PSD hybrid simulation. A multi-axial loading system is prone to errors and cross-talk which cannot be observed or accounted for by internal

measurements; a corresponding systematic calibration method for multi-axial loading systems using external measurement based on the sensitivity of global coordinates was proposed by Nakata et al. (2010). The method was tested at UIUC and found to improve control accuracy and reduce cross-talk of multi-axial loading systems in global Cartesian coordinates. Reinhorn et al. (2004) conducted physical testing using large shake tables, dynamic actuators and strong walls at the University of Buffalo (UB), combined with the numerical computation in developing *real time dynamic hybrid simulation* method. The unique aspect of this simulation method is the versatile implementation of inertia forces and a force-based substructuring. A reconfigurable reaction wall was constructed at the University of California, Berkeley (UCB) facilitating large scale PSD hybrid simulation of versatile specimens at real time or slow rates.

Table 3.2. NEES Structural Hybrid Simulation Facilities

Site	Large scale structural testing facility	Loading rate capability
CUB	Fast hybrid simulation (FHT) facility	Real time
UIUC	Multi-axial full-scale substructure testing and simulation (MUST-SIM)	Slow
UM	Multi-axial subassemblage testing (MAST) facility	Slow
UCB	Reconfigurable reaction wall, strong floor and 4million pound test machine	Real time
Lehigh	Real-time multi-directional (RTMD) testing facility	Real time
UB	Real time dynamic hybrid simulation (RTDHT) facility consist of 2 shake tables, reaction wall and actuators	Real time

3.3 Physical Specimen

3.4 Structural Materials and Systems

Hybrid simulation is applied to structures built with common building materials such as steel (Table 3.3); reinforced concrete/masonry (Table 3.4) and wood and structures equipped with structural response mitigation devices (Table 3.5). Of the twenty-two NEESR projects listed in Table 3.1, seven projects evaluate *steel* moment frames or braced frames with innovative structural configurations and/or installed with special devices; seven projects investigate *reinforced concrete (RC) /masonry* structures systems such as columns, frame infill walls and bridge piers; six projects study the effects of seismic mitigation devices on structural response and one project will inspect various seismic retrofits of wood frame buildings with soft story. Projects 711, 648, 72 and 973 are real time hybrid simulation development projects during which large scale magneto-rheological (MR) dampers were utilized as the test specimen. Project 685 is a simulation development project in which small scale (1/25) bridge pier modules were used to develop the framework for hybrid simulation in earthquake impact assessment.

Table 3.3. NEESR Hybrid Simulation of Steel Specimen

ID	HS method	Specimen	Scale
570; 605	PSD	2-story/1-bay conventional concentric braced frame (CBF) with diamond shape brace	Full
24	PSD (slow and RT)	Chevron brace and connections	1/3
	Distributed	Chevron braces and connections (1st and 2nd story)	1/3

77	PSD	4-story/2-bay, self-centering (SC) moment resisting frame and SC-CBF assemblies	0.6
75	PSD	3-story steel frame with various steel slit fuses	0.43
912*	PSD (local & distributed)	Steel moment frame	1/8
921*	Subst. STT	CFS framed building with (a) only the lateral system (b) the lateral and gravity system (c) structural and nonstructural systems.	Large

* Information provided is based on project proposal, NEESHub data incomplete.

Table 3.4. NEESR Hybrid Simulation of RC Specimen

ID	HS method	Specimen	Scale
135	PSD	Two single frames w/ and w/out URM infill walls	¾
Error! Not a valid result for table.; 201	Distributed PSD	Two RC piers of five-span bridge in separate facilities	1/2
47	PSD	2-story, 1- bay steel moment frame retrofitted with High-Performance Fiber-Reinforced Cementitious (HPFRC) panels	2/3
71*	PSD	22 (14 NEESR funded) RC piers of two different bridges	Small-Large
676*	Hybrid STT	RC squat shear walls (low aspect ratio)	Large
685	PSD	Pier module of MRO bridge	Small
922*	PSD	3-story RC building w/ coupled walls and foundation	~1/2
1084*	Dist. PSD	RC frame building	Large

* Information provided is based on project proposal, NEESHub data incomplete.

3.5 Specimen Scaling

A review of the scaling for NEESR hybrid simulation projects in Table 3.3~Table 3.5 demonstrates that scaling of the experimental specimen depends on the material and capacity limitations of the laboratory. Concrete and wood structures shall be as close to the full prototype scale as possible as the dynamic behavior of these materials does not scale well. Projects 135 and 47 adopted concrete/masonry specimens greater than ¾ scale. To satisfy capacity limitations, project 120 adopted a

½ scale RC specimen. The RC pier modules of project 685 are small scale as the objective of this project was to integrate hybrid simulation with free field and structure sensor measurements. On the other hand, the dynamic behavior of steel tends to scale more accurately, therefore specimens may be slightly smaller scale (~1/2 scale). Project 24 adopted a 1/3 scale steel braced frame while projects 77 and 75 investigated steel moment frames at approximately ½ scale. Steel frames to be evaluated in project 912/974 are proposed to be $\frac{1}{8}$ scale based on a STT of the same. specimen (Lignos 2008). Six projects included large scale MR dampers as the experimental substructure but no physical structural system. Details of the physical specimen and scale for all reinforced concrete (RC)/masonry, steel, and wood and structural control devices are presented in Table 3.3, Table 3.4 and Table 3.5, respectively.

Table 3.5. NEESR Hybrid Simulation of Control Devices/Wood Specimen

	ID	HS method	Specimen	Scale
Control Devices	711	RT-PSD	Elastomeric damper	Large
	21, 973		MR dampers as semi-active control	
	648, 1018*		MR dampers as passive damping	
	72	Dist. RT-PSD	MR dampers at separate facilities	Small & Large
wood	934*	PSD	Upper stories of a multi-story woodframe building	Large

* Information provided is based on project proposal, NEESHub data incomplete.

3.6 Substructuring and Analytical Specimen

The substructuring technique is a main feature of real-time dynamic hybrid simulation, PSD, and RT-PSD hybrid simulation and has been utilized in thirteen of fourteen complete NEESR projects as listed in Table 3.1. It offers versatility in terms of the experimental specimen, such as those exhibiting highly nonlinear or complex behavior. Additionally, the economic and capacity limitations of fully physical simulations are addressed by introducing a numerical component. Physical and numerical substructures can be simulated locally in one laboratory or distributed among several NEES equipment sites.

Hashemi (2007) conducted local PSD hybrid simulation during which the interactions between the RC frames and the unreinforced masonry (URM) infill walls were evaluated in project 135. The prototype structure was a five-story, three-bay by two-bay RC building with unreinforced masonry infill walls. A benchmark STT was conducted using the first-story interior bays as the specimen with post-tensioned columns and additional mass in the top connecting RC slab to better match the mass requirement of the prototype structure. In the following PSD hybrid simulation, one RC frame with a URM infill wall which was the center bay of the STT, became the physical substructure and the remaining bare frame was considered as the numerical substructure.

Wight et al. (2011) physically simulated high-performance fiber-reinforced cementitious (HPFRC) material panels as if it had been installed in a steel moment frame that was being simultaneously numerically simulated in project 47. Yang et al. (2009) conducted PSD hybrid simulation of a three story one bay prototype steel frame in project 24with a physical substructure consisting of a Chevron brace and its

connection at the first story . In projects 77 and 75, Ricles et al. (2009) and Eatherton and Hajjar (2010) evaluated the seismic performance of self-centering steel frames and steel frames with steel fuse configurations , respectively.

Chen and Ricles (2008, 2009), Lin (2009), and Chae et al. (2010) considered high damping rubber bearings as an experimental substructure and conducted RT-PSD hybrid simulation to see their effects on the seismic response of the remaining numerical steel structure in projects 711, 21, and 973, respectively. A single degree of freedom steel moment frame was the numerical substructure in project 711 (Chen and Ricles 2008,2009), while a three story SAC steel moment frame was the numerical specimen in project 21 (Lin 2009). In project 973 the analytical substructure consisted of moment frame, damped braced frame (DBF) and gravity frame. Two physical MR dampers were installed on the second and third story DBF (Chae et al. 2010). Details of NEESR local and distributed substructured PSD hybrid simulations are presented in Table 3.6.

Table 3.6. Substructuring in NEESR Projects

	ID	Testing objectives	Physical Substructure	Numerical Substructure
Local	21,711, 973, 648	Steel structures' response to control techniques; control strategy	Full scale dampers	Prototype structural system with physical specimen vs. damping model
	135	Dynamic response of STT specimen with URM infill walls	Two single outer frames w/ and w/out URM infill walls	Remaining STT specimen (symmetry) & RC slab (spring)
	47	Evaluate new critical connection (HPFRC) of steel building	2-story, 1- bay steel moment frame retrofitted with HPFRC panels	2nd and 3rd bay
	24	Effect of brace behavior	1st story steel Chevron brace & connections	2nd and 3rd stories of single bay frame
	77	Energy dissipation of connection subassembly in SC steel frames	2-bay, 4-story SC-CBF, adjacent gravity columns, basement substructure	Lean-on column, mass tributary to a single frame; viscous damping
	75	Energy dissipation performance of new steel fuse configurations	3-story steel frame assembly equipped with various steel slit fuses	P-Δ effect; interior wall partitions; beam-to-column connections
Distributed	120, 201	Response of continuous 5-span bridge's piers, deck and foundation	Pier 1 & 3 (2 facilities)	Box girder deck, 3 foundation-soil modules & pier 2

Table 3.6. - Continued

ID		Testing objectives	Physical Substructure	Numerical Substructure
Distributed	24	Study brace configurations without changing physical specimen	1st and 2nd story brace with connections (2 facilities)	3rd story brace, remainder of frame
	72	Communication framework and compensation for distribute RT testing	Small scale MR damper at UCONN	2-story steel structure at UIUC

3.7 Numerical Integration Algorithms

Explicit algorithms such as Newmark (Newmark 1959) and central difference methods (CDM) were adopted in early simulation projects but presented stability issues with substructured and real-time experiments. In project 24 the initial stiffness of the physical 1st story brace within a 3-story prototype steel braced frame was determined from a QST test. In the following PSD hybrid simulation, an explicit Newmark integration utilized this initial stiffness to carry out the first step integration (Shing 2006).

A significant contribution of NEESR projects has been the continued improvement of stability and accuracy in integration algorithms. Stability conditions of the Newmark method and CDM make them unsuitable for substructuring and real-time testing. Chen and Ricles (2008) proposed the CR algorithm in simulation development project 711. The CR algorithm is explicit in terms of velocity; and therefore unconditionally stable for RT- PSD simulation. It was adopted in a RT-PSD hybrid simulation of single degree of freedom numerical structures equipped with rate dependent devices to verify its stability in real-time applications. Roke et al. (2009) adopted the CR algorithm for slow and real time simulation of self-centering braced and moment frame performance in project 77; CR algorithm was also adopted by Chae et al. (2010) in projects 648 and 973 to develop a test-bed for evaluating MR damper control strategies.

As discussed in Chapter 2, implicit algorithms are superior in stability and accuracy; however require iterations, which are not possible with a physical experiment. Implicit algorithms have been modified to limit the number of iterations

per step, such as the HHT α-method, or to eliminate iterations all together with predictor-corrector methods, such as the α-OS method. Lin (2009) and Shing et al. (2004) adopted the HHT α-method , modified with a set number of iterations, in projects 21 and 24 for RT-PSD simulations to study the seismic performance of semiactive control of nonlinear steel moment frames and an innovative steel brace configuration (namely zipper frame), respectively. Kwon (2005) and Eatherton and Hajjar (2010) adopted the α-OS method in slow PSD tests projects 120 and 75. Table 3.7 provides a summary of the integration used in the NEESR projects.

Table 3.7. Integration Algorithms in NEESR Projects

	Project	Rate	Integration algorithm	Remark
Explicit	24	Slow	Newmark	Initial stiffness measured by QST; uncond. stability for slow tests
	711, 973, 77, 648	Slow & Real-Time	CR	Explicit velocity, unconditional stability for RT-PSD tests
	72	Real Time	Runge-Kutta	Distributed test
Implicit	21,24	Real-Time	HHT α-method	Set number of iterations to preserve stability
Mixed implicit & explicit	120, 75	Slow	α-OS: Implicit α-method for numerical portion; explicit OS for experimental portion	Stability maintained even in high stiffness degradation
	135	Slow		Implicit force control for high stiffness states

3.8 Real-Time and Geographically Distributed Hybrid Simulation NEESR Projects

Structural systems installed with seismic response mitigation devices exhibit rate-dependent behavior that requires real-time pseudodynamic (RT-PSD) hybrid simulation for evaluation. A total of seven NEESR RT-PSD simulation projects have been conducted and one is in progress. MR dampers, supplemental passive damper systems and self-centering steel frames are experimentally investigated using RT-PSD simulation in projects 21 (CUB FHT), 77 and 1018 (Lehigh) respectively. In project 648, both Lehigh and UIUC conducted a RT-PSD hybrid simulation of a simple linear passive and semi-actively controlled structure to confirm the compatibility of the unique real-time experimental framework of laboratories.

To make the best use of the large scale testing facility available at the NEES equipment sites, the robust internet communication tools and the substructuring techniques, four geographically distributed hybrid simulation projects were conducted via substructuring (see Table 3.6). In project 120, Kwon et al. (2005) implemented the multi-site soil-structure-foundation interaction test (MISST), a distributed PSD hybrid simulation of a five-span continuous bridge was conducted at three NEES equipment sites: UIUC, Lehigh and Rensselaer Polytechnic Institute (RPI). Piers one and three were experimentally modeled at UIUC and Lehigh while the deck, pier two and soil interactions were numerically modeled at UIUC and RPI (soil only). The five modules were integrated using the UI-SimCor that conducted the alpha -OS integration to attain seismic response of the entire prototype system. UI-SimCor enabled all testing facilities to communicate essential information for the smooth execution of hybrid simulation, including test initialization, stiffness estimation, integration parameters and loading commands.

To address errors introduced by inherent actuator and communication delay in RT-PSD simulation, NEESR projects develop and implement control compensation based on predictive and adaptive control theory (see Table 3.8). In project 21, Lin (2009) adopted virtual coupling in RT-PSD hybrid simulation of in a numerical three-story building installed with physical large scale semiactive MR fluid dampers. The seismic performance of this controllable device was studied with passive-off, passive-on and active control strategies. A virtual parallel spring-damper was placed between the physical and numerical substructures with a virtual stiffness smaller than that of the physical component to increase stability. Stability is improved as it the virtual stiffness becomes smaller, relative to the physical specimen. The ratio of virtual stiffness to virtual damping becomes greater than the system dynamics, counterbalancing time delay. However the increased stability is an inherent tradeoff for decreased system performance seen when virtual restoring force is not greater than that of the physical specimen. As discusses in Chapter 2, Chen and Ricles (2009, 2010) proposed an adaptive compensation method, which improved the inverse compensation method (Chen 2007) in simulation development project 711. Through comparison to inverse and dual compensation techniques, it was shown that the adaptive compensation scheme is able to achieve more accurate actuator control in a RT-PSD hybrid simulation.

Table 3.8. Real Time Compensation in NEESR Projects

	Actuator Delay Compensation	Compensation
21	Virtual Coupling	Parallel virtual spring -damper $(k_c - c_c)$ placed between numerical and physical components. k_c adjusts to provide stability
711	Inverse Compensation; Adaptive Inverse Compensation	Inverse of the discrete z- transform of measured and command displacements sends measured displacement associated with actuator delay to controller.
72	Smith's Predictor	Estimated model of the physical setup to predict its delayed behavior and compensated in the controller

The Smith predictor method (Smith 1959) employs an estimated model of the physical system to predict its delayed behavior and compensates for such in the controller. In project 972 Christenson et al. (2008) conducted small scale geographically distributed RT-PSD tests between University of Illinois-Urbana Champagne (UIUC) and University of Connecticut (UCONN) adopting a Smith predictor to accommodate for communication time delay following the previous local RT-PSD tests. The experiment will be repeated on a large scale between Lehigh and UIUC.

Neither of the two software platform for distributed hybrid simulation, UI-SimCor and OpenFresco, are able support hard real time distributed hybrid simulation, which was addressed in projects 24 and 972. In project 24, Leon et al. (2004) attempted a distributed RT-PSD simulation between UCB and CUB on a three story steel braced frame. It was noted that true real time interactions were not achieved due to the latency in the network and the complexity of the specimen. In

project 972, distributed RT-PSD hybrid simulation was successfully conducted at a small scale between UIUC and UCONN and at a large scale between UIUC and Lehigh. First, MR dampers were tested physically at UCONN as part of a two-story sheer frame structure that was numerically modeled at UIUC. Second, two MR dampers were placed on the first and second floor of a numerical three-story sheer frame at UIUC and Lehigh, respectively.

3.9 Validation of NEESR Hybrid Simulation Projects

One of the main objectives of the NEESR projects is to validate the experimental procedure and the associated simulation results as they serve as a basis for future research development. NEESR projects adopt full dynamic simulation and/or component level experiments to validate simulation results. To validate experimental protocol, an incremental approach builds on small scale simulations and experimenting with a predictable specimen.

Hashemi and Mosalam (2006) conducted STT as a benchmark for a PSD hybrid simulation and achieved reasonable agreement between the two simulation results in project 135. Subsequently hybrid simulation responses were used to develop and calibrate analytical models, and to validate the associated PSD hybrid simulation platform. Lai and Mahin (2010), Ricles et al. (2009), and Wight et al. (2011) compared structural responses obtained from PSD hybrid simulation of a steel braced frame, a self-centering frame and a steel frame equipped with novel connections (projects 570; 605, 77, and 47, respectively) against those obtained from QST tests of the critical components. Structural responses obtained from PSD hybrid simulation of braced frames in project 24 and controlled rocking frames in project 75 were

compared to both STT of the prototype specimen and QST tests of critical components.

The hybrid simulation techniques developed to improve the reliability of the simulation results also requires validation. For example in project 711, the actuator delay compensation method and integration algorithm for RT-PSD simulation was validated through the comparison between the hybrid simulation results and numerical simulation of a simple single degree of freedom frame equipped with an elastomeric damper (Chen and Ricles 2008,2009). Development of the distributed slow PSD hybrid simulations in project 120 were approached incrementally; first the communication protocol was validated by a purely analytical distributed simulation, followed by small amplitude tests to verify proper communication between the distributed simulation sites and finally successful large scale distributed simulation among three experimental and numerical simulation sites (Kwon et al. 2005).

Small scale distributed RT-PSD simulation with the Smith predictor compensation using the hardware and software particular to UCONN and the Runge-Kutta integration method was conducted on a prototype specimen previously characterized by STT (Chung et al. 1989) and local RT-PSD simulations (Christenson et al. 2008). The results were a basis for developing communication framework for large scale distributed real-time hybrid testing in project 72. Projects described in Table 3.9 were successfully validated by reasonable agreement with their respective tests and used in developing analytical models.

Table 3.9. Validation of NEESR Hybrid Simulation Projects

Project	Test to be Verified	Verification Process	Remarks
711	RT-PSD test of rate dependent device	Predictable specimen	Developed RT delay compensation & integration algorithm
135	PSD hybrid simulation	Benchmark STT	Basis for future analytical models
120	Distributed slow PSD test	Analytical model and small scale tests	Developed UI-SimCor
570; 605, 77, 47	Scaled slow PSD sim. of steel frame components	QST tests of critical component	Results of QST test calibrate analytical model
24, 75	Scaled slow PSD and RT-PSD sim. of steel frame components	STT of scaled prototype specimen & QST tests of critical component	Results of QST test calibrate analytical model
648	Separately developed RT-PSD hardware, software and integration schemes	Predictable specimen; comparison between facilities	Basis for distributed RT-PSD experiment
72	Small scale distributed RT-PSD sim.	Simple specimen already tested several RT-PSD and STT	Results will be used for large scale distributed RT-PSD framework

3.10 Summary of the State-of-the-Practice of NEESR PSD Hybrid Simulation

NEESR facilities are capable of local and geographically distributed hybrid simulation techniques at slow or real time loading rates. Real time hydraulic actuator control system and reaction walls facilitate RT-PSD hybrid simulation methods. Strong walls and multi-axial control systems facilitate multi-directional PSD hybrid simulation. Large shake tables, dynamic actuators and strong walls conduct real time dynamic hybrid simulations. Large reconfigurable reaction walls facilitate large scale

PSD hybrid simulation of versatile specimens at real time or slow rates. Twenty two NEESR sponsored projects have adopted PSD hybrid simulation. By validating the experimental procedure and the associated simulation results, each project serves as a basis for future research development.

A significant contribution of NEESR projects has been the continued improvement of stability and accuracy in integration algorithms. With improvements in modified implicit integration algorithms, substructuring has become a key feature of PSD and dynamic hybrid simulation in NEESR projects, driving further development of real time and geographically distributed projects. Improved accuracy and stability of both implicit and explicit algorithms, along with control compensation techniques have made accurate RT-PSD hybrid simulation, local and geographically distributed, more achievable. The feasibility of geographically distributed simulations is improved with the introduction of flexible software such as UI-Simcor and OpenFresco to quickly communicate essential information. Nevertheless, as NEESR experimental objectives become more complex, further development of stable integration algorithms for large scale substructured experiments and real time local and geographically distributed PSD simulations is needed to produce reliable and accurate results. Neither of the two software platform for distributed hybrid simulation, UI-SimCor and OpenFresco, are able support hard real time distributed hybrid simulation.

3.11 Future Work

Much advancement has been made in hybrid simulation, such as expanding testing application examples, minimizing experimental errors, developing more

accurate algorithms and stable control compensations. However there are still challenges faced by the researchers in earthquake engineering to further improve this advanced experimental simulation method. The following provides a summary of future development concluded from the previous discussions in this paper and the other two documentations on hybrid simulation needs (Dyke et al. 2011; NEES Consortium 2007). Advancing slow and real-time PSD simulation and other hybrid simulation methods as reliable experimental method for earthquake engineering, efforts shall be made in two areas:

1)Further develop hybrid simulation methods that will provide more realistic structural responses.

- Large scale hybrid simulation to achieve system level structural responses through substructuring techniques with accurate application of boundary condition and geographically distributed substructuring testing.
- Real time simulation of rate dependent structural elements and devices by speeding up loading rate of hydraulic testing equipment; developing more stable and accurate integration algorithms with reduced computational time and time delay compensations; develop real-time or fast simulation capabilities in UI-SimCor, OpenFresco or similar for real time distributed hybrid simulation.
- Increased confidence in hybrid simulation providing realistic structural responses by developing systematic hybrid simulation validation procedure with quantification method of experimental errors for both numerical simulation and physical experiment

2)Provide validated general hybrid simulation procedure suitable to various testing facilities and projects with various testing purposes for broader application.

- Develop a benchmark hybrid simulation bed to validate various improvements made in the first area. The benchmark test bed shall:
  - contain nonlinear structural components that are easy to be replaced
  - be easily integrated with seismic response mitigation devices and various structural control techniques
  - accommodate different simulation platforms; numerical algorithms, hydraulic loading controllers
  - be easily applied to new approaches for quick comparison / contrasting of different testing methods

3.12 Conclusion

Since the completion of the NEES equipment sites construction in 2004, its capability of conducting the most advanced large-scale earthquake simulation has been utilized in evaluating various structural materials, up to full scale, and validating the analytical simulation results. Chapter 0 provides an overview of PSD hybrid simulation conducted in more than twenty NEESR projects. The NEES equipment sites that are capable of conducting hybrid simulation are discussed, highlighting the accompanying hybrid simulation development. The chapter goes on to elaborate on details of each experiment including the physical specimen material and scaling, substructuring method, and numerical integration algorithm. Research contributions and the implementation of RT-PSD and geographically distributed PSD hybrid

simulation are described. In summary, the efforts and contributions of NEESR projects to hybrid simulation, especially real-time and distributed PSD hybrid methods, have been helping make it a viable approach in earthquake engineering to generate reasonable structural seismic responses at the system level through large scale simulation . Further research is necessary in the areas of substructuring and boundary condition replication, real time compensation and stable and accurate integration algorithm to advance both local and geographically distributed hybrid simulation.

CHAPTER 4

BENCHMARK SCALE PSEUDODYNAMIC HYBRID SIMULATION

4.1 Introduction

The following chapter describes a series of small scale pseudodynamic (PSD) hybrid simulations were conducted at the Laboratory Earthquake and Structural Simulation (LESS) of Western Michigan University (WMU). The objective of this chapter is to develop versatile control schemes for slow and real time PSD hybrid simulations to eventually be adopted in the large scale experiment at the University of Alabama (UA) and contribute to the development of six DOF PSD hybrid simulation of the NEES-Soft project. An overview of the equipment at LESS utilized in this study is presented first followed by the details of the physical specimen, numerical models and the Newmark-β time-step integration. Three phases of PSD hybrid simulation tests are conducted at various amplitudes to characterize the control system at LESS and develop appropriate error compensation methods. Details of the experimental procedure, validation and final control scheme are provided herein.

4.2 Experimental Equipment

As discussed in Chapter 2, specific experimental equipment is needed for conducting PSD hybrid simulation. The following sections provide a detailed description of the equipment available for PSD hybrid simulation at LESS and Figure 4.1 illustrates the equipment connections Refer to the LESS website (http://homepages.wmich.edu/~dpb8848/Facilities.html) and Shao and Enyart(2012) for more information.

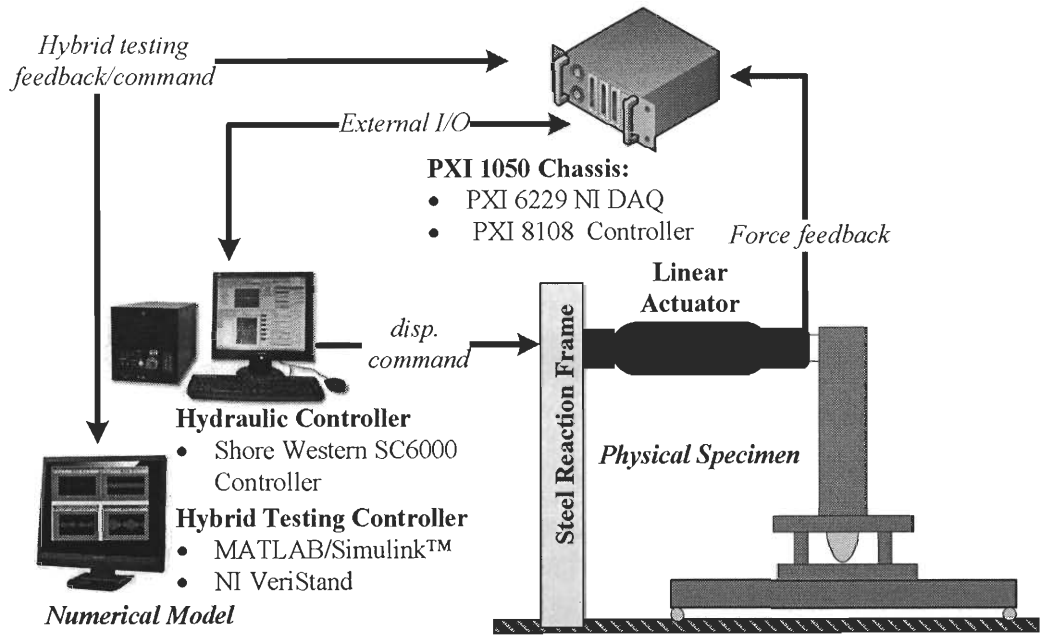

Figure 4.1. PSD Hybrid Simulation Experimental Setup at LESS

4.3 Hydraulic Control System

The hydraulic controller and actuator are required to apply the step-by-step simulated displacement responses on the physical substructure during PSD hybrid simulation. The Shore Western linear hydraulic actuator (Model 910D-1.08-6(0)-4-1348) has a force rating of ± 3,240 lbs and a six inch stroke (±3 inches). The actuator, attached to the reaction frame to apply displacement command at the desired height between 0~15 ft, is equipped with an internal linear variable differential transducer (LVDT) and a load cell transducer with 2.5 kip fatigue rated 300% overload capacity. A desktop computer houses the 2.13 GHz processor of the 2 channel Shore Western SC6000 Servo Hydraulic Controller. TheSC6000 hydraulic controller is built with data acquisition (DAQ) to acquire sensor readings from the actuator. A MOOG G781-3002 servo-valve controls the actuator's hydraulic flow

with a maximum flow rate and pressure of 2.5 gpm at 1000 psi and a maximum velocity performance of 9.1 inches per second (velocity = flow rate/piston area). The hydraulic controller adopts proportional-integral-derivative (PID) error feedback control (Figure 4.2); proportional gain is related to present error ($e(t)$), integral gain to accumulation of past error, ($\int_0^t e(\tau)d\tau$) and derivative to future error ($\frac{de(t)}{dt}$). The proportional, integral and derivative gains, K_p, K_i and K_d , respectively, are tuned in the hydraulic controller for actuator's command tracking optimal performance.

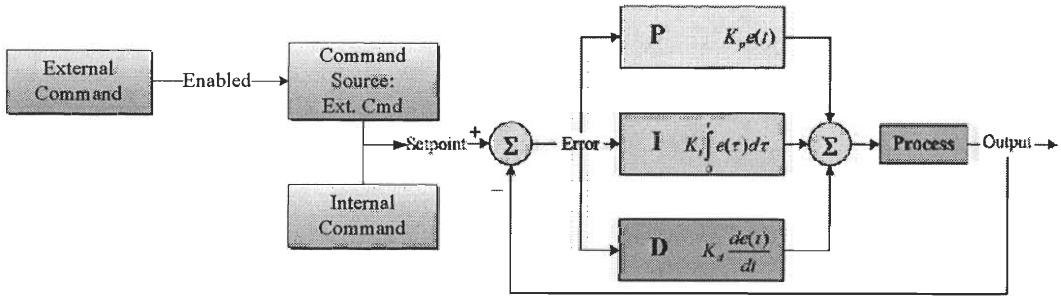

Figure 4.2. Proportional-Integral-Derivative Error Feedback Control

To tune the actuator at LESS, white noise with a frequency range of interest1.5~2.5 Hz and 0.3" amplitude was generated in SC6000. Fast Fourier transform (FFT) plot of the command and the feedback displacement was generated in the VeriStand (discussed below) while increasing the proportional gain in the SC6000. Focusing mainly 1.5~2.5 Hz, a proportional gain of 18% provided the most accurate agreement between the command and measured values (see Figure 4.3). The integral and the derivative gains were set to 0. SC6000 is equipped with an "external command" function (shown in Figure 4.2), enabling it to be controlled by the external real-time controller. The external control function is essential to hybrid simulation as

it allows the real time controller to simultaneously execute the inputs and outputs of the hybrid simulation model, as discussed below.

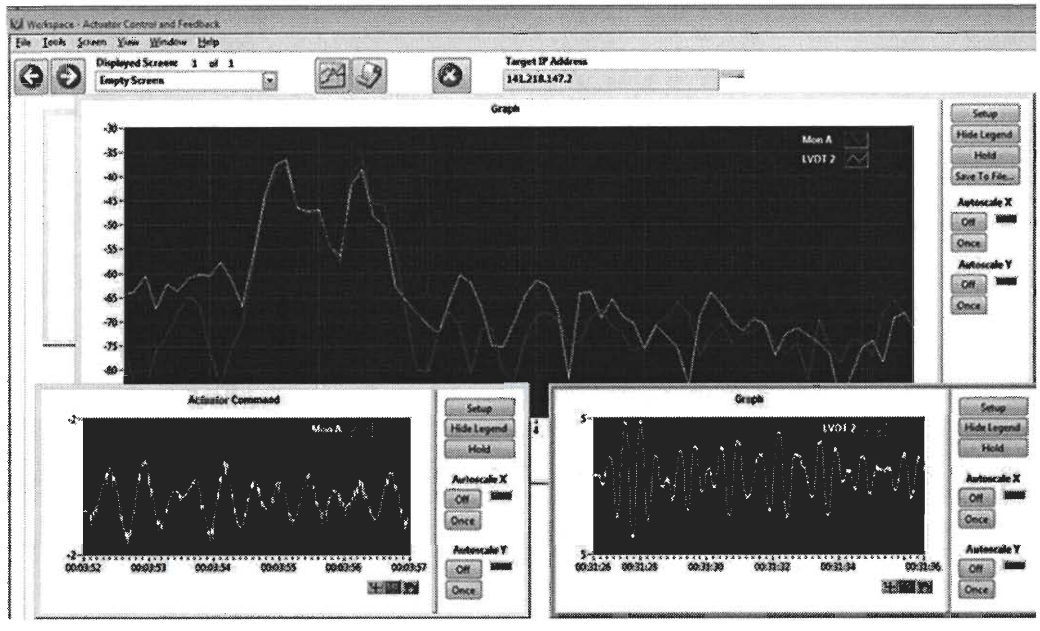

Figure 4.3. FFT Plot for Actuator Tuning

4.4 Real-Time Controller and Data Acquisition System

The National Instruments (NI) PXI 1050 Chassis houses the NI 2.53 GHz Dual-Core PXI 8108 embedded real-time controller and the multifunction M series PXI-6229 DAQ modules at LESS. The real-time controller simultaneously executes the I/O of the hybrid simulation model code via the DAQ analog input (AI) and analog output (AO) channels. An SCB-68 connector block handles real-time data exchange between SC6000 and the NI-DAQ. AI channel data is acquired from force and displacement feedback signals of the actuator load cell and LVDT, respectively. When SC6000 is enabled with external control, displacement command signals are sent through AO channel data generated by the hybrid simulation model running in the real time controller during the testing. NI SCB-68 connector block is the

hardware required to interface inputs/outputs (I/O) between DAQ devices; LESS has three SCB-68 connector blocks, one is used in the PSD hybrid simulation to connect the real-time controller and SC6000. The hybrid testing controller, as described below, provides a user interface with the real-time controller (through NI Veristand); the simulation model and DAQ channel system map is configured within the hybrid testing controller and downloaded onto the real-time controller before execution of a PSD hybrid simulation.

4.5 Hybrid Testing Controller

A second desktop is used as the hybrid testing controller, which integrates the structural properties of the numerical substructure with the physical restoring force of the specimen to simulate the overall system's seismic response via the integrated simulation (MATLAB/Simulink™) and controller configuration software, (NI VeriStand). The numerical substructure model of the prototype mass, viscous damping and the analytical force-displacement relationship of the numerical degree of freedom (DOF) are developed in MATLAB/Simulink™ simulation modeling software. VeriStand provides the interface between DAQ channels with the dynamic link library (.dll) simulation model in a system map configuration. Simulink blocks 'NIVeriStandSignalProbe', 'NI In' and 'NI Out' (see Figure 4.4) identify the destination of AI channel data and the source of AO channel data, respectively. Using VeriStand, the simulation model and system map configuration is downloaded to the real-time controller, referred to above as the hybrid simulation model. Sensor readings, in voltage are scaled using VeriStand setting to appropriately read as force

and displacement values. Data readings can be monitored and/or logged in a customizable VeriStand workspace (Figure 4.5).

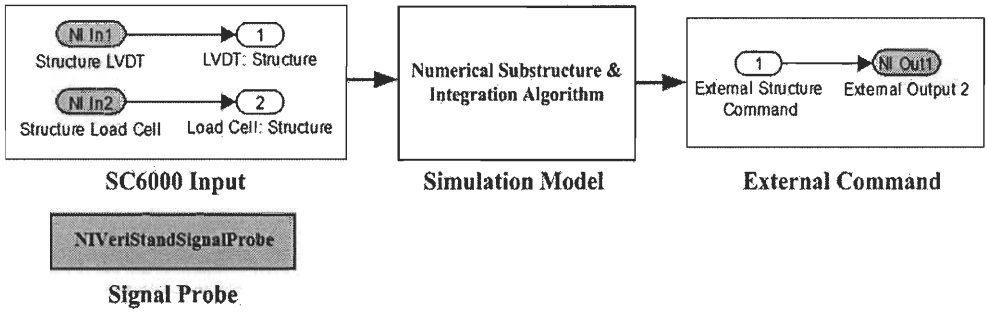

Figure 4.4. Simulink Model VeriStand Signal Probe and I/O

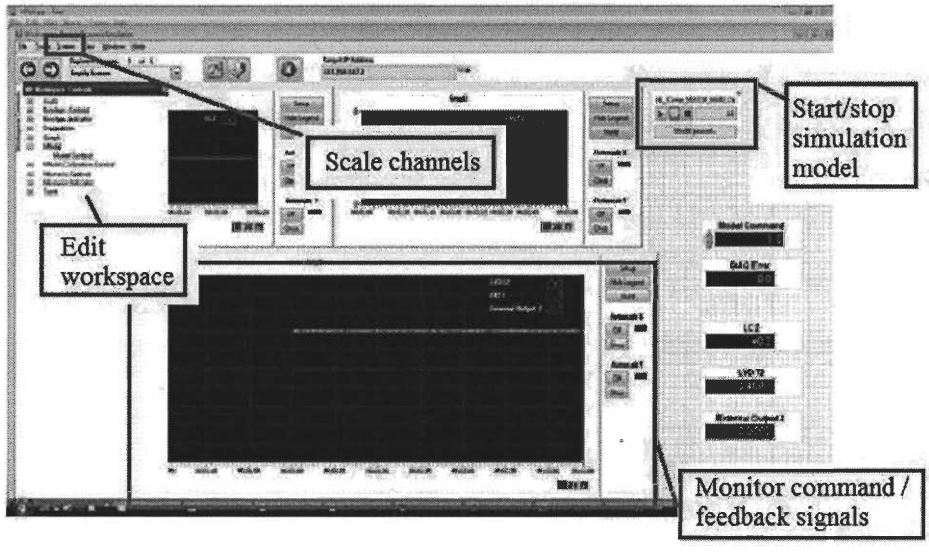

Figure 4.5. Customizable VeriStand Workspace

4.6 Physical Specimen

4.7 Description of Physical Specimen

Physical experimentation is generally conducted to study unpredictable behavior of a structure, as often experienced during nonlinear response to large

earthquake excitation. However, as discussed in Chapter 2, as a relatively new topic, the hybrid simulation protocol itself often requires validation. Equipment setup, structural idealization, numerical algorithms and compensation techniques are all major sources for unexplained error within hybrid simulation experiments. Therefore a predictable specimen, small scale simulations, and an incremental approach are usually adopted to verify the overall hybrid simulation procedure.

Mosqueda (2005) evaluated experimental errors utilizing a small scale steel cantilever column with an idealized plastic hinge connection which is adopted in this study. The plastic hinge was designed with bolts much weaker than the overall specimen, known as coupons, to emulate plastic behavior. It can be used in nonlinear tests and easily replaced after yielding without permanent damage to the other components of the specimen, making it ideal for simulation control development purposes. The test column and its plastic hinge connection were designed and fabricated based on the capacity limitations of the hybrid simulation equipment at LESS (Phillips 2012). A key feature of using a specimen of this nature is the ease and accuracy in formulating an analytical model (see Section 4.11) for validation purposes. The overall specimen can be seen in Figure 4.6 with a close up view of the plastic hinge connection in Figure 4.7.

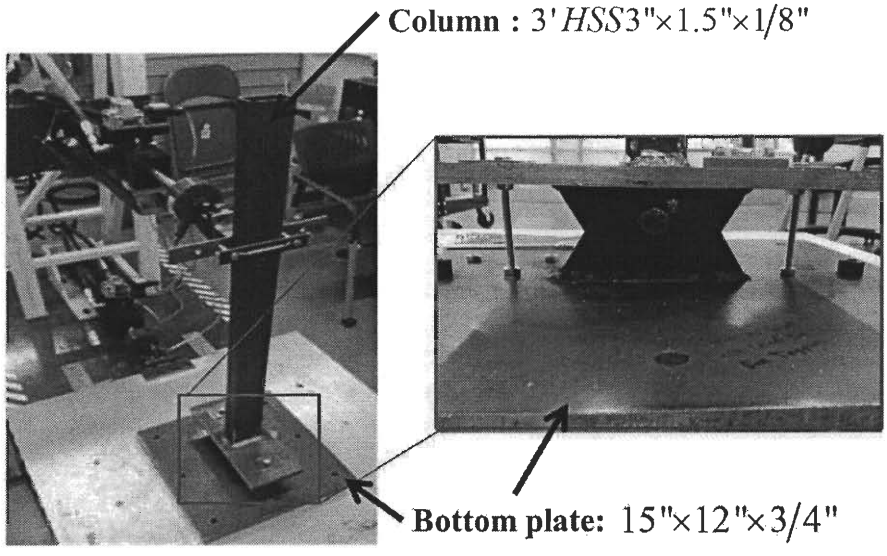

Figure 4.6. Physical Specimen at WMU

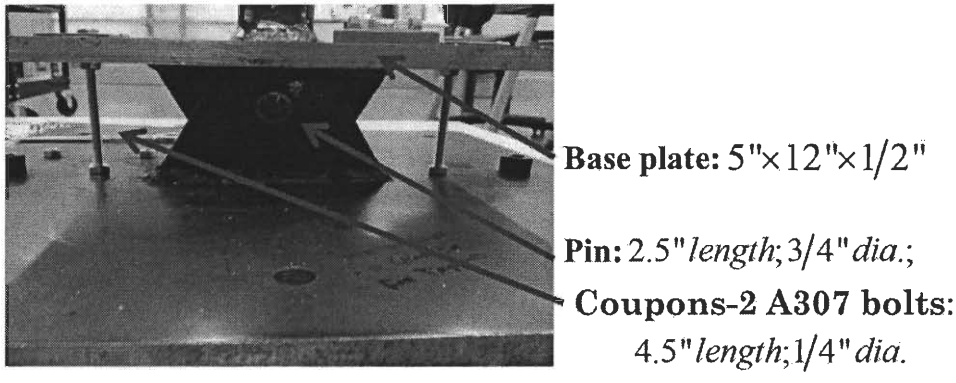

Figure 4.7. Pin Connection and Coupons

The steel column was a $3'\ HSS3\times1.5\times\frac{1}{8}"$ welded at the base to a $5\times12\times\frac{1}{2}"$ steel plate. The steel plate was welded to a steel pin connection which was welded at the bottom to a $15\times12\times\frac{3}{4}"$ plate. Two $4.5"$ long $\frac{1}{4}"$ diameter A307 steel bolts acted as coupons on either side of the pin connection are fastened from the top plate through bottom plate. Nuts were tightened at the bottom plate and underneath the top plate to

ensure proper boundary conditions. The center to center distance between the two coupons is 8". The pin connection, fastened by a ¾" bolt, resists axial and shear forces and moment resistance is formed by the coupons through force couple. A detailed description of the specimen design is available in Phillips (2012)

4.8 Physical Specimen Installation Procedure

It should be noted that slippage was observed in the pin connection in early testing phases, reducing the initial stiffness. This was addressed by tightening the pin and adding grease. It was also observed that improper coupon installation leads to the coupon experiencing uneven initial torque, and becoming damaged very early in the test. Instructions for proper coupon installation procedure are as follows:

1. Fasten structure to actuator at '0' position, ensure plates are level and column is centered with the actuator. This allows the user to monitor force readings in the SC6000 screen while tightening the coupon to ensure they are equally fastened.
2. Thread coupon through top plate; add two nuts per coupon, ensuring that the nuts are ***not*** tightly fastened.
3. Fasten coupon into bottom plate as tightly as possible. As they are being tightened, monitor the force measurement, keeping as close to zero as possible by alternating between the two coupons.
4. Tighten top nuts, monitoring force measurement and alternating between the two to keep the reading at 0.
5. Repeat step 4 with bottom nuts.

4.9 Numerical Model

Two numerical models were created in this series of small scale PSD hybrid simulation tests. The first one was used to verify experimental setup and preliminary procedures and only adopted in the first slow PSD hybrid simulation (see Table 4.4) and in the real time hybrid simulation (Section 4.7), which is a one-story structure

idealized as a single degree of freedom (SDOF) lumped-mass model. The mass and the damping properties are determined based on the predefined natural period (0.35 sec) and damping ratio (2%). The initial stiffness (k) of $0.950\,^{kip}/_{in}$ was quantified from the cyclic test (Section 4.11). Then the mass (m) and the damping coefficient (c) of the SDOF structure were computed as $0.0028\,^{kip\cdot s^2}/_{in}$ and $0.0021\,^{kip\cdot s}/_{in}$, respectively.

The second structural model was a two story building that was developed by the collaborators from Clemson University for the large scale PSD hybrid simulation of a woodframe building that was carried out at the University of Alabama (see Chapter 5). The structural model was idealized as a two DOF lumped mass model (Figure 4.8) and scaled down to be compatible with the LESS equipment capacity. The numerical substructure model consisted of the mass of both DOFs, the damping properties of the two modes, and a hysteretic model representing the first story. The physical substructure was hysteretic behavior of the second story.

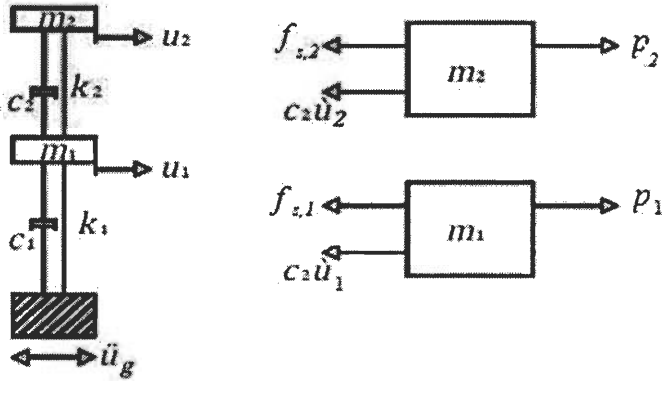

Figure 4.8. Idealized Two DOF Structural Model

As discussed in Chapter 2, the numerical substructure for a PSD hybrid simulation with a numerical first story and a physical second story is as follows:

$$\begin{bmatrix} m_1 & \\ & m_2 \end{bmatrix}\begin{Bmatrix} \ddot{u}_1 \\ \ddot{u}_2 \end{Bmatrix}+\begin{bmatrix} c_1+c_2 & -c_2 \\ -c_2 & c_2 \end{bmatrix}\begin{Bmatrix} \dot{u}_1 \\ \dot{u}_2 \end{Bmatrix}+\begin{bmatrix} f_{s,1} \\ f_{s,2} \end{bmatrix}=\begin{bmatrix} p_1 \\ p_2 \end{bmatrix} \qquad 4.1$$

The first story's initial stiffness was predefined as $10.2\,{}^{kip}/_{in}$ by the woodframe prototype structure. To account for the significant difference between the first story stiffness ($10.2\,{}^{kip}/_{in}$) and the physical substructure's initial stiffness ($\sim 0.95\,{}^{kip}/_{in}$), a scaling factor (WS_Scale) was introduced to the force-displacement relationship of the physical substructure in the hybrid simulation model. The scaling factor was defined by the ratio of the first story numerical stiffness, k_1 to the second story physical stiffness, k_2 , therefore the stories are identical:

$$WS\_Scale = {}^{k_1}/_{k_2} \qquad 4.2$$

The mass and damping matrices, as with the previous SDOF model, were determined by the modal natural periods and modal damping ratios, respectively. Table 4.1 summarizes the structural dynamic properties of both the SDOF and 2DOF structural models.

Table 4.1. Structural Dyanmic Properties in Numerical Models

Property	SDOF	MDOF
k $\left({}^{kip}/_{in}\right)$ (physical)	0.95	$\begin{bmatrix} 0 \\ 0.950 \end{bmatrix}$
k $\left({}^{kip}/_{in}\right)$(hysteretic parameters)	-	$\begin{bmatrix} 20.44 & -10.22 \\ -10.22 & 10.22 \end{bmatrix}$
m $\left({}^{kip\cdot s^2}/_{in}\right)$	0.0028	$\begin{bmatrix} 0.249 & 0 \\ 0 & 0.249 \end{bmatrix}$
ω_n / T_n $\left({}^{rad}/_{\sec}\right)$	18.4 / 0.34	$\begin{Bmatrix} 12.5 \\ 32.8 \end{Bmatrix} / \begin{Bmatrix} 0.5 \\ 0.19 \end{Bmatrix}$
ξ	2%	2% of each mode
c $\left({}^{kip\cdot s}/_{in}\right)$	0.0021	$\begin{bmatrix} 0.129 & -0.0645 \\ -0.0645 & 0.0645 \end{bmatrix}$

4.10 Numerical Integration Algorithm

The simulated dynamic response of the prototype structure was calculated in an implicit Newmark integration algorithm modified to be suitable for experimentation. Per the procedure discussed in Section 2.4.2, initial calculations are conducted before the hybrid simulation as shown in Table 4.2. An average acceleration approximation was adopted; parameters β and γ were ¼ and ½, respectively. The time step, Δt, was 0.01 seconds. The earthquake excitation is calculated from 1994's Northridge (MUL009) ground acceleration, which exhibits a peak ground acceleration of 0.42g ; ground acceleration was scaled to the capacity limits of the specimen and loading equipment.

Table 4.2. Calculation Steps for Newmark-β Nonlinear Integration Algorithm

4.2.0 Initial Calculations:

4.2.1 $$k_{C1}+k_{C2}=\frac{1}{\beta\Delta t^2}\begin{bmatrix} m_1 & 0 \\ 0 & m_2 \end{bmatrix}+\frac{\gamma}{\beta\Delta t}\begin{bmatrix} c_1+c_2 & -c_2 \\ -c_2 & c_2 \end{bmatrix}=\begin{bmatrix} 9998 & -12.9 \\ -12.9 & 9972 \end{bmatrix}$$

4.2.2 $$dp_{C1}+dp_{C2}=\frac{1}{\beta\Delta t}\begin{bmatrix} m_1 & 0 \\ 0 & m_2 \end{bmatrix}+\frac{\gamma}{\beta}\begin{bmatrix} c_1+c_2 & -c_2 \\ -c_2 & c_2 \end{bmatrix}=\begin{bmatrix} 99.9 & -0.258 \\ -0.258 & 99.7 \end{bmatrix}$$

4.2.3 $$dp_{C3}+dp_{C4}=\frac{1}{2\beta}\begin{bmatrix} m_1 & 0 \\ 0 & m_2 \end{bmatrix}+\Delta t\left[\frac{\gamma}{2\beta}-1\right]\begin{bmatrix} c_1+c_2 & -c_2 \\ -c_2 & c_2 \end{bmatrix}=\begin{bmatrix} 0.498 & 0 \\ 0 & 0.498 \end{bmatrix}$$

4.2.4 $$v_{C1}=\frac{\gamma}{\beta\Delta t}=200 \quad v_{C2}=\frac{\gamma}{\beta}=2 \quad v_{C3}=\Delta t\left[1-\frac{\gamma}{2\beta}\right]=0$$

4.2.5 $$[k]_1=[k]_{initial}$$

In PSD hybrid simulation, an updating tangent stiffness matrix replaced the secant stiffness matrix that requires iteration to be obtained; the stiffness of each DOF for the next time step was calculated based on the displacement and measured restoring force of the current step (Equation 4.3.6). To correct for error associated with inaccurate stiffness estimation, acceleration was calculated at the end of the time step with the measured restoring force to ensure dynamic equilibrium (Equation 4.3.8). An explicit target displacement for the first time-step was calculated by assigning the initial stiffness, measured from a cyclic test, to the first step (Equation 4.2.5). The derivation of the implicit Newmark time-step integration with iterations and its modified version with an updating stiffness are presented in Chapter 2. Step by step calculations carried out as programmed in the Simulink model (see Appendix A) are listed in Table 4.3.

Table 4.3. Step by Step Procedure for Newmark –β Integration

4.3.0 Calculations for each step ($i=1:n$):

4.3.1 $$\begin{bmatrix}\Delta\hat{p}_1\\ \Delta\hat{p}_2\end{bmatrix}_i=\begin{bmatrix}\Delta p_1\\ \Delta p_2\end{bmatrix}_i+\begin{bmatrix}99.9 & -0.258\\ -0.258 & 99.7\end{bmatrix}\begin{Bmatrix}\dot{u}_1\\ \dot{u}_2\end{Bmatrix}_i+\begin{bmatrix}0.498 & 0\\ 0 & 0.498\end{bmatrix}\begin{Bmatrix}\ddot{u}_1\\ \ddot{u}_2\end{Bmatrix}_i$$

4.3.2 $$\begin{bmatrix}\hat{k}_{11} & \hat{k}_{12}\\ \hat{k}_{21} & \hat{k}_{22}\end{bmatrix}_i=\begin{bmatrix}k_{11} & k_{12}\\ k_{21} & k_{22}\end{bmatrix}_i+\begin{bmatrix}9998 & -12.9\\ -12.9 & 9972\end{bmatrix}$$

4.3.3 $$\begin{Bmatrix}\Delta u_1\\ \Delta u_2\end{Bmatrix}_i=\begin{bmatrix}\hat{k}_{11} & \hat{k}_{12}\\ \hat{k}_{21} & \hat{k}_{22}\end{bmatrix}_i^{-1}\begin{bmatrix}\Delta\hat{p}_1\\ \Delta\hat{p}_2\end{bmatrix}_i$$

4.3.4 $$\begin{Bmatrix}\Delta\dot{u}_1\\ \Delta\dot{u}_2\end{Bmatrix}_i=200\begin{Bmatrix}\Delta u_1\\ \Delta u_2\end{Bmatrix}_i-2\begin{Bmatrix}\dot{u}_1\\ \dot{u}_2\end{Bmatrix}_i$$

4.3.5 $$\begin{Bmatrix}\ddot{u}_1\\ \ddot{u}_2\end{Bmatrix}_{i+1}=\begin{bmatrix}0.249 & 0\\ 0 & 0.249\end{bmatrix}^{-1}\left[\begin{bmatrix}p_1\\ p_2\end{bmatrix}_{i+1}-\begin{bmatrix}f_{s,1}\\ f_{s,2}\end{bmatrix}_{i+1}-\begin{bmatrix}0.129 & -0.0645\\ -0.0645 & 0.0645\end{bmatrix}\begin{Bmatrix}\dot{u}_1\\ \dot{u}_2\end{Bmatrix}_{i+1}\right]$$

Update story stiffness, k:

4.3.6 $k_{1,i}=\frac{\Delta f_{s,1,i}}{\Delta u_{1,i}}, k_{2,i}=\frac{\Delta f_{s,2,i}}{\Delta u_{2,i}-\Delta u_{1,i}}$

Update stiffness matrix:

4.3.7 $$\begin{bmatrix}k_{11} & k_{12}\\ k_{21} & k_{22}\end{bmatrix}_{i+1}=\begin{bmatrix}k_1+k_2 & -k_2\\ -k_2 & k_2\end{bmatrix}$$

4.3.8 $\{u\}_{i+1}=\{\Delta u\}_i+\{u\}_i;\{\dot{u}\}_{i+1}=\{\Delta\dot{u}\}_i+\{\dot{u}\}_i$

A time history plot of the displacement responses of the analytical first and second stories is shown in Figure 4.9.

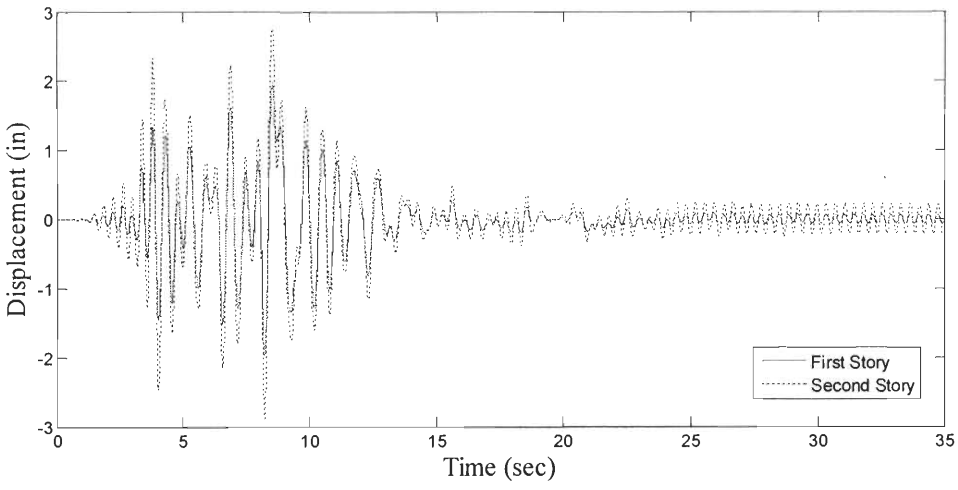

Figure 4.9. Analytical Displacement of First and Second Story

4.11 Cyclic Testing

Hysteretic behavior of the specimen was characterized through the cyclic QST test, during which a slow predetermined cyclic loading history was applied to the specimen. First monotonic loading in the positive and negative direction verified the axial symmetry of the coupons. The triangle waveform (Figure 4.10) function available in the he hydraulic controller (SC6000) was used in QST test. The maximum displacement of the waveform was approximately 1.2" applied over 800 seconds . No inertial or viscous damping effects are captured during the QST test resulting in only the hysterics of the specimen. The DAQ embedded in the SC6000 hydraulic controller collected force and displacement data from the actuator's load cell and LVDT. The initial stiffness, peak restoring force and yield displacement of the specimen were then determined by plotting the data in a force vs. displacement plot (Figure 4.10).The specimen's initial stiffness was determined to be $0.950\,^{kip}/_{in}$ with a yield displacement of 0.75" and yield force of approximately 0.7 kip.

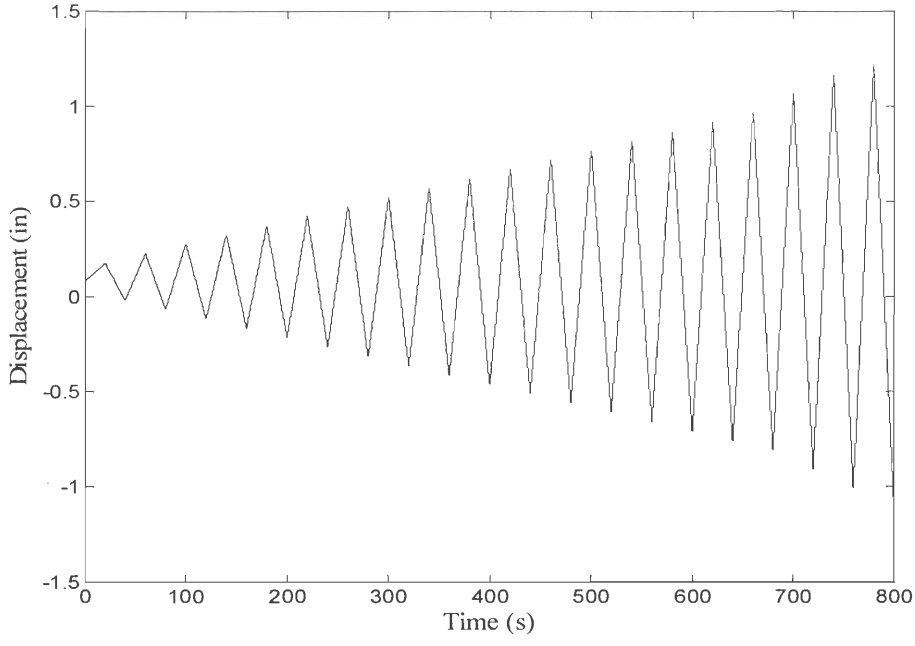

Figure 4.10. Cyclic QST Test Loading History

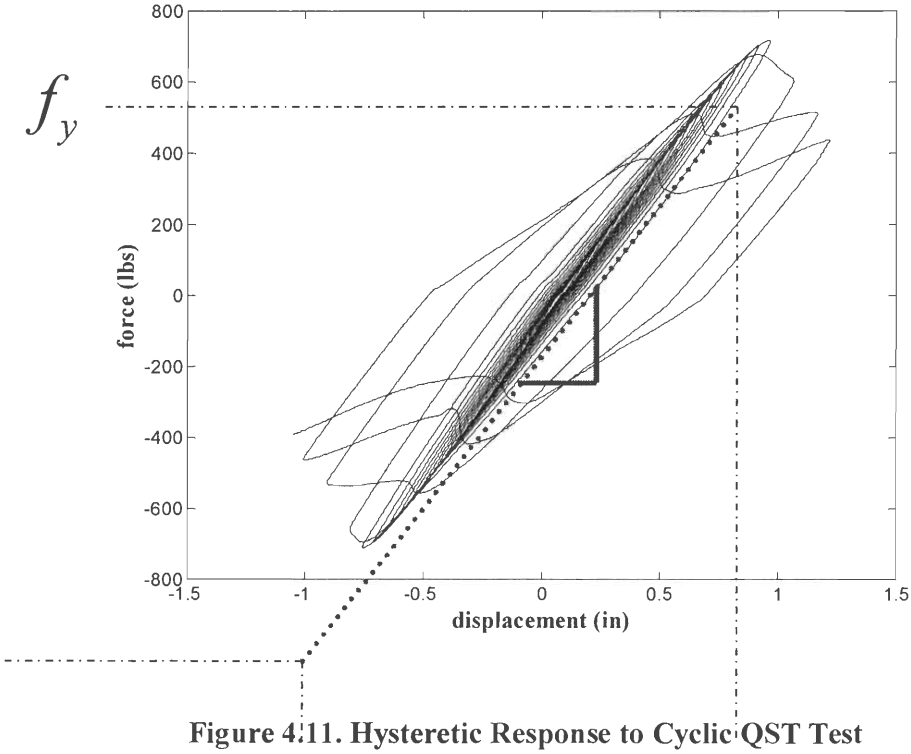

Figure 4.11. Hysteretic Response to Cyclic QST Test

4.12 Slow PSD Hybrid Simulation Control Scheme Development

Developing the control scheme for slow PSD hybrid simulations was approached in three empirical phases; each phase included multiple PSD simulations, modified slightly from the last one to examine the effect of individual parameters. First, control parameters specific to LESS facilities were characterized and methods of slowing down the loading rate and triggering the force measurement were examined. Second, a more complex numerical model and error compensation were introduced into the control scheme. Last, the hybrid controller's execution rate was increased to a speed closer to UA and UB controllers. The results of each test were validated by comparing to the results obtained from the numerical simulation of the specimen's response predicted by the initial stiffness. Each phase of testing and validation is discussed herein. Table 4.5 lists all the slow PSD hybrid simulations discussed in this section. For reference, the Simulink model of the control scheme for slow PSD hybrid simulation is pictured in Figure 4.12. The MATLAB initialization code, embedded subsystems, and embedded MATLAB scripts are all provided in Appendix A

Table 4.4. Summary of Stable Slow PSD Simulation Experiments

		ID	Slow Rate	eScale	Hit/Force Delay	Remark
SDOF Phase 1		1	40	0.7	40/30	Step/hold command and force feedback delay
MDOF	*Phase 2*	2	40	0.5	40/30	Tracking error compensation. Increased force feedback delay.
		4	20	0.9	20/18	
		5	40	0.5	40/35	Error tracking compensation (future work)
	Phase 3	7	20	0.7	200/150	Simulation step(sdt) = 0.001; Controller running at 1000 Hz
		8	20	0.5	200/150	

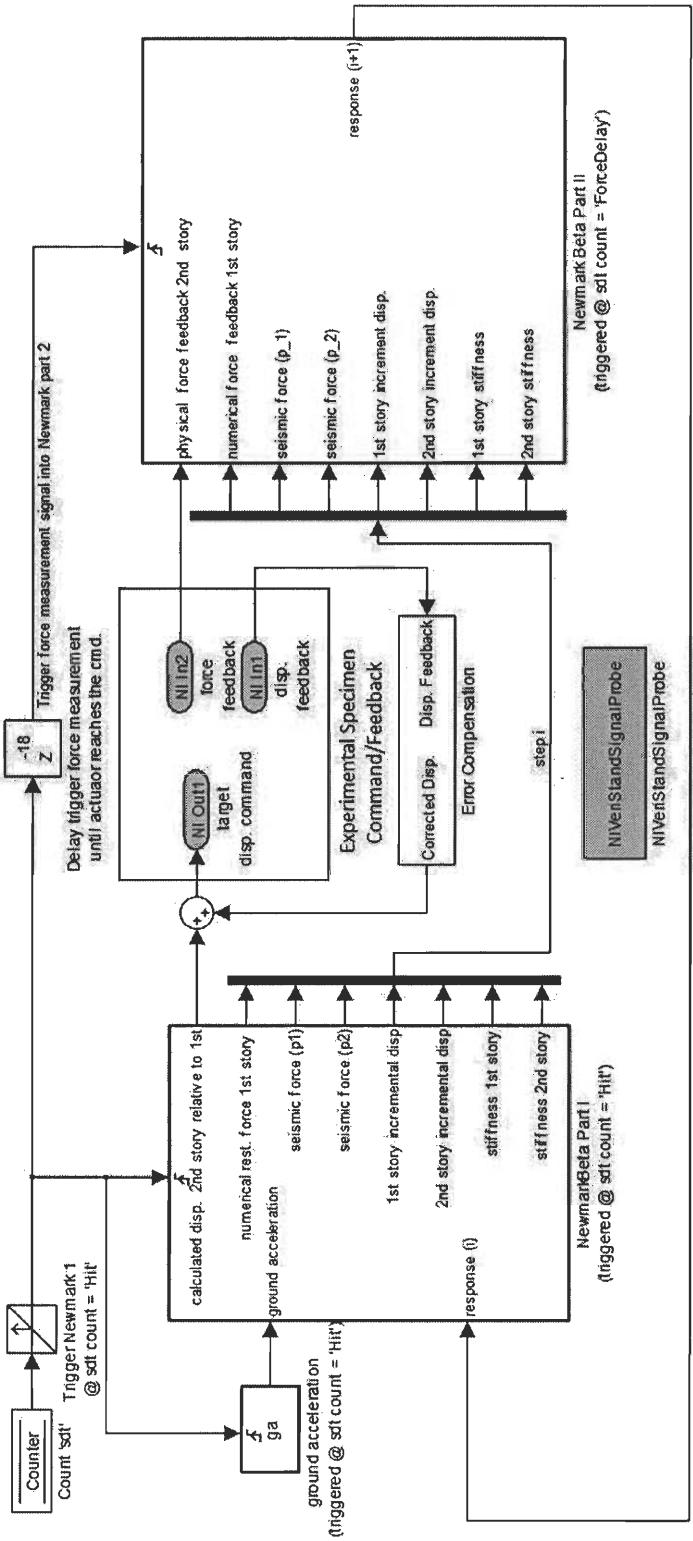

Figure 4.12. Simulink Model with NI Signal I/O: Control Scheme for Slow PSD Hybrid Simulation

4.13 Phase One: Step/Hold Loading Pattern

The objective of the first phase of simulation development characterized the performance of the LESS hydraulic and real time controllers and proposed the strategy to slow down the actuator loading rate accordingly. Initially, the use of the 'decimation' function in the real-time controller was attempted to slow the rate. In a decimated PSD hybrid simulation, the primary control loop passes through a predefined number of iterations (decimation factor) before calling the next command signal from the DAQ. For example, if a decimation factor of 10 is set in the real time controller, and the restoring force value is read every 0.01 seconds (the integration time step), the primary control loop will run 10 iterations with the same restoring force value, before calling the next value . This causes vibration in the specimen during the command holding phase and force feedback not at the desired time; therefore no stable PSD hybrid simulations were obtained using decimation slow down method.

A controlled step/hold loading pattern was then developed to slow down the loading rate and to delay the force feedback until the actuator reaches its target displacement. This method is appropriate when there are no velocity dependent devices present, in other words, time can be considered irrelevant to the structural dynamic response.

The step loading pattern was achieved by introducing a triggered signal block in the Simulink model and defining a factor by which the loading rate is slowed (slow) and a simulation step (sdt) in the initialization script. Figure 4.13 illustrates the Simulink model for a step loading pattern command. Each integration step (i) (Δt in integration) is carried over a predetermined number of simulation steps, initially

defined (Hit). The following script was included in the Matlab initialization file do define the slow rate; simulation step, Hit value and ForceDelay, where ForceDelay defines the number of simulation steps carried out before the force is measured and fed into the second portion of the Newmark integration.

```
%% Trigger Integration Algorithm
slow=40;
sdt=0.01;
Hit=dt*slow/sdt;
ForceDelay=0.75*Hit;
```

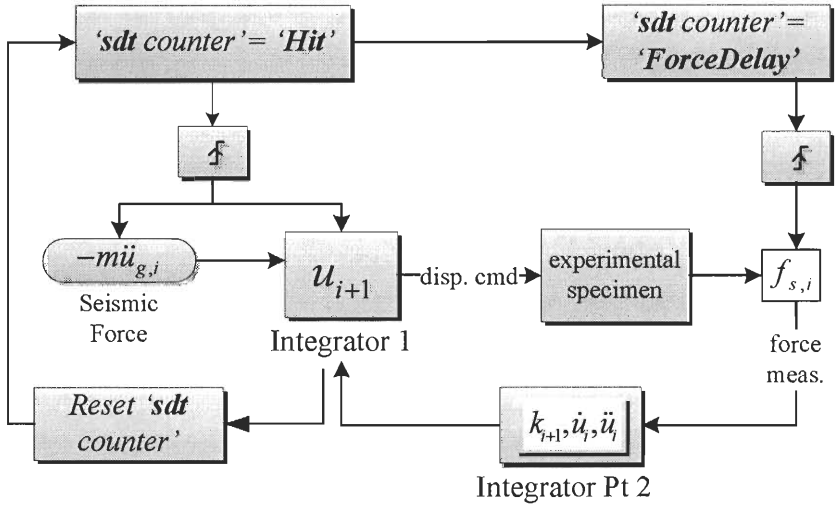

Figure 4.13. Diagram of Triggered Step/Hold Pattern

A counter function within the Simulink model counts the simulation steps, triggering the next integration step when the 'Hit' value is reached. The target displacement of one integration step generates an identical command signal for each simulation step execution, thus resembling a step. For example, a simulation slowed by a factor of forty generates forty identical command signals to the controller from a single target displacement value. Upon reaching the fortieth execution, the next integration step is triggered. In this phase, the controller was running at 100 Hz, thus a single integration step lasts 0.4 seconds in real time. This slowed step command

allows a slow actuator to "catch up" with the command displacement, as illustrated in Figure 4.14. Ideal loading rate depends on system performance; however, the target displacement must be achieved by the actuator within a single integration step to ensure stability of the test.

In a closed loop simulation with a slowed loading rate as discussed above, an accurate force measurement corresponds to the target displacement. The force feedback signal generated upon the execution of the first simulation step provides a restoring force measurement before desired target displacement is achieved. An integer delay block in the Simulink model defines a number of simulation steps (ForceDelay) to be executed before generating a force feedback with a triggered signal as a portion of the 'Hit' value (for example z^{-18} in Figure 4.13 delays force measurement 18 simulation steps). As with slowed loading rates, the ideal force measurement delay depends on the control system performance. Figure 4.14 illustrates the ideal point of feedback signal generation with respect to actuator lag. Triggering force feedback signal too early or too late in the time-step will cause inaccurate simulation responses and/or propagation of errors that jeopardized the system stability.

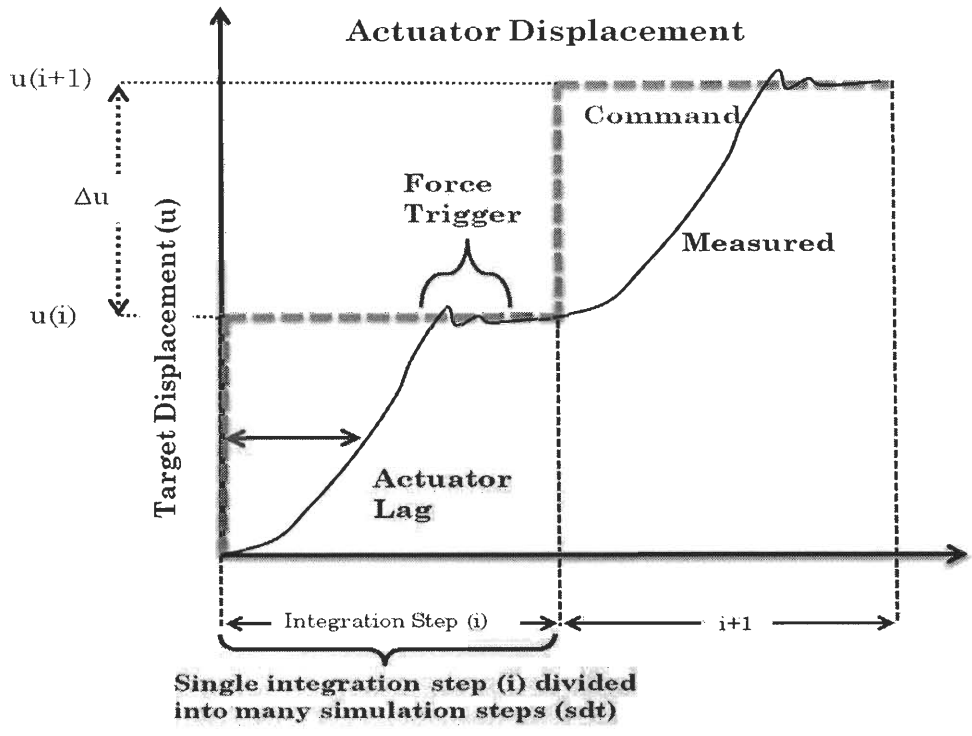

Figure 4.14. Ideal Force Feedback Signal Delay

A slow PSD simulation of the SDOF specimen was conducted at forty times slower than real time with force measurement delayed by thirty steps. The specimen experienced a maximum displacement of approximately 0.5"; the analytical model predicted a maximum displacement of approximately 0.7". Ground acceleration was scaled by 0.7 to maintain linear behavior in specimen (Figure 4.15). The slight slippage observed at the 'zero' displacement is attributed to the imperfect pin connection fabrication described in Section 4.8. To verify signal compatibility the simulation was replicated, replacing the SDOF numerical model with Clemson's MDOF numerical model, described in Section 4.9. Similar results were observed and Clemson's numerical model was implemented in all of the following simulations.

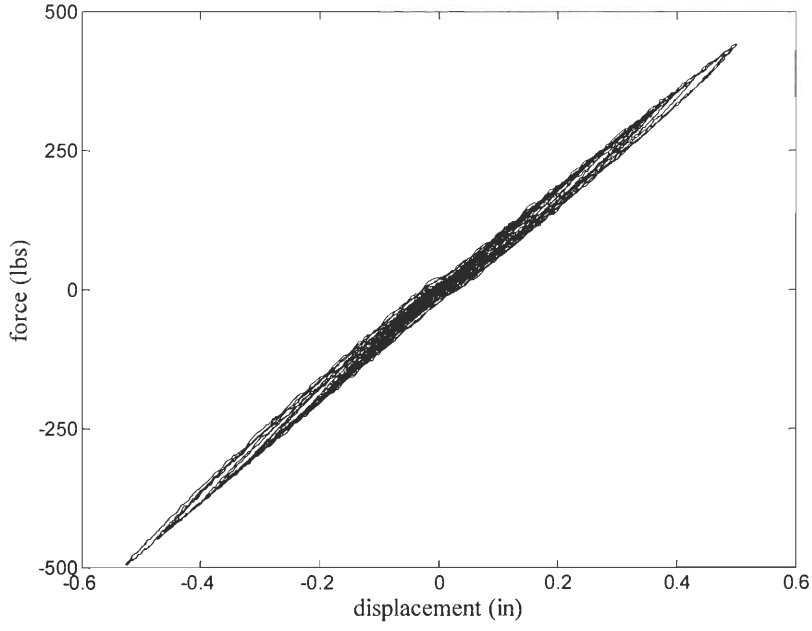

Figure 4.15. Linear Hysteretic Response (Phase 1: triggered force measurement)

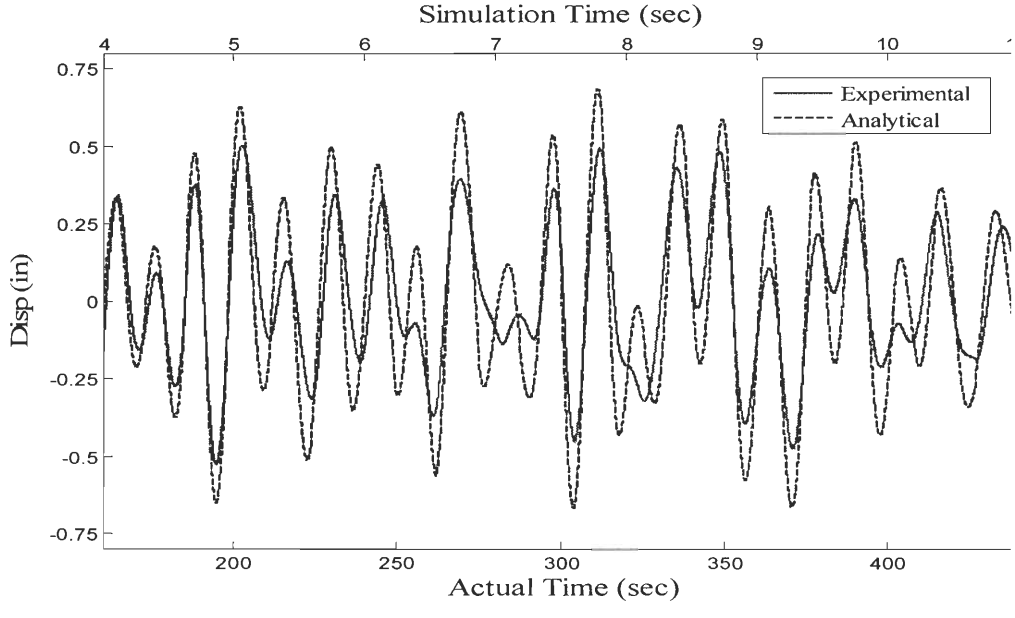

Figure 4.16. Peak Experimental and Analytical Displacement Response (Phase 1: triggered force measurement)

For validation, the results of the experiment are compared to a numerical model in which the specimen's initial stiffness determines the restoring force. Significant error was observed in the displacement response of the experiment and numerical model (Figure 4.16).

Actuator tuning, specimen installation and loading rate were all inspected as sources of inaccuracy. Another test was attempted at twenty times slower resulting in instability. It was determined the actuator does not reach the desired target displacement within the time-step, with the actuator tuned to its best performance using the hydraulic controller discussed in Section 4.2.1. Figure 4.17 and Figure 4.18 illustrate the actuator tracking error, leading to an unstable test. Therefore an error compensation was introduced into the control scheme as discussed next.

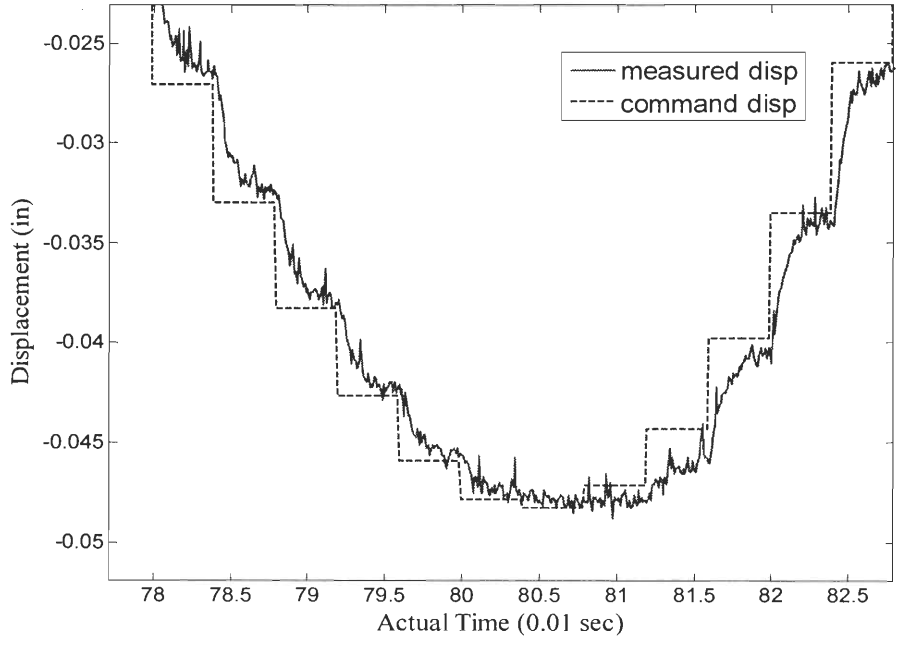

Figure 4.17. Inherent Time Delay in Actuator

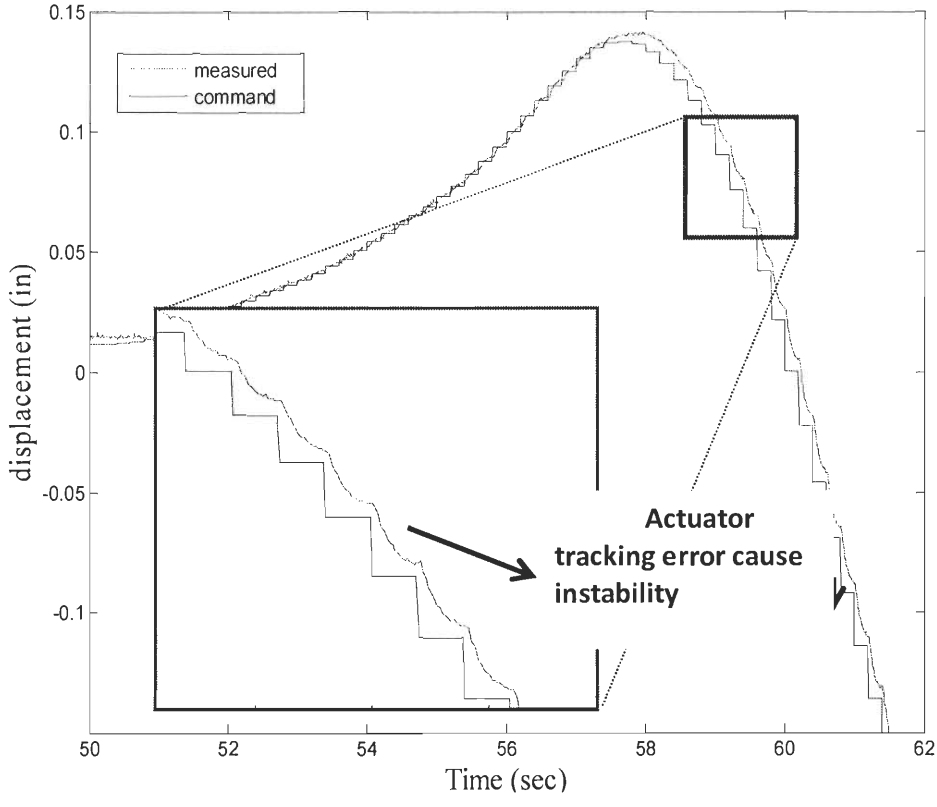

Figure 4.18. Unstable Slow PSD Hybrid Simulation at 20X Slower

4.14 Phase Two: Error Compensation

The objective of the second phase development of slow PSD hybrid simulation was to introduce error compensation to the existing control scheme. Due to inherent actuator delay and its imperfect performance of tracking the command, the target displacement of the previous control scheme is not reached within a single integration step. A feed forward error compensation method was adopted. The discrepancy ("Error" in Figure 4.19) between the command target displacement and target displacement feedback feeds into the next integration step to be added to the calculated displacement for the corrected target displacement command signal.

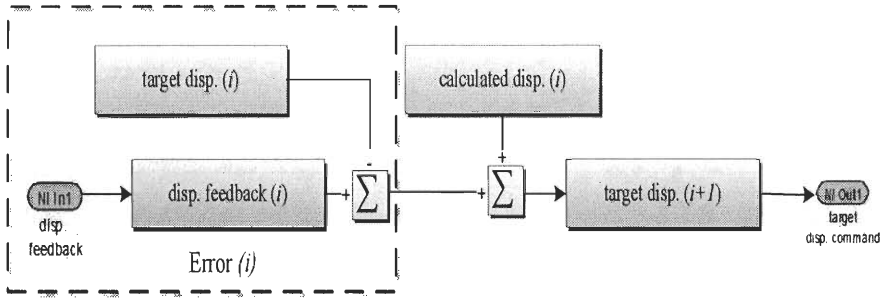

Figure 4.19. Error Compensation Scheme

Three slow PSD simulations were conducted in this phase; first, displacement error compensation was added to the control scheme described in Section 4.13 with other parameters unchanged. Figure 4.19 shows the Simulink subsystem for error compensation shown in Figure 4.12. Next, it was repeated at a loading rate twenty times slower with a ground acceleration scale of 0.5 to maintain linear behavior in the specimen to verify its performance for a faster (twice faster) hybrid simulation. Reasonable agreement was seen between the experimental response and the numerical response of the specimen. The displacement response is shown in Figure 4.20.

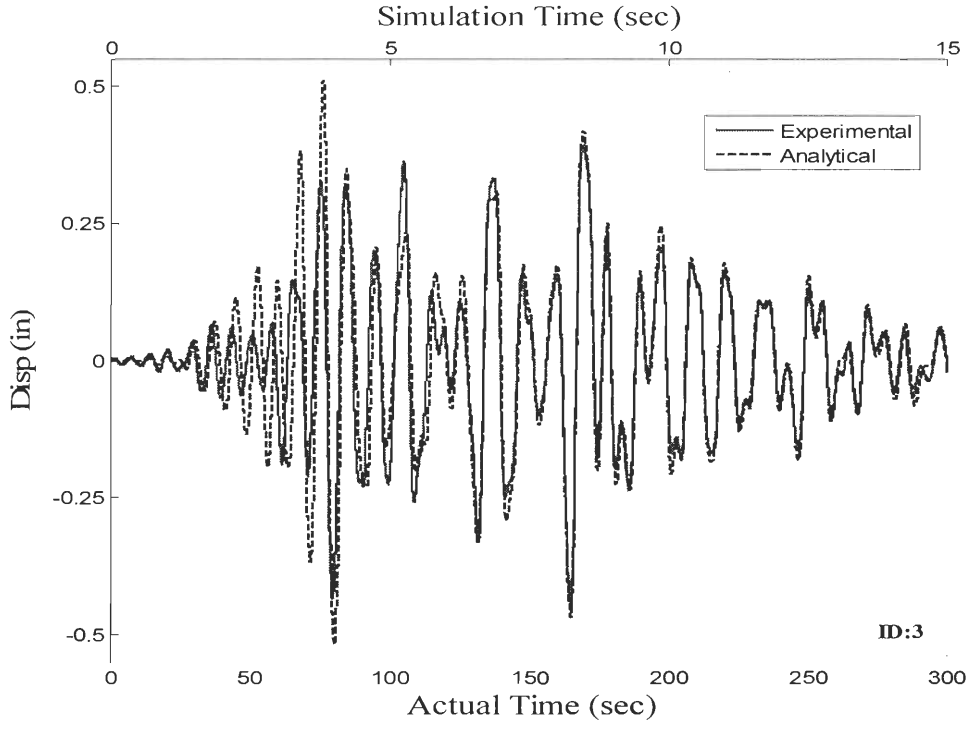

Figure 4.20. Linear Experimental and Analytical Displacement Response (Phase 2: feed forward error compensation and triggered force)

Finally, the control scheme was repeated at a loading rate twenty times slower at a ground acceleration scale of 0.9 to observe the controller's performance when specimen reaches nonlinear response. Figure 4.21 shows the displacement response around the peak. As expected, reasonable agreement is seen until the yield displacement, after which the specimen became nonlinear which is not accounted for in the numerical model. The results were compared to a nonlinear range QST (Figure 4.22) demonstrate reasonable agreement.

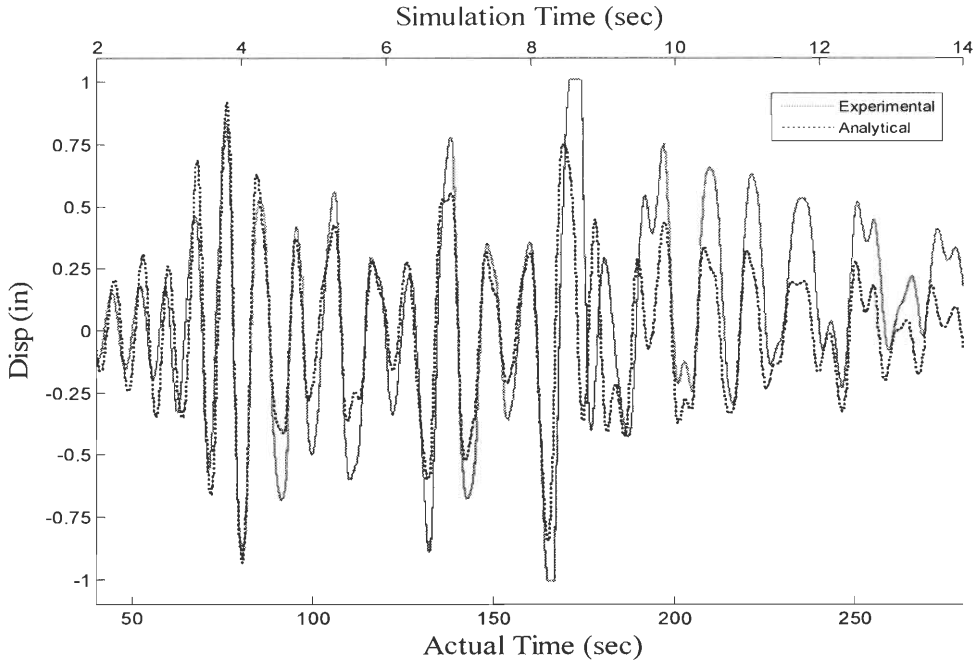

Figure 4.21. Nonlinear Experimental and Analytical Displacement Response (Phase 2: feed forward error compensation and triggered force)

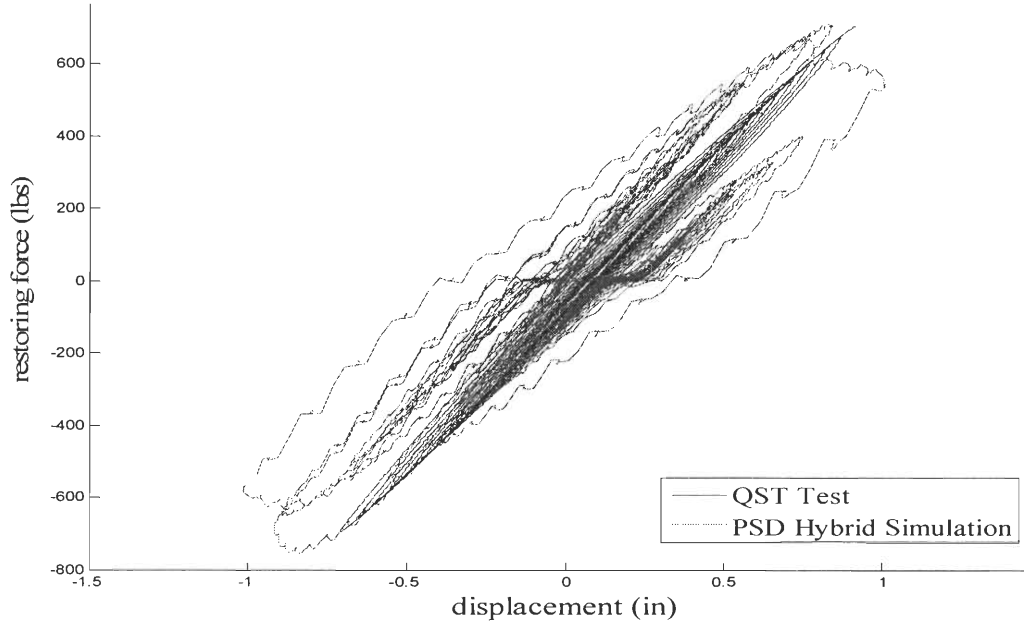

Figure 4.22. QST and PSD Simulation Nonlinear Hysteretic Response (Phase 2: feed forward error compensation and triggered force)

A second compensation technique was attempted which monitors the error between command and feedback. At each simulation step, the displacement feedback is subtracted from the displacement command. This value is fed into an "If Action" subsystem in the Simulink model which checks whether it is within a desired tolerance. If the error is within the preset tolerance, a force feedback measurement is triggered. If not, the force reading from the previous step is fed into the integrator. Due to time constraints, no further exploration of this compensation was pursued in this study.

4.15 Phase Three: Increased Controller Execution Rate

The hybrid testing controllers at the structural engineering laboratory at UA and the NEES equipment site at the State University of New York at Buffalo (UB) run at a much higher execution rate than the controller at LESS (100 Hz in the previous two phases). The objective of the third simulation development phase was to evaluate how increased controller speed would affect the control execution. A higher execution rate will potentially increase the accuracy of feedback signals but requires more computing power for data analysis. The hybrid controller execution rate was increased from 100 Hz to 1000 Hz. A PSD simulation was conducted at a loading rate slowed by a factor of twenty. The simulation step was reduced to from 0.01sec to 0.001sec; the 'Hit' value is now ten times the 'slow' value, whereas they were identical in all previous tests. Feed forward compensation described previously was also implemented in this test. The physical displacement response is compared around the peak displacement (Figure 4.23) shows agreement and that this control scheme is the most ideal.

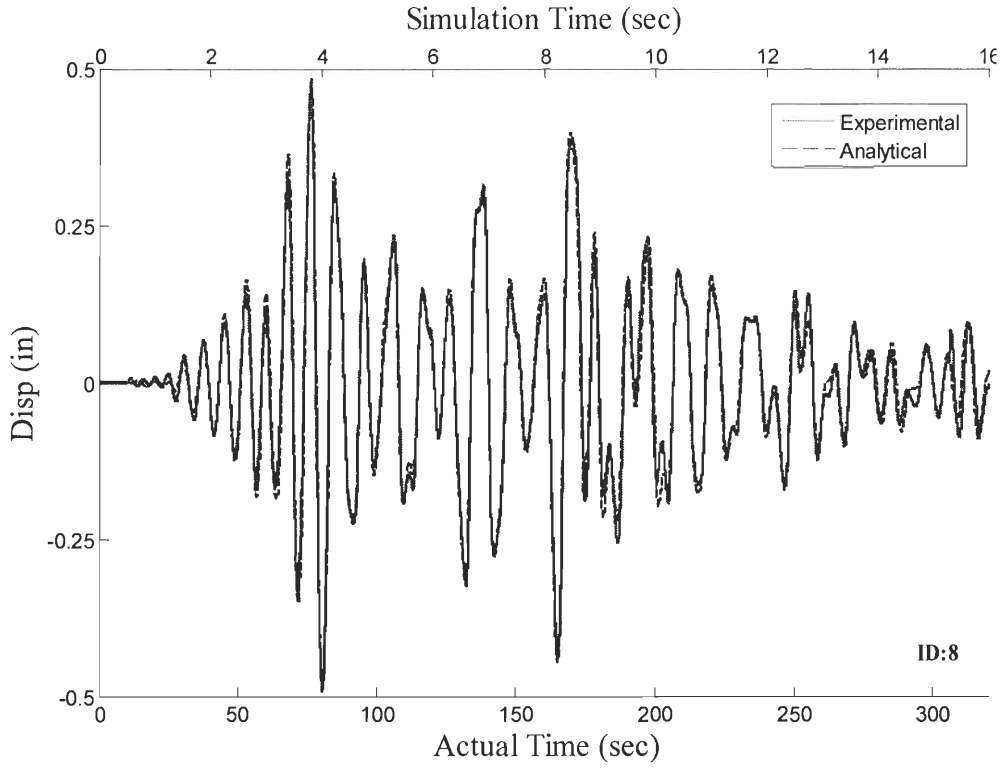

Figure 4.23. Phase 3: Peak Experimental and Analytical Displacement Response (Phase 3: increased execution rate, error compensation and triggered force)

4.16 Real Time Hybrid Simulation

Experimental evaluation of wood shear walls installed with energy dissipation devices was proposed in the NEES-Soft project. Structural systems installed with such devices exhibit rate-dependent behavior that cannot be accurately evaluated using the conventional (slow) PSD simulation. Real-time PSD (RT-PSD) hybrid simulation control scheme was attempted at LESS for the proposed experiment. As discussed in Section 4.12, the hydraulic linear actuator at LESS introduces delay to the control system which leads to instability in the experiment. Actuator delay compensation for RT-PSD was developed to account for the adverse effect of actuator delay. Figure

4.24 illustrates the actuator delay observed in Test 8 of the previous section and a 0.06sec delay in actuator response was determined.

Table 4.5. Summary of RT PSD Simulation Experiment

ID	dt/sdt (sec)	Actuator Delay (simulation step)	eScale	Model	Real time controller rate	Remark
RT1	0.01/0.01	6	0.3	SDOF	100 Hz	Tracking error compensation & Smith predictor delay compensation

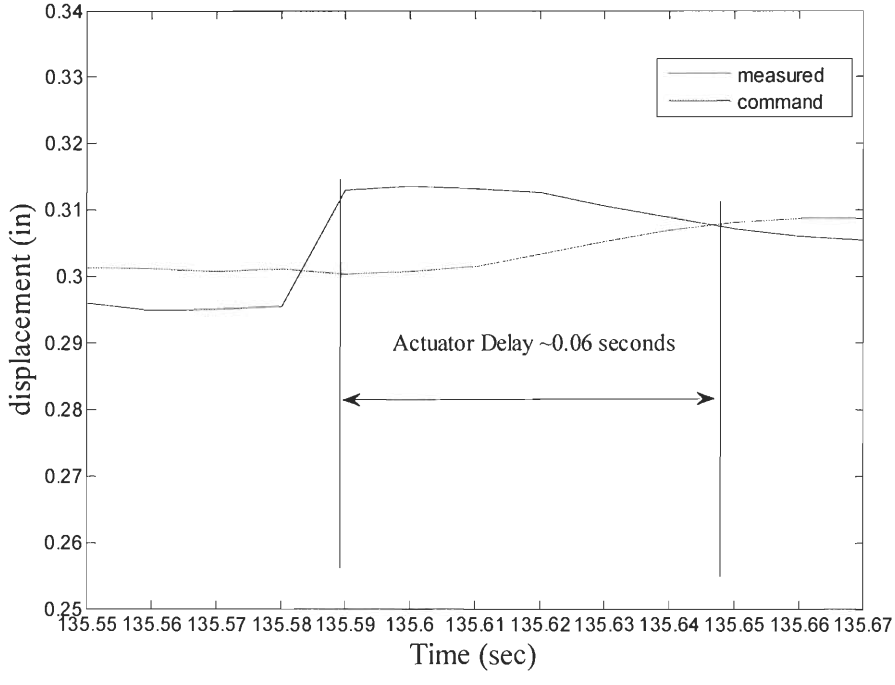

Figure 4.24. Estimated Actuator Delay

A Smith predictor (Smith 1959) was developed to account for the adverse effect of actuator lag on force feedback measurements. The Smith predictor method employs an estimated model of the physical system to predict its delayed behavior and compensates accordingly in the controller. By estimating actuator delay, the delayed restoring force can be predicted and used in determining the displacement command for the next numerical time-step. In the Smith predictor adopted in this study, the actuator was molded as a pure time delay specified by the number of simulation time-steps (sAdl=6). The structural model is the initial stiffness determined from the QST test. Figure 4.25 shows the illustration of the Smith predictor block in the Simulink model (Figure 4.26) for RT-PSD hybrid simulation. The desired target displacement is sent to the structural model to generate a predicted restoring force at that displacement. The error in restoring force measurement associated with the actuator delay is adjusted in the controller. The adjusted force is fed into the integrator for the current time step. The actuator model in Figure 4.26 defines an estimated delay; that was 0.06sec observed by comparing the actuator feedback with its command from the previous test (see Figure 4.24). A random number generator is used to consider amplitude mismatch of the actuator if necessary; in this study it was set to 0. The following code is included in the initialize file to define the Smith predictor parameters:

```
      %Smith predictor model
      SAdl=6;       %delay step in terms of sdt=0.01sec, 0.06 sec
delay total
      SAMean=1.00; %random signal to simulate error in actuator displ.
performance.
      SAVar=0.000; %when Mean =1.0, Var=0, there is no error.
      SKo=Ko;       %estimated structure stiffness
```

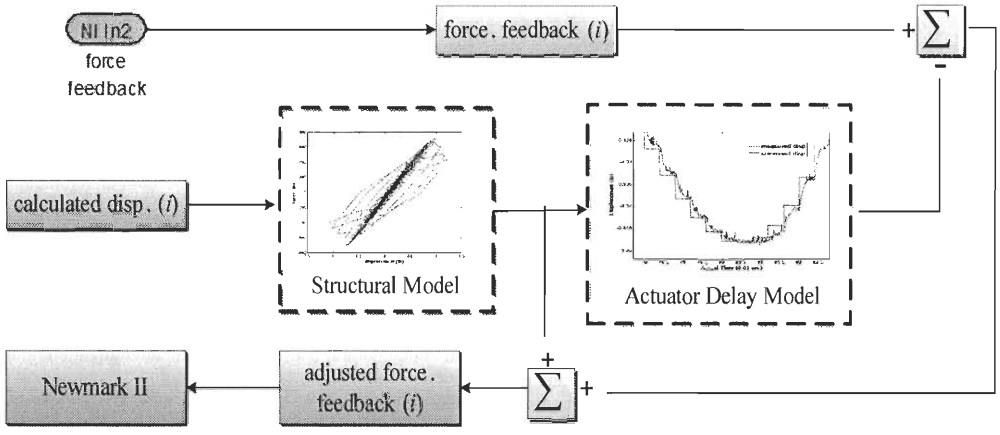

Figure 4.25. Smith's Predictor for Real-Time PSD Hybrid Simulation

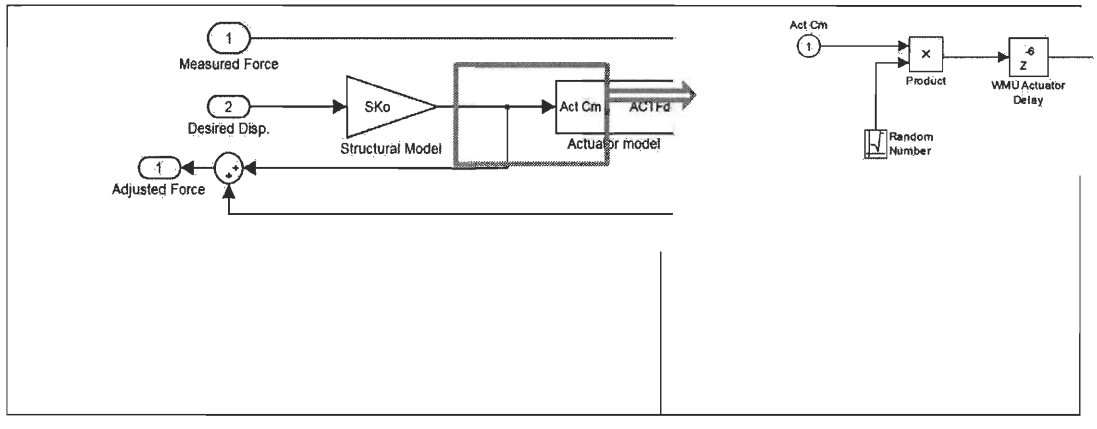

Figure 4.26. Simulink Model for Real-Time PSD Hybrid Simulation

4.17 Conclusion

A series of small scale PSD hybrid simulations were conducted at the WMU to develop a control schemes for PSD hybrid simulations. Three phases of PSD hybrid simulation tests were conducted at various amplitudes. First, a "step/hold" command was introduced ensuring the target displacement was reached in one integration step;

at this point a "triggered" force measurement for the restoring force corresponding for the target displacement is fed into the integration algorithm. Second, a method of error compensation was introduced to address the error in the actuator command tracking. Finally, the real-time controller rate was increased from 100 Hz to 1000 Hz. Results of each test were compared to purely numerical simulations of an analytical model of the specimen, based on a cyclic test. The control scheme will be adopted in the large scale experiment at the UA (Chapter 5) and contribute to the development of six DOF PSD hybrid simulation of the NEES-Soft project; therefore is suitable for multiple facilities and specimen types.

CHAPTER 5

LARGE SCALE PSEUDODYNAMIC SIMULATION AT THE UNIVERSITY OF ALABAMA

5.1 Introduction

This chapter presents the large scale hybrid simulations conducted at the newly constructed Structural Engineering Laboratory at University of Alabama (UA). Preliminary cyclic testing and single degree of freedom (SDOF) pseudodynamic (PSD) simulation was conducted to characterize the testing system and develop the corresponding control compensation method; then full scale hybrid simulations was conducted. The prototype structure is a two story wood frame building modeled as a two DOF structure with a physical first story and a numerical second story. The objective of this series of experiments was to apply the PSD hybrid simulation control scheme developed at WMU to the wood frame building. This experiment serves as a basis for the hybrid simulation of the NEES-Soft project; three of the five universities collaborating on the NEES-Soft project participated in this experiment: Colorado State University (CSU), Clemson University (CU) and Western Michigan University (WMU). The experimental protocol for hybrid simulation in the NEES-Soft project is led by WMU; therefore this chapter focuses only on the control scheme development; structural performance is not analyzed. The wood shear wall specimens are designed at CSU and the numerical models and the integration algorithm are developed at CU.

5.2 Experimental Equipment

5.3 Hydraulic Actuator and Hydraulic Controller

Hydraulic actuator and its associated controller are required to apply the step-by-step simulated displacement responses onto the physical substructure during PSD hybrid simulation as discussed in Section 2.5. The actuator used in the UA hybrid simulation was an MTS Model 244.31 hydraulic actuator with a force rating of $\pm$ 55 kip and a 40 inch stroke ($\pm$20 inches). The actuator's hydraulic flow is controlled by an electro-hydraulic servo valve (MTS Model 256.25A-01) with a maximum flow rate and pressure of 250 gpm at 2800 psi; therefore the actuator has a maximum velocity of 50 inches per second (piston area: 19 square inches). The actuator is attached to the reaction blocks to apply displacement command at the top of the wall; it is equipped with an internal linear variable differential transducer (LVDT) and a 55 kip capacity load cell transducer to measure displacement and force, respectively.

The hydraulic control of the actuator was provided by the MTS Series 793 Controller and it's on board DAQ system that provides the exchange of command and feedback data. Control channels, feedback signals, engineering unit conversions were configured in the MTS MultiPurpose TestWare® (MPT) Software (2010) and actuator turning was performed using MTS MPT software as well. Processes are modular test activities, such as command and data acquisition, and are represented by icons on the process palette in the MPT software. External control processes, which issue signals to devices external to the servo loop control system, is necessary for the proposed PSD hybrid simulation to accept simulated displacement responses of the physical substructural as displacement commands for the actuator from the real time

controller. Figure 5.1 shows the icons in the MPT software for enabling external command.

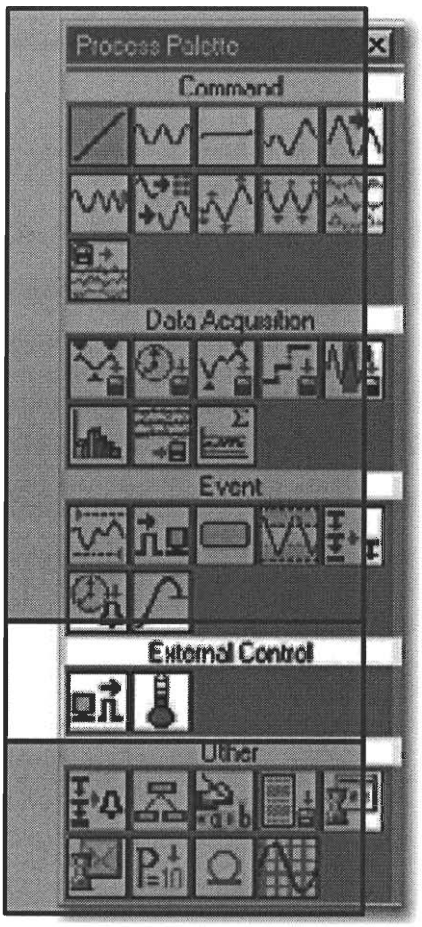

Figure 5.1. Enabling External Control in MTS Hydraulic Controller

5.4 Real-Time and Hybrid Testing Controller

Real-time control was enabled by the MPT software with the MTS Series 793 hydraulic controller and carried out by two computers: a "host" PC as the hybrid testing controller and a "target" PC as the real time controller. The data communication with the hydraulic controller is provided by the SCRAMNet Network (Systran 2006), which enables the high speed, low-latency transfer of data. This interface is fundamental to PSD hybrid simulation; it allows the real time controller to

simultaneously send target displacements calculated in the hybrid simulation model to the actuator while obtaining the force measurements used in calculating the next step's displacement.

The real time controller is a 3.0 GHz Xeon dual-core processor target PC. Inputs and outputs (I/O) are configured directly in the Simulink model in the hybrid testing controller as SCRAMNet signal blocks. A MathWorks hardware-in-loop simulation software, xPC™ Target, provides a real-time kernel that allows the execution of the numerical model by connecting the hybrid testing and the real time controllers. Within the hybrid testing controller, the structural properties of the numerical substructure are integrated with the physical restoring forces of the specimen to simulate the overall system's seismic response. The numerical model of the prototype mass, viscous damping and the analytical force-displacement relationship of the numerical DOF are developed using MATLAB/Simulink™ simulation modeling software. Additionally, discrepancies between the command and the feedback displacements are monitored and compensated accordingly in the hybrid testing controller.

Table 5.1 compares the hybrid simulation experimental facilities at UA and WMU. Both facilities have integrated hydraulic control system, real-time controller, and hybrid testing controller, as required by PSD hybrid simulation when being executed in closed loop. However, there is a significant disparity in the size and performance of the hydraulic equipment and the primary control loop execution rate between the two facilities. The MTS 244.31 linear hydraulic actuator at UA has a force rating almost 20 times that of WMU's Shore Western 910D actuator. Furthermore, a more powerful servo valve at UA results in a much larger maximum velocity of 50 inches per second versus 9 inches per second at WMU. The much faster

actuator at UA, with respect to the WMU actuator has a significant effect on the accuracy and stability of the PSD hybrid simulation control scheme developed at WMU, as will be discussed in Section 5.8.

Table 5.1. Experimental Facilities at LESS and UA

Experimental Component	Western Michigan University	University of Alabama
Linear Hydraulic Actuator	Shore Western 910D Force: ± 3.2 kip Stroke: ±3 inches Maximum velocity: 9 in/sec	MTS 244.31 Force: ± 55 lb Stroke: ± 20 in. Maximum velocity: 50 in/sec
Load Transducer	2.5 kip	55 kip
Servovalve	2.5 gpm at 1000 psi	250 gpm at 2800 psi
Hydraulic controller	SC6000 w/ on board DAQ and user interface	MTS Series 793 w/ on board DAQ and MTP software
Hybrid testing controller simulation software	Matlab/Simulink	Matlab/Simulink
Hybrid testing controller interface to Real time controller	NI-VeriStand	Matlab/xPC Target
External I/O Interface	SCB-68 Connector Block	SCRAMNet GT150
Real-time Controller	NI 2.53 GHz Dual-Core PXI 8108 Embedded Controller	3.0 GHz Xeon Dual-Core Real-time Target PC
Primary control loop execution rate	1000 Hz	4096 Hz

5.5 Physical Specimen

Two identical 'dummy' wood shear wall specimens (Figure 5.2) were constructed to calibrate the numerical substructure and validate the control scheme developed in Chapter 4, respectively. The third (final) PD1 specimen (Figure 5.3) was constructed for the final set of slow PSD hybrid simulation. All three shear wall specimens were 20 ft by 8 ft with 15/32" plywood sheathing. The lateral resistance of the PD1 specimen was significantly larger than that of the dummy specimens due to the difference in their connections to the base support and in the plywood sheathing, which can be seen by comparing Figure 5.2 and Figure 5.3. In all experiments, the specimen was bolted at the bottom to a 32 inch thick concrete strong floor and attached to the actuator which is mounted against the reaction block along the loading direction. The wall is supported transversely by the framing apparatus at the top to prevent undesired out of plane motion during the testing. Table 5.2 provides a summary of the physical specimens used in this experiment and their function.

Table 5.2. Summary of Three Physical Specimens

Specimen ID	Experiment	Function
Dummy 1	CUREE (2004) protocol cyclic test	Verify hysteretic loop of the CASHEW model (Folz 2000)
Dummy 2	Small amplitude open and closed loop PSD hybrid simulation	Verify control scheme for large scale loading equipment and specimen; modify accordingly
PD 1	Final slow PSD hybrid simulation	Verify developed control scheme with modification

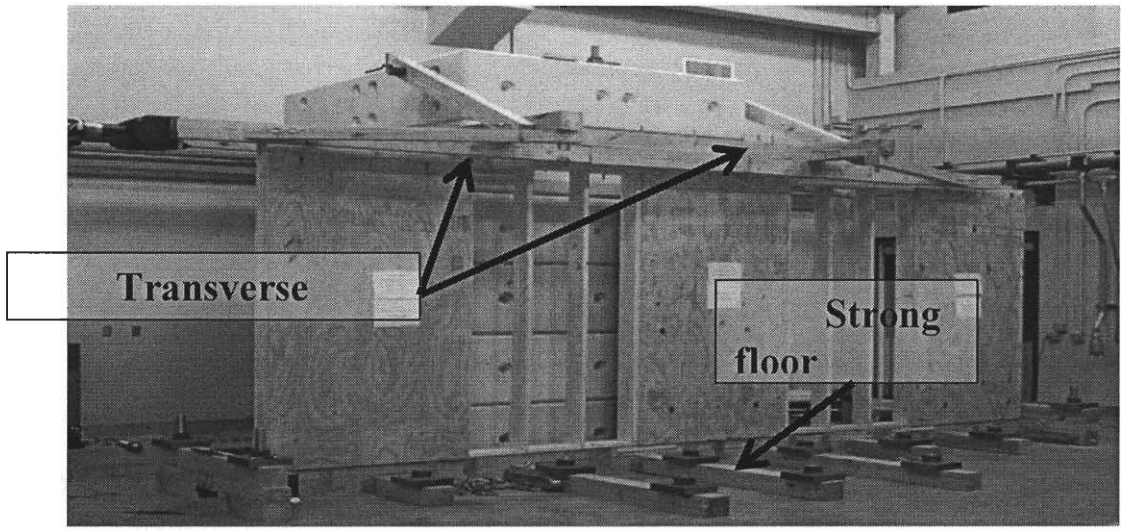

Figure 5.2. 'Dummy' Wood Shear Wall Specimen

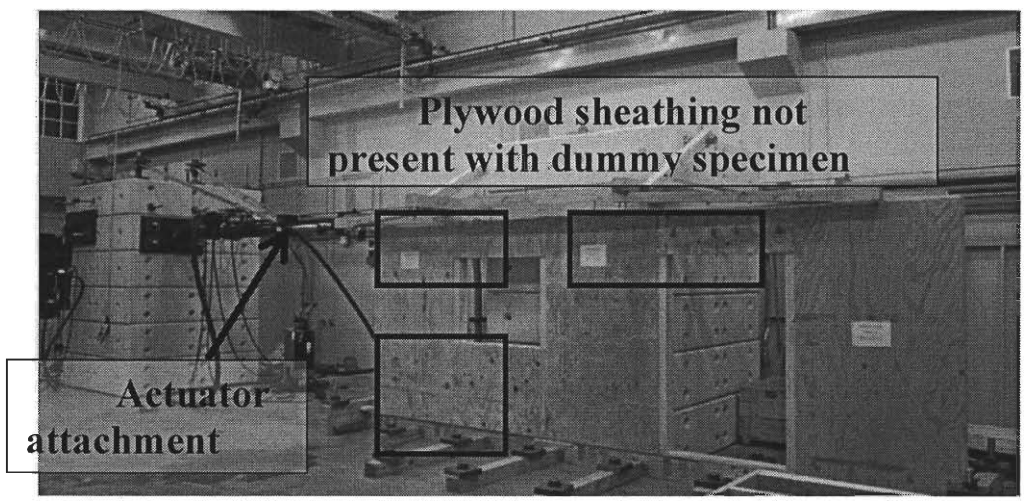

Figure 5.3. 'PD1' Wood Shear Wall Specimen

5.6 Numerical Model

The numerical substructure (DOF), the mass and damping both stories (DOFs) and the restoring force of the second story shear wall, was developed by Clemson University as part of the NEES-Soft project. Hysteretic behavior of the dummy 1 specimen was characterized in a large scale QST cyclic test. Figure 5.4 shows the

adopted CUREE protocol cyclic loading history. Figure 5.5 shows the hysteretic response of the dummy 1 specimen to the cyclic test.

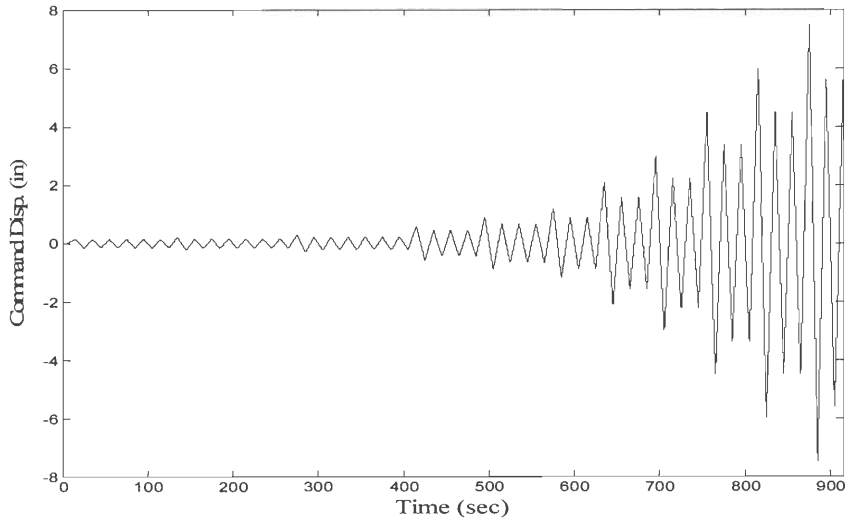

Figure 5.4. QST Cyclic Loading: CUREE Protocol

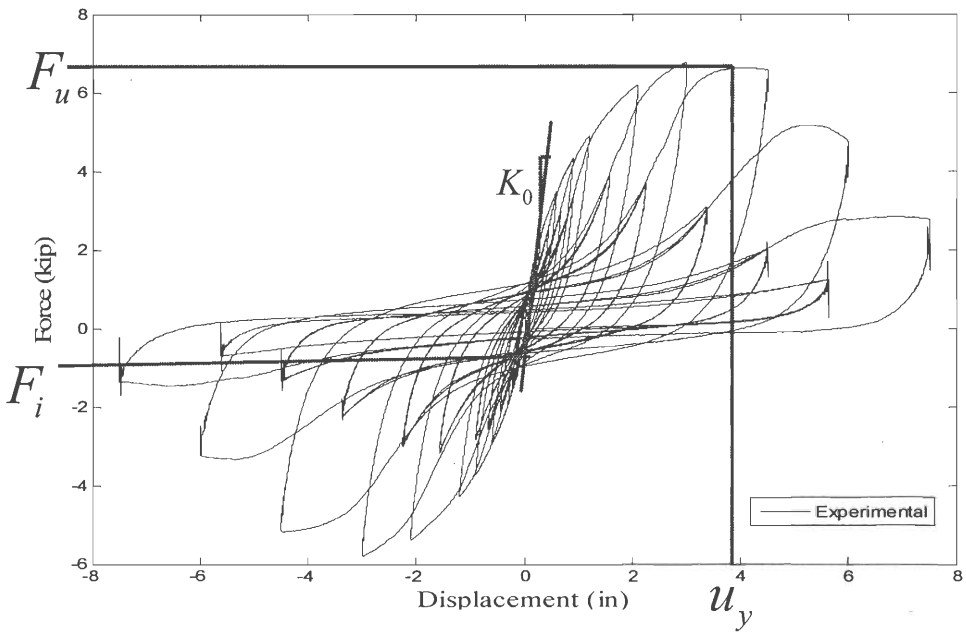

Figure 5.5. Hysteretic Response to QST Cyclic Test

The maximum displacement of the waveform was $\sim 6.3in$ applied over a 900 second span. The dummy specimen's initial stiffness was determined to be 8.2 kips/in with a yield displacement (u_y) of 3.81 inches, an ultimate force (F_u) of 6.7 kips and a loading path intersection (F_i) of -0.5 kips. The results of the cyclic test are used to calibrate the hysteretic model of the specimen based on the CASHEW model. This model serves as the numerical restoring force for the second story in all of the following PSD hybrid simulations.

5.7 Numerical Integration Algorithm

The simulated dynamic response of the two story wood shear wall assembly was computed via the implicit Newmark-β integration algorithm with a integration time step (Δt) of 1/256sec. As discussed in Chapter 2, implicit integration algorithms are superior to explicit algorithms in terms of accuracy and stability; however they require iterations, which is not feasible in this experiment. An updating tangent stiffness matrix within the numerical integration procedure was used in this set of experiments to approximate the secant stiffness that requires iteration to be obtained. An explicit target displacement for the first time-step was calculated using the initial stiffness, quantified by initial small amplitude cyclic loading. At the end of each time step, the next step's tangent stiffness was calculated. The initial and step-by-step calculations were based on the procedure outlined in Section 2.4.2 .

5.8 Incremental Simulation Procedure

As stated in Chapter 2, equipment setup, structural idealization, numerical algorithms and compensation techniques are the major sources of errors within a

hybrid simulation. A predictable specimen, small scale damage free and/or easy to be repaired physical specimen, and an incremental approach are usually used to develop and verify the overall hybrid simulation procedure. In Chapter 4, a series of small-scale hybrid simulations on a predictable specimen validated the proposed slow PSD hybrid simulation control scheme. Specifically, the method of slowing the simulation and triggering accurate force measurement and a feedforward error compensation technique were validated for the WMU facility and specimen.

However, equipment setup and the corresponding performance and physical specimen of the large-scale slow PSD hybrid simulation at UA are significantly different from those at WMU which required further development of the controller scheme discussed in Chapter 4. Again an incremental process is adopted to develop the PSD control scheme for the UA facility and wood shear wall specimen. The hysteretic behavior of the physical specimen is quantified in the large scale QST cyclic test of the dummy 1 specimen. A series of open loop then small amplitude closed loop PSD hybrid simulation tests were conducted on the dummy 2 specimen; these tests are summarized in

Table 5.3. Ground acceleration inputs were from Canoga Park (G03000) and Loma Prieta (CAP000) earthquakes. The Hit value in Table 5.3 is the number of simulation steps within each integration step. Finally, three closed loop PSD hybrid simulation tests of increasing magnitude were conducted on the PD1 specimen. The Simulink model of the slow PSD hybrid simulation control scheme is illustrated in Figure 5.6. The MATLAB initialization code, the Simulink hybrid simulation model with its embedded subsystems, and MATLAB scripts are all provided in the Appendix B.

Table 5.3. Summary of Initial Slow PSD Simulation Experiments

ID	Loading	Close/open loop	Force Trigger/ Ramp/Hit	Remark
1	G03000 (1/8 scale)	Open loop	No force feedback	5 times slower; observed excessive vibration
4	G03000 (1/8 scale)	Open loop	No force feedback/160/320	Reduced loading rate to 20 times slower; Added repeating ramp to displacement command to decrease actuator vibration.
6	G03000 (1/4 scale)	Closed loop	240/260/320	Increased ground motion scale
8	CAP000 (1/4 scale)	Closed loop	319/319/320	Changed ramp/hold value and GA record. ***Finalized Closed Loop Control Scheme***

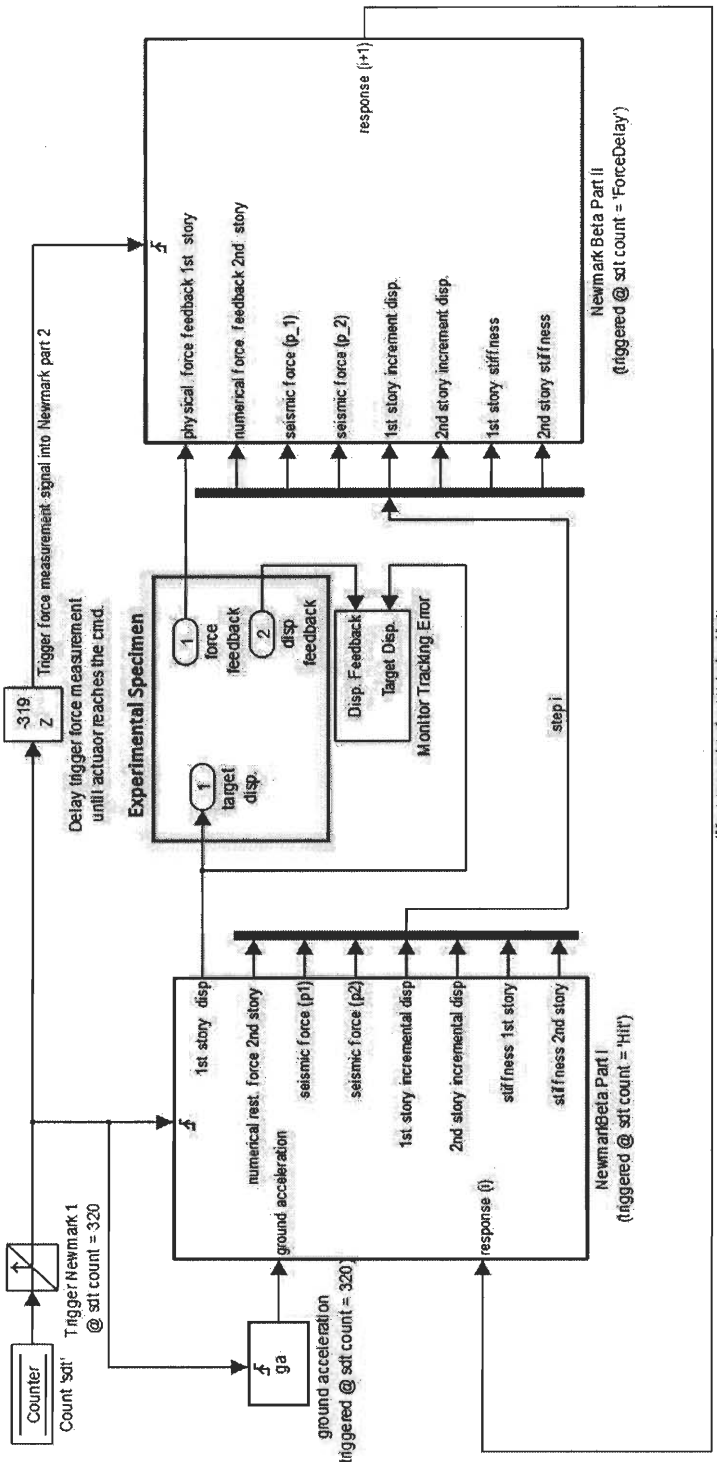

Figure 5.6. Simulink Model for UA PSD Hybrid Simulation Experiments

5.9 Ramp/Hold Loading Pattern

In Section 4.7.1, strategy to slowing down the loading rate and triggering force measurement corresponding to the target displacement was developed. This was achieved by developing a step/hold loading pattern with the definition of the *Hit* and *ForceDelay* values. The *Hit* value was defined (shown in Figure 5.8) to determine how many simulation steps to be carried out per integration step ($i = \Delta t$ in integration) with the specified slow (loading) rate. Then the "*ForceDelay*" was determined as a percentage of the *Hit* value to trigger the force reading at the desired number of simulation steps, allowing the actuator "catching up" to the command and triggering the second portion of the Newmark integration. In the final control scheme of the WMU's loading equipment and specimen, the ideal loading rate was 20 times slower, with a force measurement delay of 18 simulation steps (*ForceDelay = 0.9*Hit*).

Using the step/hold control scheme developed at WMU, excessive vibration was observed due to the very high speed UA's control system and hydraulic actuator. The primary loop rate was 4096 Hz and the MTS 244.31 actuator has a peak velocity of 50 inches per second (see Figure 5.7)

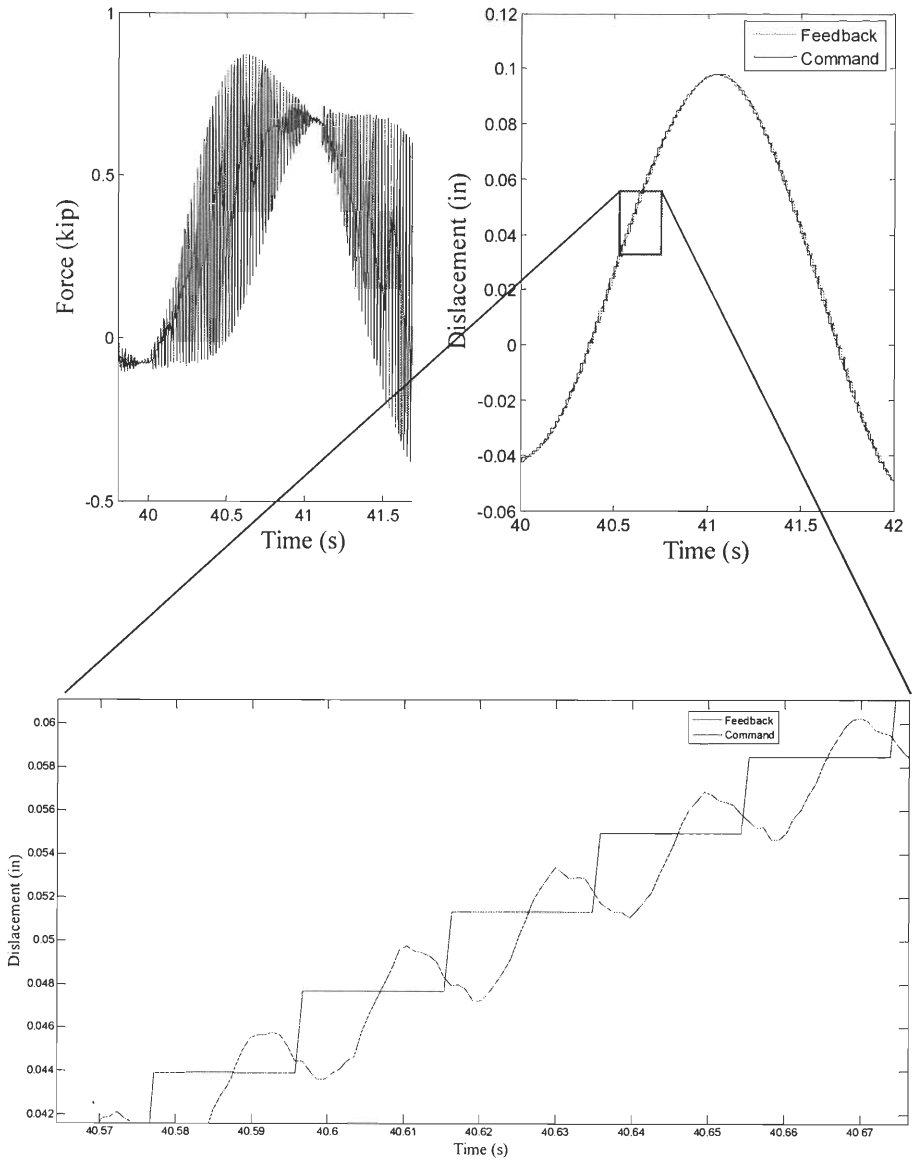

Figure 5.7. Vibration in Feedback With Step/Hold Command

Because the specimen is very lightly damped, the vibration does not have a chance to settle down before the next step command is executed, resulting in inaccurate force measurements that are not corresponding to the target displacements. This mismatch in the force reading and the displacement command causes instability in the closed loop execution of the PSD hybrid simulation. Thus a ramp/hold command was developed to minimize the vibration by "smoothing" the loading.

Figure 5.8 illustrates the ramp/hold command pattern developed specifically for UA's high performance control system and high speed actuator.

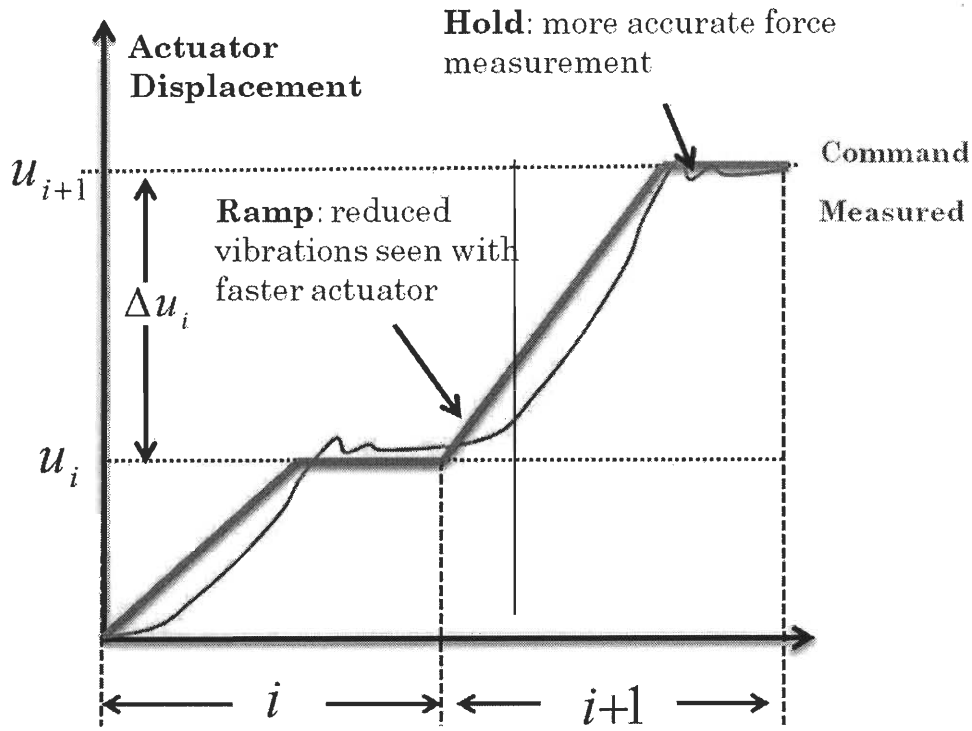

Figure 5.8. Ramp/Hold Command for UA Slow PSD Hybrid Simulation

Unlike the step/hold pattern, the ramp/hold command defines the simulation step (referred to as sub-step for clarity), h to which the command is ramped to, followed by a holding phase for the remaining sub-steps within integration step, i. The displacement at sub-step j, of integration step i, ui,j is calculated and sent to the controller at each sub-step j. A scalar factor, Rj is calculated based on the ratio of sdtj to Hit within each i. Calculation of Rj is illustrated in Figure 5.9.

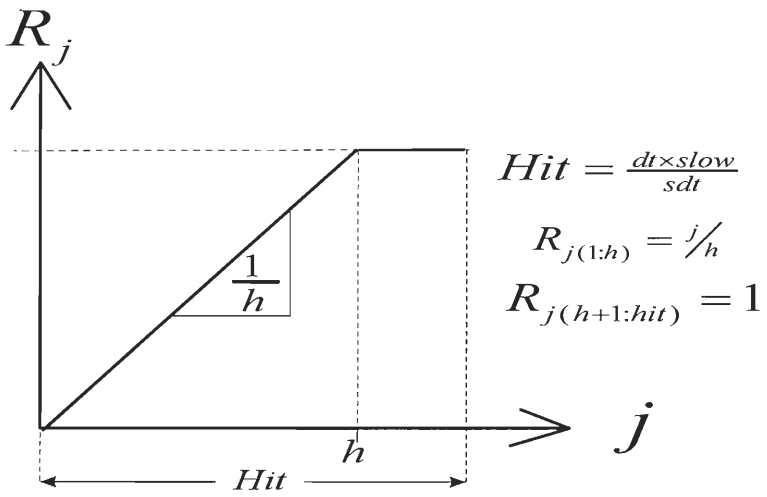

Figure 5.9. Ramp Factor of Ramp/Hold Command

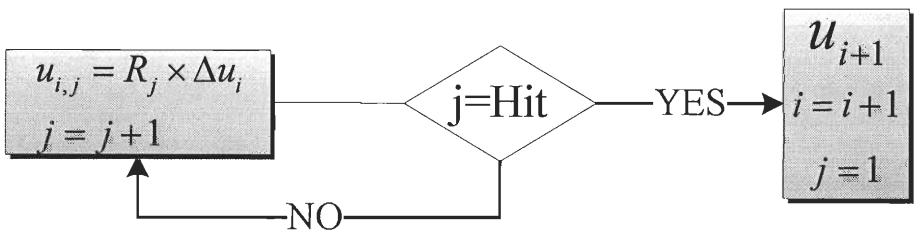

Figure 5.10. Simulation Model Input for Ramp Command

The force feedbacks of the open loop tests with (Test 4) and without the ramp command (Test 1), are compared in Figure 5.11. As is shown, the ramping command significantly reduces the vibration in the force measurements.

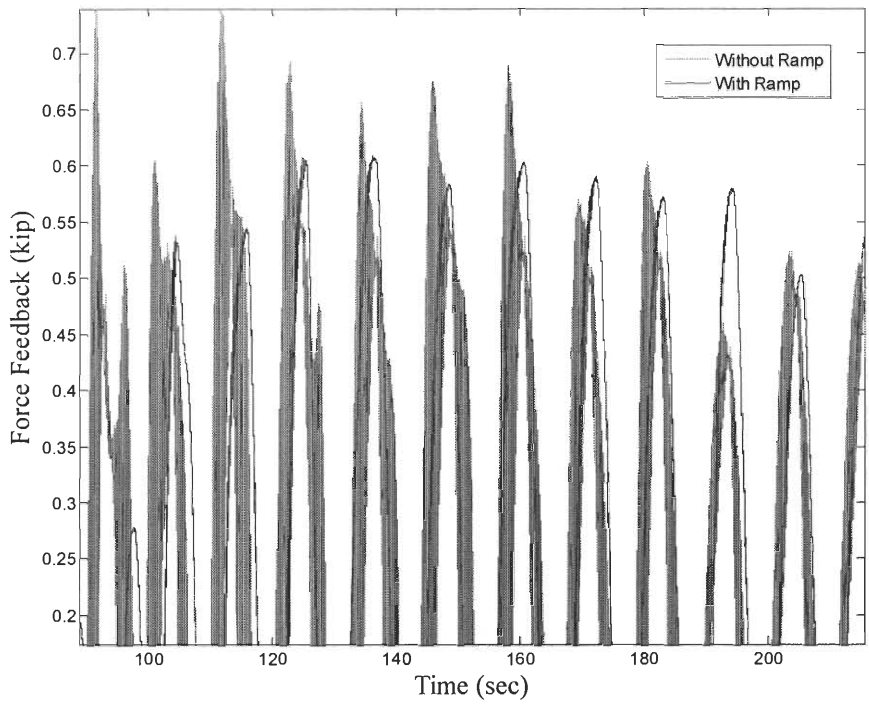

Figure 5.11. Force Readings in PSD Hybrid Simulation with Ramped Command

5.10 Actuator Command Tracking Error Compensation

Due to inherent actuator delay and its imperfect performance of tracking the command at LESS, the target displacement of each time step was not reached within a single integration step; a feed forward error compensation method was developed in to address this error. However, the actuator command tracking error was not an issue in the UA experiments; the target displacement command and feedback of Test 4 are shown in Figure 5.12 which shows an almost perfect match. Thus the error compensation developed in Section 4.7.2 was eliminated in the UA control scheme.

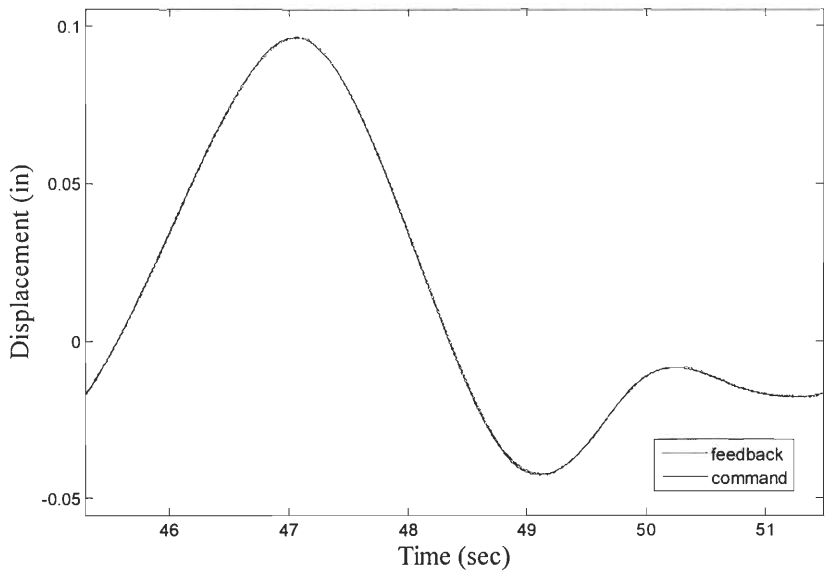

Figure 5.12. UA Actuator Command Tracking Performance

5.11 Small Amplitude Closed Loop Pseudodynamic Hybrid Simulation

Two small amplitude closed loop PSD hybrid simulations were conducted on the second dummy specimen. The first closed loop simulation, Test 6, was conducted using a ¼ scale ground acceleration. The command was ramped to sub-step 160 and held until 320, before executing the next integration step; the test verified that the ramp/hold command stabilized control scheme by reducing the vibrations observed in previous open loop tests and providing more accurate force measurements. Further reduction of vibration was achieved by adjusting the ramp and hold values in Test 8; the ramp was increased to sub-step 319, with one hold step before executing the next integration step. The reduction in vibration by increasing the ramp value is demonstrated by a much smoother force reading in Test 8 versus Test 6 as shown in Figure 5.13.

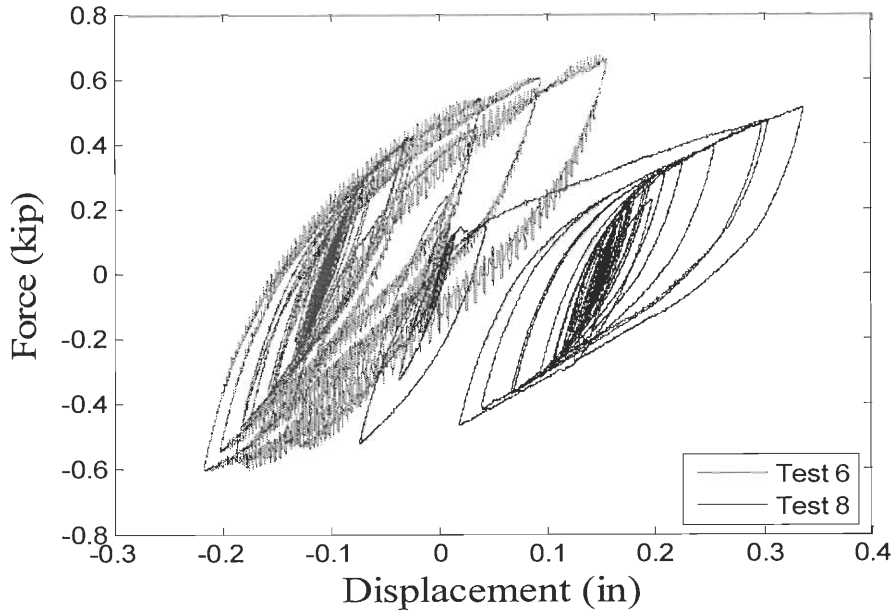

Figure 5.13. Comparison of Vibration in Hysteretic Loops of Tests 6 and 8

The control scheme adopted in the final closed loop PSD hybrid simulation of the PD1 specimen is based on the one obtained in Test 8. The hybrid simulation was executed 20 times slower. By using the UA simulation step of 1/4096sec and the predefined integration step 1/256 sec, the Hit value was calculated to be 320. The ramp was increased to sub-step 319, with one hold step before executing the next integration step.

5.12 Closed Loop Pseudodynamic Hybrid Simulation with PD1

The final control scheme modified for UA's control system and actuator performance was applied to three closed loop PSD hybrid simulations with increasing amplitudes of the PD1 specimen as the physical substructure representing the first story. The amplitude was first increased by scaling up the ground acceleration, then by scaling up the model mass. Table 5.4 summarizes the amplitudes of the ground

acceleration inputs represented by their return period and the modal mass scale of each test. The initial stiffness, quantified by the initial low amplitude cyclic loading, was 22.3 kips/in. The PD1 specimen had more plywood sheathing (discussed in Section 5.5) resulting in a much higher initial stiffness the previous specimens.

Table 5.4. Summary of Final PSD Hybrid Simulation Tests of PD-1

ID	Acceleration Return Period	Mass Scale
1	72 year	30%
2	2500 year	30%
3	2500 year	100%

All simulations were conducted at a loading rate twenty times slower, with an integration step of 1/256 sec and a simulation time step of 1/4096 sec. 320 sub-steps were executed per integration step with the actuator command ramped to sub-step 319 and held for one step for force measurement. The experimental and the analytical first story hysteretic responses of Test 2 are shown in Figure 5.14 with reasonable agreement between the experimental and analytical hysteretic models. The experimental first story hysteretic responses for all three PSD hybrid simulations are shown in Figure 5.15. In Test 3, a safety mechanism stopped the simulation when the actuator reached 5 inches. Smooth responses were observed for all three hybrid simulations and which verify that the ramp/hold control scheme was successful implemented to reduce the excessive vibration. Also the all structural responses show realistic wood shear wall behavior the loading rate and stabilizing the control scheme.

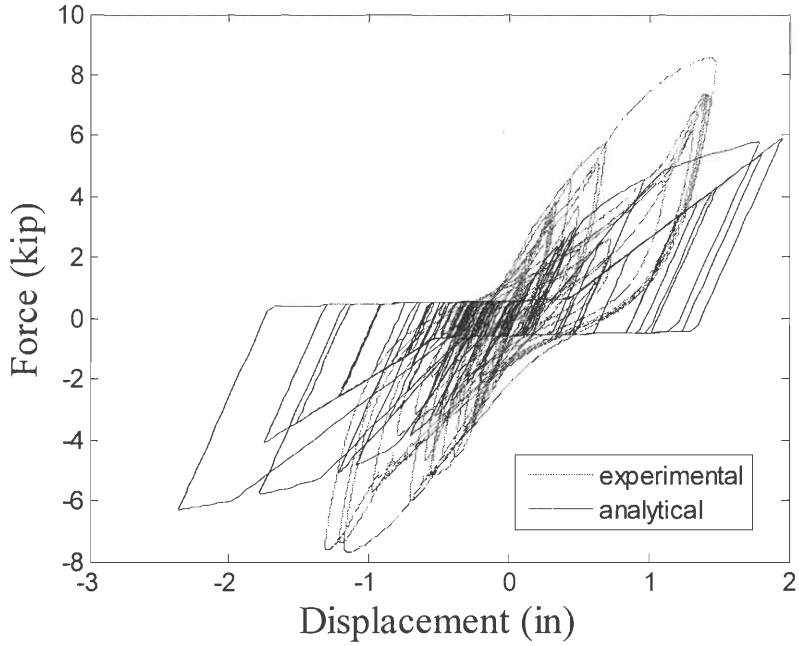

Figure 5.14. Analytical and Experimental Hysteresis for Second PSD Simulation

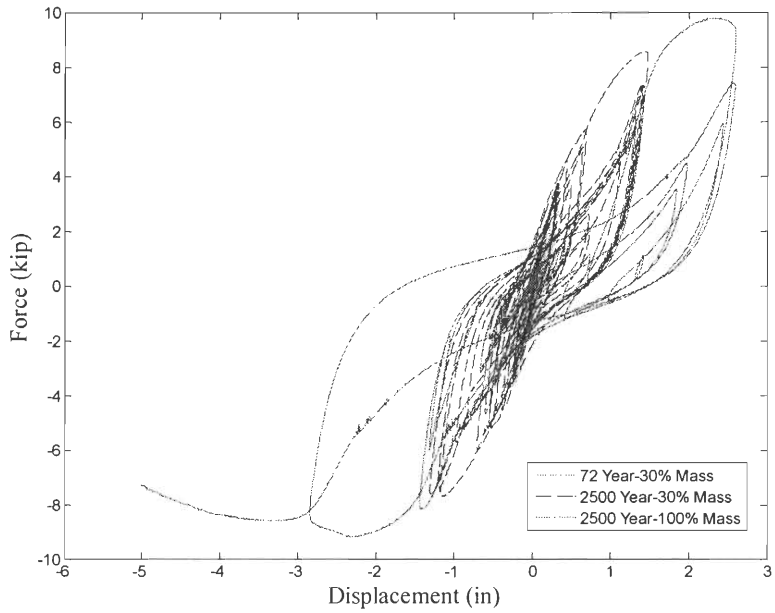

Figure 5.15. Hysteretic Loop for Three PSD Hybrid Simulations with PD1

5.13 Conclusion

A series of large scale PSD hybrid simulations were conducted at UA. The prototype structure was a two DOF wood frame building with a physical first story and a numerical second story. Three specimens were tested; each specimen was bolted at the bottom to strong floor and attached to the actuator at the top. The actuator was mounted against the reaction block along the loading direction and each wall was supported transversely by the framing apparatus at the top. A cyclic test of the dummy 1 specimen characterized its hysteretic behavior; the numerical model of the second story restoring force was developed from results based on the CASHEW model. Next a series of open and closed loop hybrid simulations of increasing amplitude were conducted with the dummy 2 specimen to investigate the testing system and appropriately modify the control scheme. Inaccurate force measurements attributed to excessive vibration of the specimen were addressed by a ramp/hold pattern was developed to replace the step/hold pattern of the original control scheme discussed in Chapter 4. Because actuator tracking error was not an issue with the higher performing actuators, the error compensation of the original control scheme was eliminated. Finally, three large scale hybrid simulations were conducted with the PD1 specimen and reasonable agreement was shown between the shape of the experimental and analytical hysteretic response. To conclude, the experiments conducted in this chapter validated the PSD hybrid simulation control scheme developed at WMU and modified at UA for a wood frame structure; they will serve as a basis for the simulation technique for the NEES-Soft project.

CHAPTER 6

CONCLUSIONS AND FUTURE WORK

6.1 Conclusions

This thesis presented an incremental approach to develop the control scheme suitable to multiple testing facilities and experimental specimens of various scale for PSD hybrid simulation. A series of PSD hybrid simulations were conducted at benchmark scale in the Laboratory of Earthquake and Structural Simulation (LESS) at Western Michigan University (WMU) and then at large scale in the Structures Laboratory at University of Alabama (UA). The final control scheme was applied the large scale PSD hybrid simulation of a two story woodframe building with a physical first story wood shear wall and numerical second story. The results of this study will serve as a basis for developing the simulation technique for the large scale hybrid simulation of a woodframe building in the NEES-Soft project. A summary of the major conclusions and contributions to the state-of-the-practice of PSD hybrid simulation are presented in this section. Contributions include a method of slowing the rate of loading and a triggered force measurement to ensure a force reading corresponding to the target displacement; a method of compensating for the error in actuator command tracking, and a ramping loading pattern with triggered force measurement.

Chapter 2 provided an overview of the fundamentals of PSD hybrid simulation. First, several components of PSD hybrid simulation were discussed, including the equation of motion, formulation of substructures, experimental integration algorithms and experimental equipment. It was found that PSD hybrid

simulation is a reliable structural seismic simulation method which addresses capacity limitations of large scale experimentation without degrading the accuracy of the results. By introducing a numerical component to the physical test through substructuring, the versatility is increased; the cost of implementing PSD hybrid simulation is decreased compared to testing the whole structural model, as is the case in alternative simulation methods such as shake table tests. Additionally, while implicit integration algorithms are superior to explicit algorithms, they are not suitable for PSD hybrid simulation as they require iteration; explicit algorithms or implicit algorithms that are modified to limit or eliminate iteration are generally adopted with experimentation. Specific experimental equipment is needed for conducting PSD hybrid simulation. Hydraulic actuators with the associated hydraulic controller are required to apply the step-by-step simulated displacement responses on the physical specimen during PSD hybrid simulation. Displacement commands are generated in a hybrid testing controller which feeds the measured responses of the physical system from the DAQ hardware to the numerical models and runs the numerical simulation.

The state-of-the-practice of PSD hybrid simulation in NEES projects was presented in Chapter 3. The large scale NEESR facilities are capable of both local and geographically distributed hybrid simulation techniques at slow or real time loading rates. Real time hydraulic actuator control systems and reaction walls facilitate real time pseudodynamic (RT-PSD) hybrid simulation methods. Strong walls and multi-axial control systems facilitate multi-directional PSD hybrid simulation. Large shake tables, dynamic actuators and strong walls conduct real time dynamic hybrid simulations. Large reconfigurable reaction walls facilitate large scale PSD hybrid simulation of versatile specimens at real time or slow rates. Twenty two NEESR sponsored projects have adopted PSD hybrid simulation. By validating the

experimental procedure and the associated simulation results, each project serves as a basis for future research development.

A significant contribution of NEESR projects has been the continued improvement of stability and accuracy in integration algorithms. Improvements in modified implicit integration algorithms have made substructuring a key feature of PSD and dynamic hybrid simulation in the NEESR projects, driving further development of real time and geographically distributed projects. Improved accuracy and stability of both implicit and explicit algorithms, along with control compensation techniques, have made accurate RT-PSD hybrid simulation, both local and geographically distributed, more achievable. The feasibility of geographically distributed simulations has improved with the introduction of flexible software such as UI-Simcor and OpenFresco to quickly communicate essential information such as test initialization, stiffness estimation, integration parameters and loading commands. Nevertheless, as NEESR experimental objectives become more complex, further development of stable integration algorithms for large scale substructured experiments and real time local and geographically distributed PSD simulations is needed to produce reliable and accurate results. Neither UI-SimCor nor OpenFresco are able to support real time distributed hybrid simulation. Future work opportunities are discussed in Section 6.2.

A series of benchmark scale PSD hybrid simulations conducted at the LESS facility were presented in Chapter 4. A strategy of slowing down the loading rate in order to achieve an accurate restoring force reading was developed through an incremental procedure in three empirical phases at benchmark scale. Each phase included multiple PSD simulations, modified slightly from the previous one to examine the effect of individual parameters. It was found that in order to achieve

stability and accuracy in a PSD hybrid simulation, the actuator must reach its target displacement within a single integration step. Additionally, the force measurement must be delayed to the point at which the actuator reaches its target displacement; delaying the force measurement to this point results in an accurate force reading, corresponding to the target displacement. A feed forward error compensation method was developed to address the inherent actuator delay and its imperfect performance of tracking the command. The results of each test were validated by comparing them to the results obtained from the numerical simulation of the specimen's response predicted by the initial stiffness; the final control scheme was found to be stable and accurate for the LESS control system. This method is appropriate when there are no velocity dependent devices present, in other words, when time can be considered irrelevant to the structural dynamic response.

A series of large scale PSD hybrid simulations conducted at the newly constructed Structural Engineering Laboratory at University of Alabama (UA) are presented in Chapter 5. The method of ramping the loading rate was developed in the same incremental procedure consisting of a series of open then closed loop PSD hybrid simulations of increasing amplitudes. The ramp/hold command pattern was developed to address the excessive vibration in the specimen experienced with the step/hold command due to UA's high performance control system and high speed actuator relative to the corresponding parts in the LESS. Smooth responses were observed for the final large amplitude closed loop hybrid simulations, which verify that the ramp/hold control scheme was successfully implemented to reduce the excessive vibration. Also, all structural responses show realistic wood shear wall behavior response and that the ramped loading rate stabilized the control scheme. The

control scheme developed in Chapter 4, with the modifications in Chapter 5, will serve as a basis for developing the simulation technique of the NEES-Soft project.

6.2 Future Work

The NEESHub project warehouse provides a repository for information on all NEESR projects. A review of this information demonstrates that future work is needed in the areas of substructuring and boundary condition replication, real time compensation; stable and accurate integration algorithms to advance both local and geographically distributed hybrid simulation. The following section presents future work opportunities, especially those relating to LESS, to further develop PSD hybrid simulation.

An incremental approach is often adopted in validating new and complex hybrid simulation techniques. Potential errors due to equipment setup, structural idealization, numerical algorithms and compensation techniques are investigated by using a benchmark scale or predictable specimen. LESS can contribute to the aforementioned research needs by conducting benchmark scale PSD hybrid simulations to develop and validate real time and geographically distributed hybrid simulation techniques much like the method presented in this study.

In this study, a real time simulation control technique was developed by using the Smith predictor to compensate for actuator delay. Stability was achieved; however the results of the test indicated that there was still significant inaccuracy. More work is needed in developing actuator delay compensation techniques and conducting real time simulations at an execution rate of 1000 Hz or higher. A higher performing control system, capable of accurate RT-PSD hybrid simulation is needed for efficient

development; however, these are considerably expensive goals of LESS so they may be considered long term. Alternatively, future work in developing a more efficient hybrid testing controller and a more precise physical specimen are relatively inexpensive, shorter term research opportunities for LESS.

More reliable benchmark simulation results can be achieved at LESS by developing a more modular simulation model within the hybrid testing controller and a precisely machined versatile physical specimen. In the current state of the hybrid testing controller, the simulation model and system mappings are configured for each PSD hybrid simulation; this tends to be a lengthy process which leaves room for mistakes in the testing and data logging procedures. Future development in methods of adjusting parameters such as the slow rate, ground acceleration scale, force measurement trigger, and the ramp/step values within the customizable VeriStand workspace will increase the versatility of the simulation model; additionally it will save time and mitigate mistakes in configuring system mappings, engineering unit conversions, data logging and deploying new simulation models for each test.

The physical specimen at LESS is a significant source of error in a PSD hybrid simulation. The coupons are not perfectly symmetric and the pin connection experiences a slight amount of slippage; the actuator connection is also not symmetric in the loading direction. Imperfections such as these result in inaccurate force measurements and an inaccurate analytical model; they can by addressed by machining the specimen using computer numerical control (CNC). A more versatile specimen capable of serving as a more complex substructure would be beneficial to developing more accurate boundary conditions and substructure partitions.

Also, an actuator command tracking error compensation was developed in this study that showed promise in increasing the accuracy of slow PSD hybrid simulation.

At each simulation step, the Simulink model checks whether the actuator tracking error is within a desired tolerance. If the error is within the preset tolerance, a force measurement is triggered. If not, the force reading from the previous step is fed into the integrator. Future work is needed in developing a command for this method which eliminates the possibility of spurious loading. Any development in compensation techniques for real time or slow PSD hybrid simulation may serve as a basis for the future development of a communication framework at LESS for geographically distributed PSD hybrid simulation.

In order for PSD hybrid simulation to be more widely adopted in structural seismic simulation, future work is needed in providing well-documented general testing procedures. Benchmark PSD hybrid simulations may be conducted to validate testing protocols which have not been well established such as RT local and geographically distributed PSD projects and large, complex physical substructures. Establishing a more general simulation framework will allow researchers to easily pick up where others left off; as better technology becomes available, research may also revisit previously validated projects in an attempt to achieve the same accurate results in a more economic and efficient manner.

REFERENCES

Ahmadizadeh, M., Mosqueda, G., and Reinhorn, A. (2008). "Compensation of actuator delay and dynamics for real-time hybrid structural simulation." *Earthquake Eng.Struct.Dyn.,* 37(1), 21-42.

Bahmani, P., and van de Lindt, J. W. (2012). "Numerical Modeling of Soft-Story Woodframe Retrofit Techniques for Design." *Structures Congress 2012,* ASCE, 1755-1766.

Carrion, J., and Spencer, B. (2007). "Model-based Strategies for Real-time Hybrid Testing. Newmark Structural Engineering Laboratory Report Series." *University of Illinois at Urbana-Champaign: Urbana, IL* .

Chae, Y., Ricles, J. M., and Sause, R. (2010). "Evaluation of structural control strategies for improving seismic performance of buildings with MR dampers using real-time large-scale hybrid simulation." *Proceedings of the 19th Analysis and Computation Specialty Conference,* 335-346.

Chen, C. (2007). "Development and numerical simulation of hybrid effective force testing method". Ph.D. Lehigh University, United States -- Pennsylvania.

Chen, C., and Ricles, J. M. (2012). "Analysis of implicit HHT-? integration algorithm for real-time hybrid simulation." *Earthquake Eng.Struct.Dyn.,* 41(5), 1021-1041.

Chen, C., and Ricles, J. M. (2010). "Tracking error-based servohydraulic actuator adaptive compensation for real-time hybrid simulation." *J.Struct.Eng.,* 136(4), 432-440.

Chen, C., and Ricles, J. M. (2009). "Analysis of actuator delay compensation methods for real-time testing." *Eng.Struct.,* 31(11), 2643-2655.

Chen, C., and Ricles, J. M. (2008). "Stability analysis of SDOF real-time hybrid testing systems with explicit integration algorithms and actuator delay." *Earthquake Eng.Struct.Dyn.,* 37(4), 597-613.

Chen, C., Ricles, J. M., Marullo, T. M., and Mercan, O. (2009). "Real-time hybrid testing using the unconditionally stable explicit CR integration algorithm." *Earthquake Eng.Struct.Dyn.,* 38(1), 23-44.

Christenson, R., Lin, Y., Emmons, A., and Bass, B. (2008). "Large-Scale Experimental Verification of Semiactive Control through Real-Time Hybrid Simulation1." *J.Struct.Eng.,* 134(4), 522-534.

Chung, L., Lin, R., Soong, T., and Reinhorn, A. (1989). "Experimental Study of Active Control for MDOF Seismic Structures." *J.Eng.Mech.,* 115(8), 1609-1627.

Combescure, D., and Pegon, P. (1997). "α-Operator splitting time integration technique for pseudodynamic testing error propagation analysis." *Soil Dyn.Earthquake Eng.,* 16(7–8), 427-443.

Darby, A. P. (1999). "Real-time substructure tests using hydraulic actuator." *J.Eng.Mech.,* 125(10), 1133.

Darby, A. P., Blakeborough, A., and Williams, M. S. (2001). "Improved control algorithm for real-time substructure testing." *Earthquake Eng.Struct.Dyn.,* 30(3), 431-448.

Dermitzakis, S. (1986). "Development of substructuring techniques for on-line computer controlled seismic performance testing." *Dissertation Abstracts International Part B: Science and Engineering[DISS.ABST.INT.PT.B- SCI.& ENG.],* 46(9).

Dimig, J., Shield, C., French, C., and Bailey, F. (1999). "Effective Force Testing: A Method of Seismic Simulation for Structural Testing." *J.Struct.Eng.,* 125(9), 1028-1037.

Dyke, S., Hachem, M., Irfanoglu, A., McKenna, F., Lynett, P., Lowes, L., and Mejia, L. (2011). "NEES 2011 Vision Report on Computational and Hybrid Simulation: Needs and Opportunities." .

Eatherton, M., & Hajjar, J. F. (2010). Large-scale cyclic and hybrid simulation testing and development of a controlled-rocking steel building system with replaceable fuses. *Report No. NSEL–024, Newmark Structural Engineering Laboratory Report Series (ISSN 1940–9826), Department of Civil and Environmental Engineering, University of Illinois at Urbana-Champaign, Urbana, IL.*

Hashemi, A., and Mosalam, K. M. (2006). "Shake-table experiment on reinforced concrete structure containing masonry infill wall." *Earthquake Eng.Struct.Dyn.,* 35(14), 1827-1852.

Hashemi, S. A. (2007). *Seismic evaluation of reinforced concrete buildings including effects of masonry infill walls.* University of California, Berkeley.

Horiuchi, T., Inoue, M., Konno, T., and Namita, Y. (1999). "Real-time hybrid experimental system with actuator delay compensation and its application to a piping system with energy absorber." *Earthquake Eng.Struct.Dyn.,* 28(10), 1121-1141.

Horiuchi, T., Konno, T., Horiuchi, T., and Konno, T. (2001). "A new method for compensating actuator delay in real–time hybrid experiments." *Philosophical Transactions of the Royal Society of London.Series A: Mathematical, Physical and Engineering Sciences,* 359(1786), 1893-1909.

Igarashi, A., Iemura, H., and Suwa, T. (2000). "Development of substructured shaking table test method." *Proceedings of the 12th World Conference.*

Kim, S. J., Christenson, R., Phillips, B., and Spencer, B. (2012) "Geographically Distributed Real-Time Hybrid Simulation of MR Dampers for Seismic Hazard Mitigation." *20th Analysis and Computation Specialty Conference,* ASCE, 382-393.

Kumar, , Itoh, Y., Saizuka, K., and Usami, . (1997). "Pseudodynamic Testing of Scaled Models." *J.Struct.Eng.,* 123(4), 524-526.

Kwon, O. -., Nakata, N., Elnashi, A., and Spencer, B. (2005). "A Framework for Multi-Site Distributed Simulation and Application of Complex Structural Systems." *J.Earth.Eng.,* 09(05), 741-753.

Leon, R., Yang, C., DesRoches, R., and Reinhorn, A. (2004). "Results of Early Collaborative Research on Behavior of Braced Steel Frames with Innovative Bracing Schemes (Zipper Frames)." *Advances in Experimental Structural Engineering,* 525-532.

Lai, J. W., and Mahin, S. A. (2010). "Experimental Study of Tomorrow's Steel Braced Frames in Building Structures." *9th US National and 10th Canadian Conference on Earthquake Engineering,* 25-29.

Lin, Y. Z. (2009). *Real-time hybrid testing of an MR damper for response reduction* (Vol. 70, No. 09).

Lignos, D. (2008). "Sidesway collapse of deteriorating structural systems under seismic excitations". Ph.D. Stanford University, United States -- California.

Mosqueda, G. (2005). *Continuous hybrid simulation with geographically distributed substructures.* University of California, Berkeley.

MTS Systems Corporation (2010), *MultiPurpose TestWare Software.*

Nakashima, M., Ishii, K., Kamagata, S., Tsutsumi, H., and Ando, K. (1988). "Feasibility of Pseudo Dynamic Test Using Substructuring Techniques." *Proceedings of Ninth World Conference on Earthquake Engineering* .

Nakashima, M. (1990). "Integration techniques for substructure pseudo-dynamic test." *4th US National Conference on Earthquake Engineering, 1990.5* .

Nakashima, M. (2001). "Development, potential, and limitations of realâ??time online (pseudoâ??dynamic) testing." *Philosophical Transactions - Royal Society.Mathematical, Physical and Engineering Sciences,* 359(1786), 1851.

Nakashima, M., Kato, H., and Takaoka, E. (1992). "Development of real-time pseudo dynamic testing." *Earthquake Eng.Struct.Dyn.,* 21(1), 79-92.

Nakata, N., Spencer, B., and Elnashai, A. (2010). "Sensitivity-Based External Calibration of Multiaxial Loading System." *J.Eng.Mech.,* 136(2), 189-198.

NEES Consortium, I. (2007). "Issues and research needs in simulation development." NEES Consortium, Inc., Chicago Hilton Hotel, O'hare Airport.

NEESHub. (2009). "A platform for research, collaboration, and education." Accessed October 20th. http://nees.org/warehouse/welcome

Newmark, N. M. (1959). "A Method of Computation for Structural Dynamics." *Proc.ASCE,* 85(3), 67.

Pang, W., and Shirazi, S. M. H. (2012). "A Co-Rotational Model for the Cyclic Analysis of Light-Frame Wood Shear Walls and Diaphragms." *J.Struct.Eng.,* 1 450.

Pang, W., and Ziaei, E. (2012). "Nonlinear Dynamic Analysis of Soft-Story Light-Frame Wood Buildings." *Structures Congress 2012,* ASCE, 1767-1777.

Reinhorn, A., Sivaselvan, V., Liang, Z., and Shao, X. (2004). "Real-time dynamic hybrid simulation of structural systems." *Proceedings of the 13th World Conference on Earthquake Engineering, .*

Ricles, J. M., Sause, R., Roke, D., and Gonner, N. (2009). "Design Concepts for Damage-Free Seismic-Resistant Self-Centering Steel Concentrically Braced Frames." American Society of Civil Engineers, 1.

Roke, D., Sause, R., Ricles, J. M., and Gonner, N. (2009). "Design concepts for damage-free seismicresistant self-centering steel concentrically-braced frames." *ASCE Structures Congress,*

Schellenberg, A., and Mahin, S. (2006). "Integration of hybrid simulation within the general-purpose computational framework OpenSees." *100 th Anniversary Earthquake Conference Commemorating the 1906 San Francisco Earthquake, .*

Schellenberg, A., Kim, H. K., Takahashi, Y., Fenves, G. L., and Mahin, S. A. (2007). "OpenFresco Framework for Hybrid Simulation: Installation and Getting Started Manual." *Department of Civil and Environmental Engineering, .*

Shao, X. (2012). "Benchmark Problem and Future Development in RTHS." *Advances in Real-Time Hybrid Simulation Workshop, .*

Shao, X., Enyart, G. "Development of a Versatile Hybrid Testing System for Seismic Experimentation" *Experimental Techniques.* doi: 10.1111/j.1747-1567.2012.00837.

Shao, X., Reinhorn, A., and Sivaselvan, M. (2011). "Real-Time Hybrid Simulation Using Shake Tables and Dynamic Actuators." *J.Struct.Eng.,* 137(7), 748-760.

Shing, P., and Mahin, S. A. (1983). "Experimental error propagation in pseudodynamic testing." *Rep.no.UCB/EERC-83,* 12.

Shing, P. B. (2006). "Validation of a fast hybrid test system with substructure tests." 1.

Shing, P. B. (1996). "Application of Pseudodynamic Test Method to Structural Research." *Earthquake Spectra,* 12(1), 29.

Shing, P. B., Wei, Z., Jung, R. Y., and Stauffer, E. (2004). "NEES Fast Hybrid Test System at the University of Colorado." *13th World Conference on Earthquake Engineering,* Vancouver, B.C., Canada, .

Smith, O. J. M. (1959). "A controller to overcome dead time." *ISA Journal,* 6(2), 28.

Takahashi, Y., and Fenves, G. L. (2006). "Software framework for distributed experimental–computational simulation of structural systems." *Earthquake Eng.Struct.Dyn.,* 35(3), 267-291.

Takanashi, K., and Nakashima, M. (1987). "Japanese activities on on-line testing." *J.Eng.Mech.,* 113(7), 1014-1032.

Takanashi, K. (1987). "Japanese activities on on-line testing." *J.Eng.Mech.,* 113(7), 1014.

Thewalt, C. R., and Mahin, S. A. (1995). "Nonplanar Pseudodynamic Testing." *Earthquake Engineering Structural Dynamics,* 24(5), 733-746.

Tian, J., and Symans, M. D. (2012). "High-Performance Seismic Retrofit of Soft-Story Wood-framed Buildings using Energy Dissipation Systems." *Structures Congress 2012,* ASCE, Chicago, IL, 1790-1801.

van de Lindt, J. W., Rosowsky, D., Pang, W., and Pei, S. (2012). "Performance-Based Seismic Design of Mid-Rise Woodframe Buildings." *J.Struct.Eng.,* 489.

J. Wight, Parra-Montesinos, G. and Lequesne, R. (2011). "HIGH-PERFORMANCE FIBER REINFORCED CONCRETE FOR EARTHQUAKE-RESISTANT DESIGN OF COUPLED WALL SYSTEMS." https://nees.org/resources/2843/download/RILEM_HPFRCC-5-_Wight_Parra_Lequesne.pdf .

Wu, B., Xu, G., Wang, Q., and Williams, M. S. (2006). "Operator-splitting method for real-time substructure testing." *Earthquake Eng.Struct.Dyn.,* 35(3), 293-314.

Yang, T. Y., Stojadinovic, B., and Moehle, J. (2009). "Hybrid simulation of a zipper-braced steel frame under earthquake excitation." *Earthquake Eng.Struct.Dyn.,* 38(1), 95-113.

Appendix A

MATLAB/Simulink Programs of Chapter 4

MATLAB script which initializes PSD hybrid simulation

```
      %% Begin - Input Variables
      g = 386.089;                                % Gravitational
Constant

      %% seismic mass and damping
      mass = [1.2*8/g; 1.2*8/g] ;                 % WMU seismic mass
      m1 = mass(1);
      m2 = mass(2);
      zeta = 0.02;                                % damping ratio
(fraction of critical damping)

      %% Wall parameters
      % Modified Stewart Hysteretic Model wall parameters for 8ft x
8ft wall
      parameters_1st = [10.2189
                         0.047972
                        -0.056668
                         1.1359
                         0.012125
                         6.318
                         0.543345
                         2.45293
                         0.91419
                         1.2339];

      %  WMU stiffness replace second story wall

      %% Ground Motion
      ga_scale = 1; % scale for ground motion
      [ga,dtga]=readAccPEER('MUL009_Northridge.AT2');
      pga = max(abs(ga))*g*ga_scale; % peak ground acceleration


      %% integration time step
      Ko_1 = parameters_1st(1);                   % initial stiffness
of first story
      Ko_2 = 10.2189;                       % WMU added initial
stiffness of second story

      syms x
      k = [Ko_1+Ko_2 -Ko_2 ; -Ko_2 Ko_2];
      m = [m1 0 ; 0 m2];
      Wn = solve(det(k-(m.*(x^2))));              % initial natural
frequency
      Wn = double(Wn);
      Tn = 2*pi./Wn;                              % initial natural
period
      Tn_max = max(Tn);

      %% preprocessing

      % - ground motion
      % Scaling ground motion
      scale = pga/max(abs(ga));
      ga = scale.*ga;
```

```
      t = t(:);
      ga = ga(:);
      tga = [t,ga];                          % simulink ground motion
input


      %% wall parameters
      % calculate additional internal parameters
      parameters2_1st = addparaMSTEW(parameters_1st);

      % loading history for first story
      hyst_1st = zeros(1,16);
      hyst_1st(1) = 1; %LPATH
      hyst_1st(2) = 1; %LPREV

      WallPara_1st =
[parameters_1st(:);parameters2_1st(:);hyst_1st(:)]';

      %% Compute Newmark Beta integration coefficients
      %     select method
      imethod = 1;
      if imethod == 1                        % Average acceleration
method
          ngamma = 0.5; nbeta = 0.25;
      elseif imethod == 2                    % Linear acceleration
method
          ngamma = 0.5; nbeta = 1/6;
      end

      % calculate constants
      kc1 = m./nbeta./dt./dt;
      kc2 = ngamma/nbeta/dt;

      dpc1 = m./nbeta./dt;
      dpc2 = ngamma/nbeta;
      dpc3 = m./2./nbeta;
      dpc4 = dt*(ngamma/2/nbeta - 1);

      vc1 = ngamma/nbeta/dt;
      vc2 = ngamma/nbeta;
      vc3 = dt*(1-ngamma/2/nbeta);

      ac1 = 1/nbeta/dt/dt;
      ac2 = -1/nbeta/dt;
      ac3 = -1/2/nbeta;

      cc1 = 2.*zeta.*(mass.^0.5);
      Cc = cc1.*[Ko_1;Ko_2];      % viscous damping constant
      Cc_1 = Cc(1);
      Cc_2 = Cc(2);
      C = [Cc(1)+Cc(2) -Cc(2) ; -Cc(2) Cc(2)];
```

MATLAB additional script which initializes slow PSD hybrid simulation

```
      %% WMU time step
      dt=0.01;                                  %WMU integration step
      sdt=0.01;                                 %WMU simulation step
      slow=40;                                  %WMU slow rate
      Hit=dt*slow/sdt;                          %WMU number of
simulation steps for each integration time step


      %% WMU initialize conditions
      WKo=0.95;                                 % WMU stiffness
      WS_Scale=Ko_2/WKo;                        % WMU scale of
physical stiffness to numerical
      eScale=0.5;                               % WMU earthquake
scale to reduce amplitude
```

MATLAB additional script which initializes RT-PSD hybrid simulation

```
      %% Real time simulation parameters
      sdt=0.01;                          % WMU simulation time step
      eScale=0.3;                               % WMU earthquake
ground motion scale

      %Smith predictor model
      SAdl=6;                                   %delay step in terms
of sdt=0.01sec, 0.2sec delay total
      SAMean=1.00;                              %random signal to
simulate error in actuator displ. performance.
      SAVar=0.000;                              %when Mean =1.0,
Var=0, there is no error.
      SKo=Ko;                                   %estimated structure
stiffness
```

Simulink subsystem (slow and RT): Newmark Beta Part 1

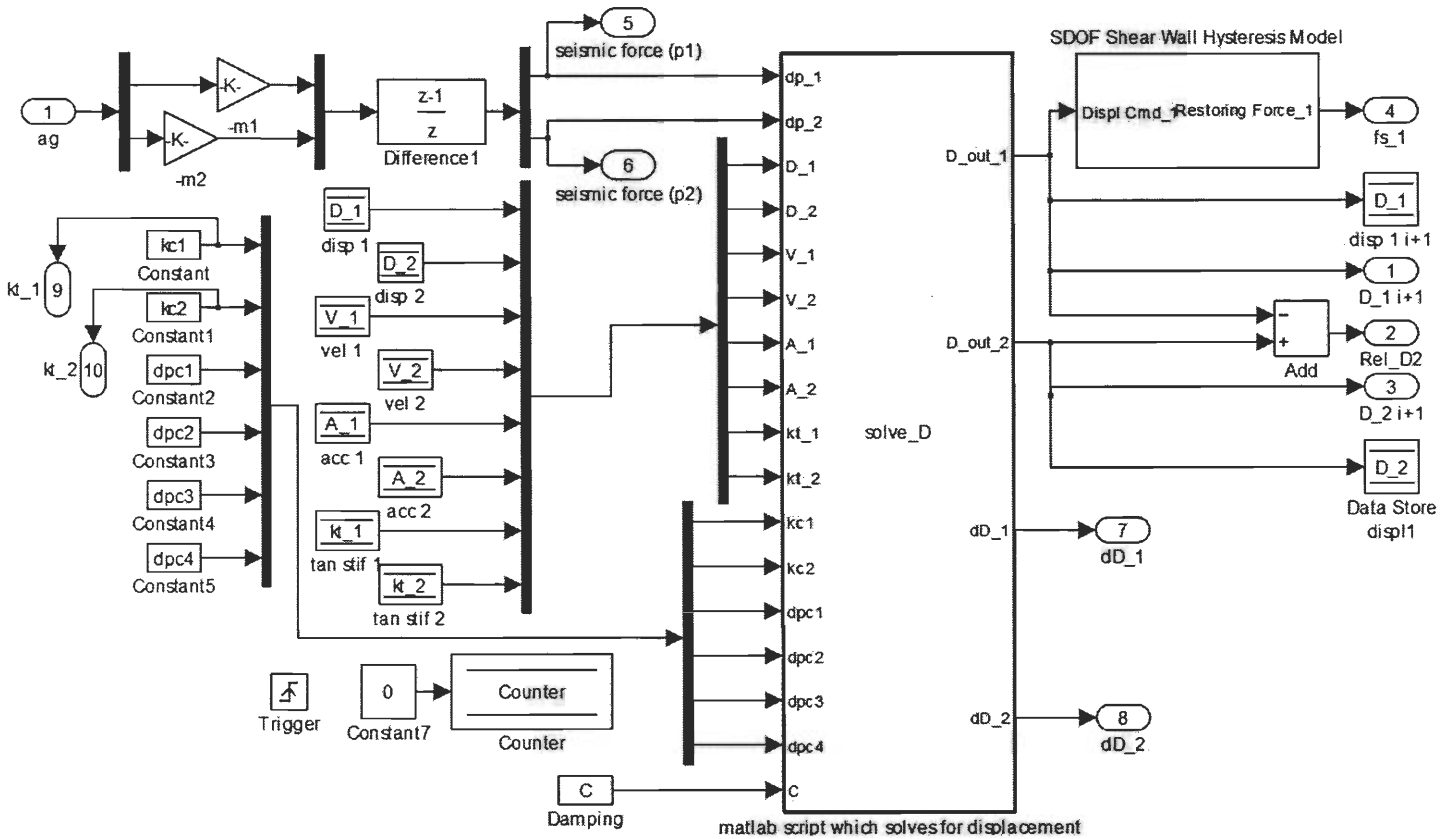

Embedded MATLAB script to calculate displacement

```
      function [D_out_1,D_out_2,dD_1,dD_2] =
solve_D(dp_1,dp_2,D_1,D_2,...
          V_1,V_2,A_1,A_2,kt_1,kt_2,kc1,kc2,dpc1,dpc2,dpc3,dpc4,C)
      %#codegen

      % equivalent stiffness
      kt = [kt_1+kt_2 -kt_2 ; -kt_2 kt_2]; % tangent stiffness
      kt_ = kt + kc1 + kc2*C;              % khat stiffness

      % equivalent force
      dp = [dp_1;dp_2];
      A = [A_1;A_2];
      V = [V_1;V_2];
      dp_ = dp + (dpc1 + dpc2*C)*V + (dpc3 + dpc4*C)*A;     % phat

      % solve for displacement increment and new displacement
      D = [D_1;D_2];                       % displacement matrix (i)
      dD = kt_\dp_;                        % change in displacement
      dD_1 = dD(1);                        %      "      1st  story
      dD_2 = dD(2);                        %      "      2nd  story
      D_out = D + dD;                      % displacement matrix (i+1)
      D_out_1 = D_out(1);                  %      "      1st  story
      D_out_2 = D_out(2);                  %      "      1st  story
```

Simulink subsystem wood shear wall hysteresis model

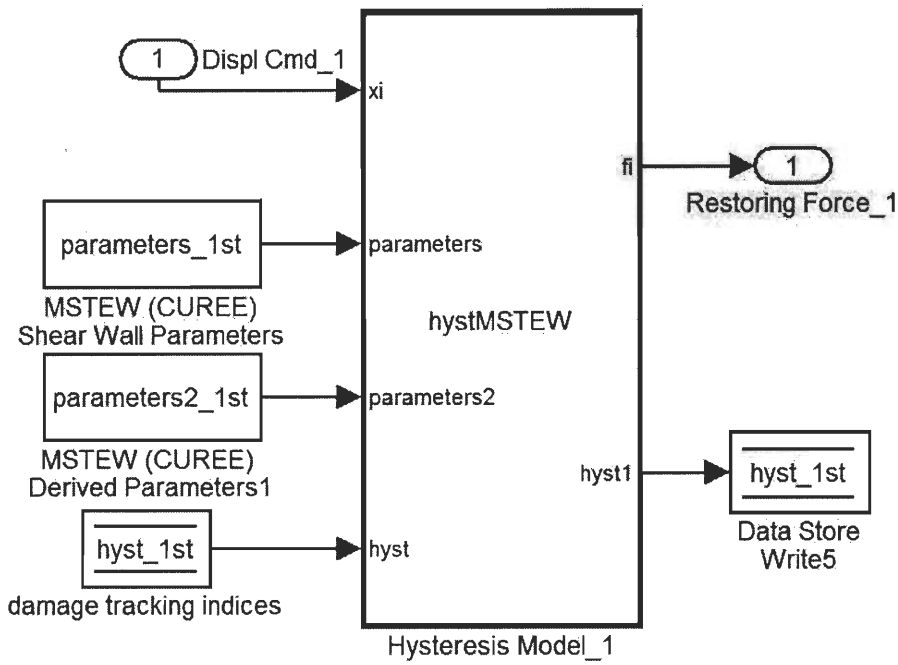

Simulink subsystem (slow and RT) model of Newmark Part 2

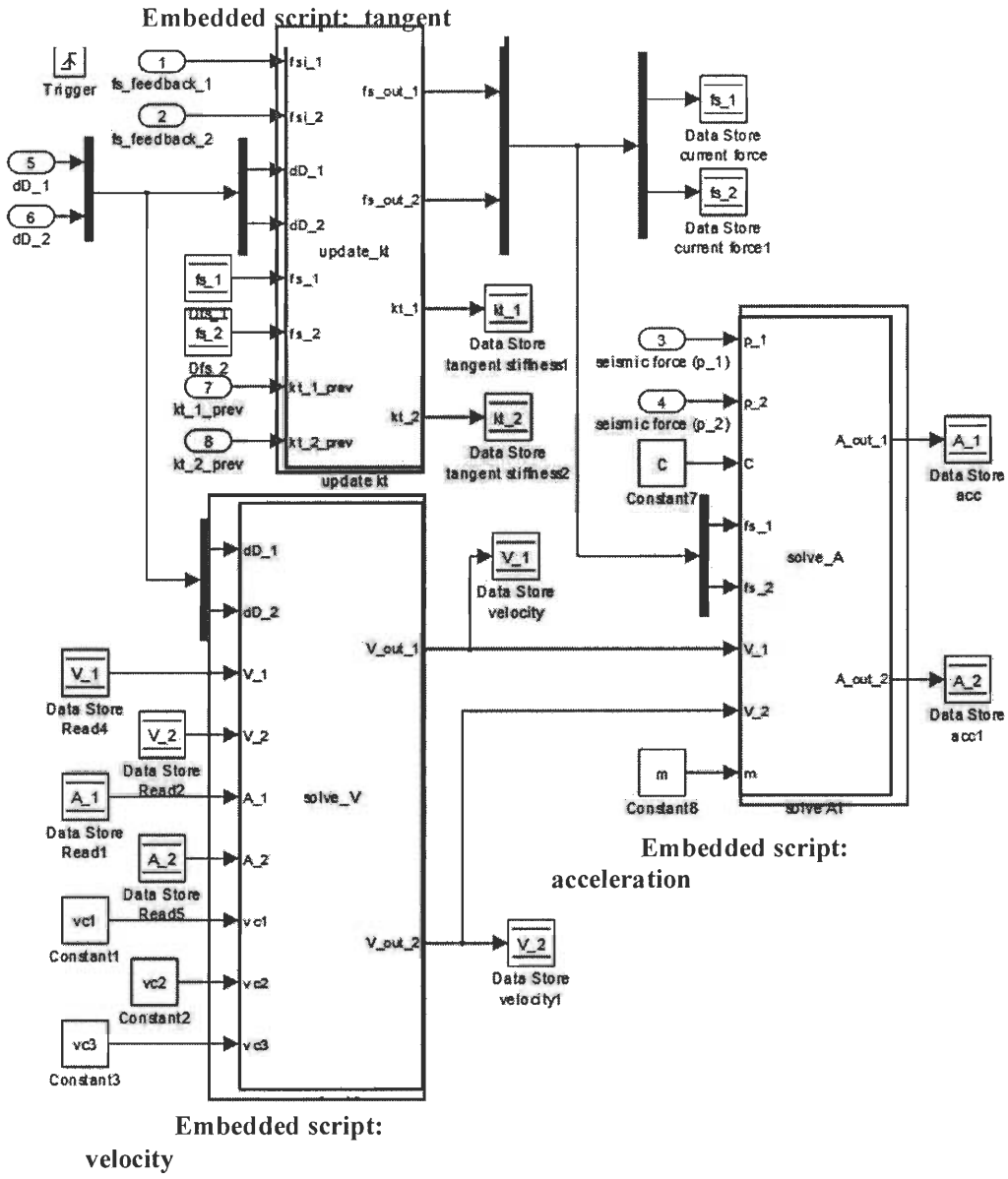

Embedded MATLAB script which solves for updated tangent stiffness

```
      function [fs_out_1,fs_out_2,kt_1,kt_2]  =
update_kt(fsi_1,fsi_2,dD_1,dD_2,fs_1,fs_2,kt_1_prev,kt_2_prev)
      %#codegen

      %% update tangent stiffness
      % change in restoring force
      dfs_1 = fsi_1 - fs_1;
      dfs_2 = fsi_2 - fs_2;
```

```
% stiffness= deltaFs/deltaD (if deltaD is zero, use k(i-1)

if dD_1 ~= 0
    kt_1 = dfs_1/dD_1;
else
    kt_1 = kt_1_prev;
end

if (dD_2-dD_1) ~= 0
    kt_2 = dfs_2/(dD_2-dD_1);
else
    kt_2 = kt_2_prev;
end

% output restoring force
fs_out_1 = fsi_1;
fs_out_2 = fsi_2;
```

Embedded MATLAB script which solves for velocity

```
function [V_out_1,V_out_2]  =
solve_V(dD_1,dD_2,V_1,V_2,A_1,A_2,vc1,vc2,vc3)
%#codegen

% solve for velocity increment

A = [A_1;A_2];                          % acceleration vector
V = [V_1;V_2];                          % velocity vector
dD = [dD_1;dD_2];                       % incremental displacement
vector
dV = vc1.*dD - vc2.*V + vc3.*A;         % incremental velocity
V_out = V + dV;                         %           "
vector

% output velocity
V_out_1 = V_out(1);
V_out_2 = V_out(2);
```

Embedded MATLAB script which solves for acceleration

```
function [A_out_1,A_out_2] =
solve_A(p_1,p_2,C,fs_1,fs_2,V_1,V_2,m)
%#codegen

%% modified Newmark Beta
% calculate acceleration
p = [p_1;p_2];                          % external force vector
V = [V_1;V_2];                          % velocity vector
fs = [fs_1;fs_2];                       % restoring force vector

A_out = m\(p - C*V - fs);              % acceleration @ dynamic eq.

% output acceleration
A_out_1 = A_out(1);
A_out_2 = A_out(2);
```

Appendix B

MATLAB/Simulink Programs for Chapter 5

MATLAB script which initializes slow PSD hybrid simulation

```
clear all; clc; close all
%%
nAct    = 8;                % number of actuators
nAdcU   = 8;                % number of user a/d channels
nUDPOut = 1+6*nAct+nAdcU;   % no. of outputs from simulink
bridge
nUDPInp = 1+5*nAct+nAdcU;   % no. of inputs to simulink bridge
% sample period parameters
controlPeriod   = 1/4096;       % sec
upsampleFactor  = 1;
samplePeriod    = controlPeriod/upsampleFactor;

scramInitialize

%% Begin - Input Variables
g = 386.089;

%% seismic mass and damping
mass = 0.3*[1.2*20/g; 0.8*20/g] ;   % scaled seismic mass
m1 = mass(1);
m2 = mass(2);
zeta = 0.02;      % damping ratio (fraction of critical
damping)

%% Wall parameters
% Modified Stewart Hysteretic Model wall parameters
% for 8ft x 8ft wall

parameters_2nd = [8.81978
                    0.0674458
                 -0.132142
                 1.16391
                 0.0122845
                 4.99853
                 0.582478
                 3.80851
                 0.75
                 1.1 ];
% Define Modified Stewart hysteretic parameters
% Ko, r1, r2, r3, r4, F0, FI, DU, Alpha, Beta

%% Ground Motion

% Test 1: Loma-Prieta Capitola
[ga,dtga]=readAccPEER('CAP000.AT2');
ga_scale = 0.593670072; % scale for ground motion, 50%/50yr

% Test 2: Loma-Prieta Capitola
% [ga,dtga]=readAccPEER('CAP000.AT2');
% ga_scale = 2.023875244; % scale for ground motion, 2%/50yr

ga = [zeros(round(0.5/dtga),1); ga]; % ga = ground acceleration
record, with 'n' data points
pga = max(abs(ga))*g*ga_scale; % peak ground acceleration
```

```
      %% CASHEW Parameters
      Ko_1 = 23.2;            % initial stiffness (from low amp
cyclic test)
      Ko_2 = parameters_2nd(1);  %% initial stiffness of second story


      syms x
      k = [Ko_1+Ko_2 -Ko_2 ; -Ko_2 Ko_2]; % stiffness matrix
      m = [m1 0 ; 0 m2];                  % mass matrix
      Wn = solve(det(k-(m.*(x^2))));      % initial natural frequency
      Wn = double(Wn);
      Tn = 2*pi./Wn;                      % initial natural period
      Tn_max = max(Tn);

      %% WMU time step
      dt=1/256;         %WMU integration step
      sdt=1/4096;       %WMU simulation step
      slow=20;
      Hit=dt*slow/sdt;

      % Calculations for ramp command
      Rratio=319;
      Rs=(0:1/Rratio:1);
      Rs(Rratio+1:Hit-1)=1;
      %% End - Input Variables

      %% preprocessing

      %- ground motion
      % Scaling ground motion
      scale = pga/max(abs(ga));
      ga = scale.*ga;
      n = length(ga);

      % Interpolate ground acceleration and caculate new time step,
dt
      t1 = linspace(0,(n-1)*dtga,n);
      ni = floor((n-1)*dtga/dt + 1);
      t = linspace(0,(ni-1)*dt,ni);
      ga = interp1(t1,ga,t);

      t = t(:);
      ga = ga(:);
      tga = [t,ga]; % simulink ground motion input



      %% wall parameters
      % calculate additional internal parameters
      parameters2_2nd = addparaMSTEW(parameters_2nd);

      %% compute Newmark Beta integration coefficients
      %  select method
      imethod = 1;
      if imethod == 1 % Average acceleration method
          ngamma = 0.5; nbeta = 0.25;
```

```
elseif imethod == 2 % Linear acceleration method
    ngamma = 0.5; nbeta = 1/6;
end

% calculate constants
kc1 = m./nbeta./dt./dt;
kc2 = ngamma/nbeta/dt;

dpc1 = m./nbeta./dt;
dpc2 = ngamma/nbeta;
dpc3 = m./2./nbeta;
dpc4 = dt*(ngamma/2/nbeta - 1);

vc1 = ngamma/nbeta/dt;
vc2 = ngamma/nbeta;
vc3 = dt*(1-ngamma/2/nbeta);

ac1 = 1/nbeta/dt/dt;
ac2 = -1/nbeta/dt;
ac3 = -1/2/nbeta;

cc1 = 2.*zeta.*(mass.^0.5);
Cc = cc1.*[Ko_1;Ko_2]; % viscous damping constant
Cc_1 = Cc(1);
Cc_2 = Cc(2);
C = [Cc(1)+Cc(2) -Cc(2) ; -Cc(2) Cc(2)];

%% WMU remove all initial conditions
```

Simulink subsystem: Newmark Beta Part 1

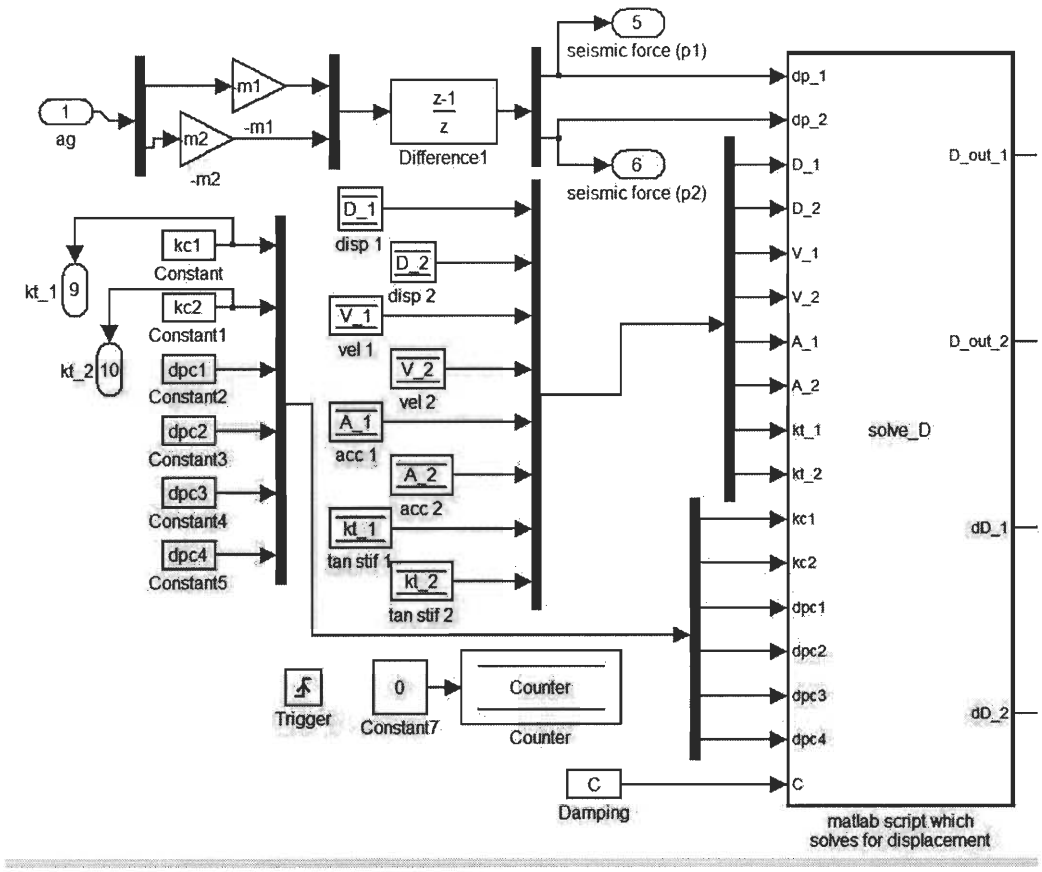

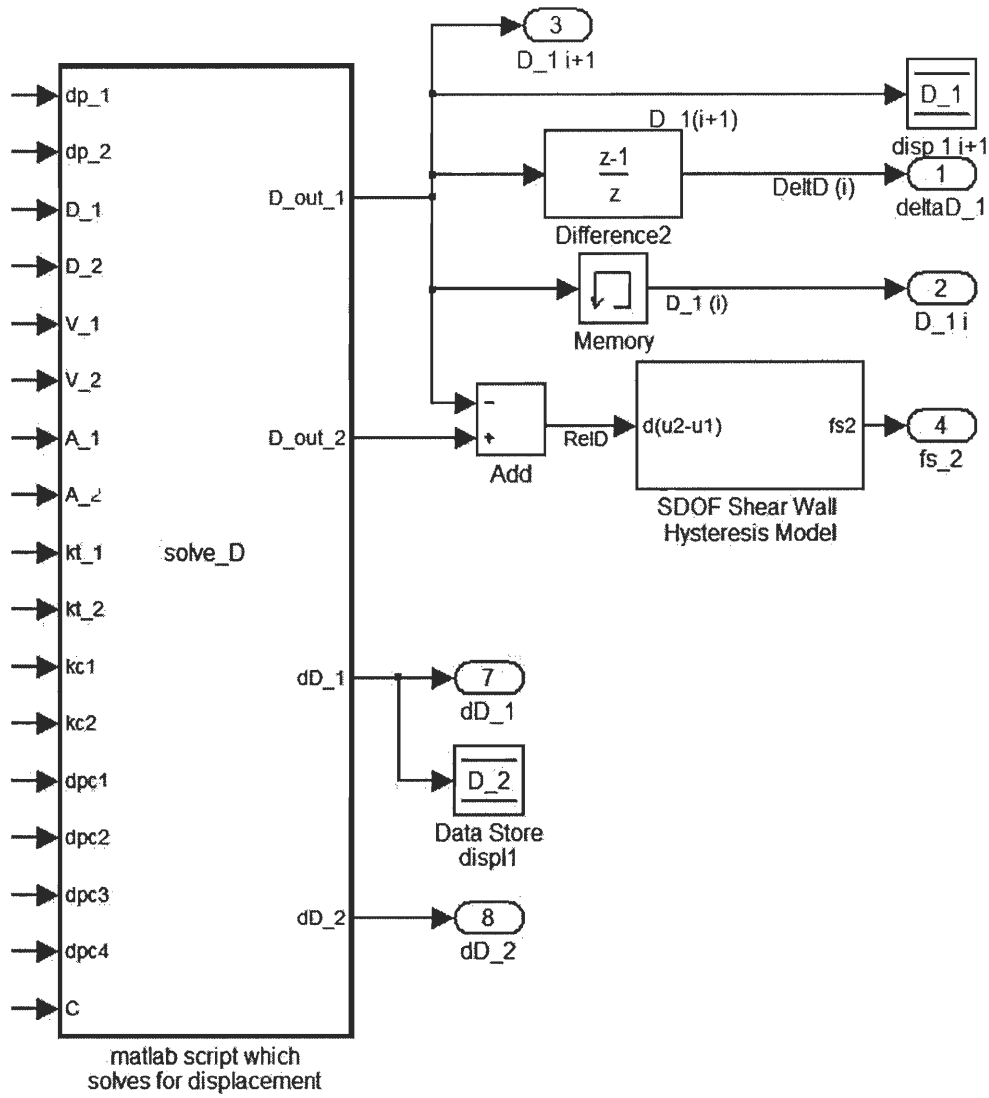

Embedded MATLAB script to calculate displacement

```
      function [D_out_1,D_out_2,dD_1,dD_2] =
solve_D(dp_1,dp_2,D_1,D_2...
          ,V_1,V_2,A_1,A_2,kt_1,kt_2,kc1,kc2,dpc1,dpc2,dpc3,dpc4,C)
      %#codegen

      % equivalent stiffness
      kt = [kt_1+kt_2 -kt_2 ; -kt_2 kt_2]; % initial tangent
stiffness
      kt_ = kt + kc1 + kc2*C;

      % equivalent force
      dp = [dp_1;dp_2];
      A = [A_1;A_2];
      V = [V_1;V_2];
      dp_ = dp + (dpc1 + dpc2*C)*V + (dpc3 + dpc4*C)*A;
```

```
% solve for displacement increment and new displacement
D = [D_1;D_2];
dD = kt_\dp_;
dD_1 = dD(1);
dD_2 = dD(2);
D_out = D + dD;
D_out_1 = D_out(1);
D_out_2 = D_out(2);
```

Simulink subsystem wood shear wall hysteresis model